

# 國立交通大學

電子工程學系 電子研究所碩士班

## 碩士論文

以 pH-ISFET 元件為基礎之尿素感測器之製造

與研究

The fabrication and study for pH-ISFET based urea  
sensors

研究生：詹昆謀

Student: Kun-Mou Chan

指導教授：張國明 博士

Advisor: Dr. Kow-Ming Chang

中華民國九十八年九月

以 pH-ISFET 元件為基礎之尿素感測器之製造  
與研究

**The fabrication and study for pH-ISFET based urea  
sensors**

研 究 生：詹昆謀

Student：Kun-Mou Chan

指 導 教 授：張國明 博士

Advisor：Kow-Ming Chang



Submitted to Department of Electronics Engineering & Institute of Electronics  
College of Electrical and Computer Engineering  
National Chiao Tung University  
in Partial Fulfillment of the Requirements  
for the Degree of  
Master  
in  
Electronics Engineering  
September 2009  
Hsinchu, Taiwan, Republic of China

中華民國九十八年九月

# 以 pH-ISFET 元件為基礎之尿素感測器之製造 與研究

學生:詹昆謀

指導教授:張國明 博士

國立交通大學

電子工程學系 電子研究所碩士班



離子感測場效電晶體(Ion-sensitive Field Effect Transistor)是由 Bergveld 在 1970 年首先提出，由於它的尺寸小、反應速度快、可承受外部應力，且與現今的 CMOS 製程相容，所以在現在的感測元件開發中具有相當大的潛力。基於以上所提之優點，製造一個以 pH-ISFET 元件為基礎之尿素感測器並研究其特性為本論文主要目標。

首先，為了將酵素薄膜有效固定在 ISFET 之  $ZrO_2$  感測層上，我們首創以 Nafion<sup>TM</sup> 混合尿素酶之結構將 Nafion<sup>TM</sup> 包埋住尿素酶以達到酵素固定化之目的。由實驗結果得知當酵素電極中尿素酶與 Nafion<sup>TM</sup> 的混合比例為 5:1 時，該 EnFET 尿素感測器具有較廣之感測範圍(8 mg/dl ~ 240 mg/dl)、高感測度 [0.64mV/(mg/dl)]、低偵測極限(8 mg/dl)、線性反應、反應時間短(25 ~ 60 sec)、生命期長(> 7 days)以及儲存穩定度佳等特性。

但是由於缺乏一個穩定且微小化的固態參考電極使得 EnFET 的應用受到很

大的限制。這個問題在藉由一個 EnFET/REFET 差動對的輸出後,固態參考電極因為金屬/溶液界面產生的不穩定電壓會以共模訊號的形式而被消除掉。

在本篇論文中，我們以 Nafion<sup>TM</sup> 混合光阻(FH-6400)或 Polyimide 的結構來修飾 ISFET 的感測層，成功地製造出一系列對尿素靈敏度極低的參考電晶體 (REFET)。並從 EnFET/REFET 差動對的輸出結果以及 EnFET/REFET 轉移電導特性比較中選擇 Nafion<sup>TM</sup> 混合光阻(FH-6400)該結構作為 REFET 感測層之材料。由實驗結果顯示對尿素的感測度達到 0.63 mV/(mg/dl)，感測範圍也達到 8 mg/dl 到 240 mg/dl 之程度，而此輸出特性非常接近由玻璃參考電極所量測之結果。

為了要實現一個最簡單且小型結構的 EnFET，在微小化的技術上，必須要整合一個固態參考電極在單一 EnFET 晶片上，不需要額外再使用到 REFET 或玻璃電極。因此，我們也把 Nafion<sup>TM</sup> 混合光阻(FH-6400)的結構應用到固態參考電極的表面修飾上，使得固態參考電極因為金屬/溶液界面產生的不穩定電壓被消除掉。因為從前面的實驗結果可知道，Nafion<sup>TM</sup> 混合光阻的結構具有使 REFET 的感測層維持在一個固定的電位且保護它不受離子的干擾的效果。由實驗結果可看出，令人困擾的電壓不穩問題，大幅地獲得改善。一個單一的 EnFET 整合固態參考電極在不需搭配 REFET 或玻璃參考電極的情況下，對尿素的感測度仍然可達到 0.47 mV/(mg/dl)而且感測範圍也達到 10 mg/dl 到 240mg/dl 之程度。

# **The fabrication and study for pH-ISFET based urea sensors**

Student: Kun-Mou Chan

Advisor: Dr. Kow-Ming Chang

Department of Electronics Engineering & Institute of Electronics  
National Chiao Tung University

## **ABSTRACT**

ISFET( Ion-sensitive Field Effect Transistor ) was first developed by Bergveld in 1970s, and because of its small size, fast response, rigidity and compatibility with standard CMOS process, ISFET is an attractive candidate of modern sensor device. Based on the advantages described previously, it is our main objective to fabricate a pH-ISFET based urea sensor and study the characteristics of it in the research.

First of all, for the purpose of enzyme immobilization, we first apply urease-mix-Nafion<sup>TM</sup> structure as enzymatic membrane coated onto ZrO<sub>2</sub> sensing layer by Nafion<sup>TM</sup> entrapment method. From the experimental results, it is obviously that when the ratio of urease to Nafion<sup>TM</sup> is 5:1, the urea-EnFET exhibits wide sensing range of between 8 and 240 mg/dl, high sensitivity of 0.64 mV/(mg/dl), low detection limit of 8 mg/dl, linear response, short response time of from 25 to 60 seconds, long lifetime, and good storage stability.

Due to the lack of a stable and miniaturized solid-state reference electrode, the application of EnFET will be restricted seriously. One approach to solve this problem is to use a differential measurement consisting of an ion-sensitive structure (EnFET)

and an ion-insensitive structure (REFET). With this arrangement, the common mode unstable voltage generated from the thermodynamically undefined metal/electrolyte interface can be eliminated.

In this thesis, we apply the Nafion<sup>TM</sup>-mix-PR or Nafion<sup>TM</sup>-mix-Polyimide structures to modify the ISFET sensing layer and successfully obtain a series of REFETs with low urea sensitivity. According to the EnFET/REFET differential measurement results with different REFET's sensing layers and the transconductance characteristics of EnFET and REFETs, we finally choose the Nafion<sup>TM</sup>-mix-PR structure as REFET's sensing layer. From the experimental results, the urea sensitivity can achieve 0.63 mV/(mg/dl), and the urea sensing range is from 8 mg/dl to 240 mg/dl because of the ultra low sensitivity REFET treated by PR-mix-Nafion<sup>TM</sup> structure. The performance is extremely close to those of glass reference electrode.

In order to realize the single EnFET integrated with the simple and compact structure of solid-state reference electrode by miniaturized technology, and the EnFET sensor is fabricated without the additional REFET or glass reference electrode. We also apply the Nafion<sup>TM</sup>-mix-PR structure to modify the surface of the solid-state reference electrode, so the unstable voltage generated from the thermodynamically undefined metal/electrolyte interface can be eliminated. From the experimental results presented previously, we can know the Nafion<sup>TM</sup>-mix-PR structure can maintain a constant voltage for the sensing layer of REFET and prevent it from disturbing by the ions. The experimental results show the troublesome and unstable problem can be greatly improved. Without EnFET/REFET arrangement in differential measurement or glass reference electrode, the urea sensitivity of single EnFET integrated with Ti/Pd/Nafion<sup>TM</sup>-mix-PR solid-state reference electrode still can reach to 0.47 mV/(mg/dl) and the sensing range is from 10mg/dl to 240 mg/dl.

## 誌 謝

能夠完成此論文，首先要誠摯地感謝張國明老師，悉心的教導使我得以順利完成碩士論文，不時的討論並指點我正確的方向，使我在這些年中獲益匪淺。老師那豁達開朗的個性，讓我印象深刻，並且也教導了我許多待人處世的道理，讓我的想法觀念成長了不少，老師對學問的嚴謹更是我輩學習的典範。

還有感謝桂正楣老師，王水進老師，賴瓊惠老師在口試中對我論文內容提出的建議及看法，讓我對研究的題目有更進一步的想法，也讓我見識到了教授思考問題的方法，確實是學生該去學習的。

其次我要感謝張知天學長，在我實驗過程中給予的建議及鼓勵，使我對於實驗充滿了信心，而且在平常的交談中也傳授了我許多人生的經驗談，讓我受益匪淺。還有感謝黃菘宏學長和憶雯晶圓的熱情贊助，使得本篇論文內容更佳的完整。另外我要感謝堃濠、成家及其他實驗室同學在儀器考核及實驗上的幫助，有了你們讓我可以很快地進行實驗，順利完成我的碩士論文。

最後要感謝我的父母，在我的求學生涯中，你們從不會給予我任何的壓力，讓我可以自由自在的學習，在我遇到挫折失敗時，你們也都給予我極大的關心與幫助，讓我覺得相當幸福及幸運，由於你們無怨無悔的付出，讓我可以無後顧之憂，順利完成我的學業，取得碩士學位。

誌于 2009.09  
詹昆謀

# Contents

<b>Abstract (in Chinese)</b>	-----	i
<b>Abstract (in English)</b>	-----	iii
<b>Acknowledgement</b>	-----	v
<b>Contents</b>	-----	vi
<b>Table Captions</b>	-----	ix
<b>Figure Captions</b>	-----	xi
<b>Chapter 1</b>	<b>Introduction</b>	
1.1	The importance of pH detection-----	1
1.2	Techniques for pH detection-----	1
1.3	The pH glass electrodes-----	2
1.4	The ISFET based pH sensors-----	3
1.5	The importance of reference electrode-----	6
1.6	Solid-state reference electrode integrated with ISFET-----	7
1.7	The ISFET/REFET configuration in differential mode-----	8
1.8	ISFET-based enzyme biosensors-----	10
1.9	Motivation of this work and thesis organization-----	12
1.10	References-----	14
<b>Chapter 2</b>	<b>Theory Description</b>	
2.1	Definition of pH-----	17
2.2	Fundamental principles of ISFET-----	17
2.2.1	From MOSFET to ISFET-----	18
2.2.2	The oxide-electrolyte interface-----	20
2.2.3	Theory for the pH sensitivity of ISFET-----	25
2.3	Basic principles of ENFET-----	27
2.3.1	The definition of system configuration-----	27
2.3.2	Enzyme-catalyzed reaction of substrate-----	28
2.3.3	Enzyme-modified ISFET-----	30
2.4	Summary-----	34
2.5	References-----	34
<b>Chapter 3</b>	<b>Experiment and Measurement</b>	



3.1	Introduction-----	37
3.2	The characteristics of the Urease, Polyimide, Nafion <sup>TM</sup> and PR-----	37
3.2.1	Urease-----	37
3.2.2	Polyimide-----	38
3.2.3	Nafion-----	39
3.2.4	PR-----	39
3.3	Fabrication process flow of co-fabricated ENFET and REFET-----	40
3.4	Key steps illustration-----	41
3.4.1	Gate region formation-----	41
3.4.2	Sensing layer deposition-----	42
3.4.3	PR-mix-Nafion <sup>TM</sup> membrane-based reference electrodes-----	43
3.4.4	PR-mix-Nafion <sup>TM</sup> and Polyimide-mix-Nafion <sup>TM</sup> membrane-based sensing layer-----	43
3.5	Packing and measurement system-----	44
3.5.1	Current-Voltage (I-V) measurement set-up-----	45
3.5.2	Current-Voltage (I-V) measurement set-up with solid-state reference electrodes-----	46
3.5.3	Reaction time measurement set-up with glass reference electrodes-----	46
3.6	References-----	47

## **Chapter 4 Results and Discussions**

4.1	Introduction-----	49
4.2	Enzyme immobilization methods-----	49
4.3	Enzyme immobilization of the pH-ISFET based urea sensor-----	53
4.3.1	pH sensitivity and linearity of the pH-ISFET and urea-ENFET-----	53
4.3.2	The proper immobilization method of enzyme membranes---	54
4.3.3	The response time of urea-ENFET-----	58
4.3.4	The influence of the titration by high concentration urea solution-----	59
4.3.5	The effect of concentration of the phosphate buffer solution-	60
4.3.6	Storage stability-----	60
4.4	Solid-state reference electrode integrated with ENFET-----	61
4.4.1	Solid-state reference electrode-----	61
4.4.2	The bare metal reference electrode-----	63

4.4.3	The PR-mix-NF coated solid-state reference electrode-----	64
4.5	The ENFET/REFET configuration in differential mode-----	66
4.5.1	ENFET/REFET differential pair with different polymer-based material-----	66
4.5.2	Coplanar ENFET/REFET differential pair with quasi-reference electrode-----	70
4.6	Conclusions-----	71
4.7	References-----	73
<b>Chapter 5</b>	<b>Future Work-----</b>	<b>75</b>

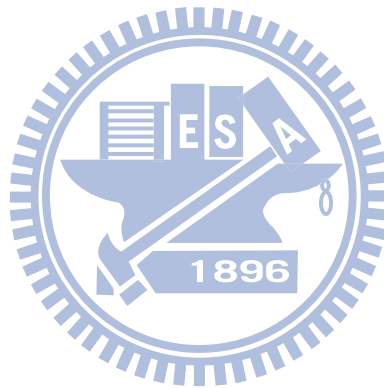


## Table Captions

Table 1-1	Sensitivity for different sensing layers	79
Table 1-2	Data on ENFETs developed	79
Table 3-1	ZrO <sub>2</sub> Sputtering parameters	92
Table 3-2	Summary of test structures	93
Table 4-1	Summary of ZrO <sub>2</sub> ISFET and ZrO <sub>2</sub> /urease-mix-NF(1:1) ENFET measure by glass reference electrode	122
Table 4-2	Summary of urea-ENFET measure by glass reference electrode	123
Table 4-3	Storage stability of ZrO <sub>2</sub> /urease-mix-NF(5:1) ENFET measure by glass reference electrode	123
Table 4-4	Summary of ZrO <sub>2</sub> /urease-mix-NF(5:1) ENFET measure by bare Ti/Pd metal reference electrode and Ti/Pd/PR-mix-NF solid-state reference electrode	124
Table 4-5	Summary of ZrO <sub>2</sub> /urease-mix-NF(5:1) ENFET measure by glass reference electrode and Ti/Pd/PR-mix-NF solid-state reference electrode	124
Table 4-6	Summary of ENFET/ISFET in differential mode measure by glass reference electrode	125
Table 4-7	Summary of ENFET/REFET in differential mode measure by glass reference electrode	125
Table 4-8	Summary of ENFET/REFET in differential mode measure by Ti/Pd quasi-reference electrode	126

Table 4-9	Summary of ENFET and ENFET/REFET differential pair measure by different reference electrodes	126
Table 4-10	Summary of ENFET and ENFET/REFET(ISFET) differential pair measure by different reference electrodes	127



## Figure Captions

Fig. 1-1	Conventional pH glass electrode	76
Fig. 1-2	Cross-Section Structure of ISFET	76
Fig. 1-3	Block diagram of a differential ISFET/REFET measuring system	77
Fig. 1-4	Schematic representation of ENFET from R&D Institute of Microdevices	77
Fig. 1-5	Organization of thesis	78
Fig. 2-1	Schematic representation of a MOSFET (a) and an ISFET (b) cross-section	80
Fig. 2-2	$I_D$ - $V_{DS}$ curve of an ISFET with $V_{gs}$ (a), and pH (b) as a parameter	80
Fig. 2-3	Electrode and electrolyte interface	81
Fig. 2-4	Schematic representation of site-binding model	81
Fig. 2-5	Hemholtz model	82
Fig. 2-6	Gouy-Chapman model	82
Fig. 2-7	Gouy-Chapman-Stern model	83
Fig. 2-8	Potential profile and charge distribution at an oxide/electrolyte solution interface	83
Fig. 2-9	Mechanisms involved in the response of pH-based enzyme sensors	84
Fig. 2-10	Schematic representation of the potentiometric biosensor using an immobilized enzyme layer	84

Fig. 3-1	The chemical structure of Helicobacter Pylori urease	85
Fig. 3-2	Chemical structure and model of Nafion <sup>TM</sup>	85
Fig. 3-3	Fabrication process flow	89
Fig. 3-4	Measurement set-up	89
Fig. 3-5	Extraction method of sensing range and sensitivity	90
Fig. 3-6	Extraction method of response time	91
Fig. 4-1	The $I_{DS}$ - $V_{GS}$ curves and sensitivity linearity of $ZrO_2$ -pH-ISFET measure by glass reference electrode	94
Fig. 4-2	The $I_{DS}$ - $V_{GS}$ curves and sensitivity linearity of $ZrO_2$ /urease-mix-NF urea-ENFET measure by glass reference electrode	95
Fig. 4-3	The $I_{DS}$ - $V_{GS}$ curves of $ZrO_2$ /urease-mix-NF(1:1) urea-ENFET measure by glass reference electrode	96
Fig. 4-4	Calibration curve of $ZrO_2$ /urease-mix-NF(1:1) urea-ENFET measure by glass reference electrode	96
Fig. 4-5	The $I_{DS}$ - $V_{GS}$ curves of $ZrO_2$ /urease-mix-NF(20:1) urea-ENFET measure by glass reference electrode	97
Fig. 4-6	Calibration curve of $ZrO_2$ /urease-mix-NF(20:1) urea-ENFET measure by glass reference electrode	97
Fig. 4-7	The $I_{DS}$ - $V_{GS}$ curves of $ZrO_2$ /urease-mix-NF(5:1) urea-ENFET measure by glass reference electrode	98
Fig. 4-8	Calibration curve of $ZrO_2$ /urease-mix-NF(5:1) urea-ENFET measure by glass reference electrode	98
Fig. 4-9	Calibration curves of $ZrO_2$ /urease-mix-NF urea-ENFET measure by glass reference electrode	99
Fig. 4-10	Summary of urea sensing range for different test structures	99

Fig. 4-11	Summary of urea sensitivity for different test structures	100
Fig. 4-12	Response signals of ZrO <sub>2</sub> /urease-mix-NF(5:1) urea-ENFET with 1.25 mg/dl urea concentration	100
Fig. 4-13	Response signals of ZrO <sub>2</sub> /urease-mix-NF(5:1) urea-ENFET with 10 mg/dl urea concentration	101
Fig. 4-14	Response signals of ZrO <sub>2</sub> /urease-mix-NF(5:1) urea-ENFET with 40 mg/dl urea concentration	101
Fig. 4-15	Response signals of ZrO <sub>2</sub> /urease-mix-NF(5:1) urea-ENFET with 80 mg/dl urea concentration	102
Fig. 4-16	Response signals of ZrO <sub>2</sub> /urease-mix-NF(5:1) urea-ENFET with 120 mg/dl urea concentration	102
Fig. 4-17	Response signals of ZrO <sub>2</sub> /urease-mix-NF(5:1) urea-ENFET with 240 mg/dl urea concentration	103
Fig. 4-18	Response signals of ZrO <sub>2</sub> /urease-mix-NF(5:1) urea-ENFET with different urea concentrations	103
Fig. 4-19	The I <sub>DS</sub> -V <sub>GS</sub> curves of ZrO <sub>2</sub> /urease-mix-NF(5:1) urea-ENFET titration by high concentration urea	104
Fig. 4-20	Calibration signals of ZrO <sub>2</sub> /urease-mix-NF(5:1) urea-ENFET titration by high concentration urea	104
Fig. 4-21	The I <sub>DS</sub> -V <sub>GS</sub> curves and calibration line of ZrO <sub>2</sub> /urease-mix-NF(5:1) urea-ENFET with different phosphate buffer solutions	105
Fig. 4-22	Calibration curves of ZrO <sub>2</sub> /urease-mix-NF(5:1) urea-ENFET in storage stability measurement	106
Fig. 4-23	The I <sub>DS</sub> -V <sub>GS</sub> curves of ZrO <sub>2</sub> /urease-mix-NF(5:1) urea-ENFET measure by bare Ti/Pd metal reference electrode	106
Fig. 4-24	Calibration curve of ZrO <sub>2</sub> /urease-mix-NF(5:1) urea-ENFET measure by bare Ti/Pd metal reference electrode	107
Fig. 4-25	The I <sub>DS</sub> -V <sub>GS</sub> curves of ZrO <sub>2</sub> /urease-mix-NF(5:1) urea-ENFET measure by Ti/Pd/PR-mix-NF solid-state reference electrode	107
Fig. 4-26	Calibration curve of ZrO <sub>2</sub> /urease-mix-NF(5:1) urea-ENFET measure by Ti/Pd/PR-mix-NF solid-state reference electrode	108

Fig. 4-27	Calibration curves of $ZrO_2$ /urease-mix-NF(5:1) urea-ENFET measure by Ti/Pd/PR-mix-NF solid-state reference electrode and bare Ti/Pd metal reference electrode	108
Fig. 4-28	Calibration curves of $ZrO_2$ /urease-mix-NF(5:1) urea-ENFET measure by glass reference electrode and Ti/Pd/PR-mix-NF solid-state reference electrode	109
Fig. 4-29	The $I_{DS}$ - $V_{GS}$ curves of $ZrO_2$ ISFET measure by glass reference electrode	109
Fig. 4-30	Calibration curve of $ZrO_2$ ISFET measure by glass reference electrode	110
Fig. 4-31	The $I_{DS}$ - $V_{GS}$ curves of $ZrO_2$ /PR-mix-NF(1:1) REFET measure by glass reference electrode	110
Fig. 4-32	Calibration curve of $ZrO_2$ /PR-mix-NF(1:1) REFET measure by glass reference electrode	111
Fig. 4-33	The $I_{DS}$ - $V_{GS}$ curves of $ZrO_2$ /PI-mix-NF(3:1) REFET measure by glass reference electrode	111
Fig. 4-34	Calibration curve of $ZrO_2$ /PI-mix-NF(3:1) REFET measure by glass reference electrode	112
Fig. 4-35	The $I_{DS}$ - $V_{GS}$ curves of $ZrO_2$ /PI REFET measure by glass reference electrode	112
Fig. 4-36	Calibration curve of $ZrO_2$ /PI REFET measure by glass reference electrode	113
Fig. 4-37	Calibration curves of REFET with different structures measure by glass reference electrode	113
Fig. 4-38	Calibration curves of ENFET/ISFET( $ZrO_2$ ) in differential mode measure by glass reference electrode	114
Fig. 4-39	Calibration curves of ENFET/REFET( $ZrO_2$ /PR-mix-NF) in differential mode measure by glass reference electrode	114
Fig. 4-40	Calibration curves of ENFET/REFET( $ZrO_2$ /PI-mix-NF) in differential mode measure by glass reference electrode	115
Fig. 4-41	Calibration curves of ENFET/REFET( $ZrO_2$ /PI) in differential mode measure by glass reference electrode	115
Fig. 4-42	Calibration curves of ENFET/REFET in differential mode measure by glass reference electrode	116



Fig. 4-43	Transconductance curves of ENFET/ISFET( $ZrO_2$ ) in differential mode measure by glass reference electrode	116
Fig. 4-44	Transconductance curves of ENFET/REFET( $ZrO_2$ /PR-mix-NF) in differential mode measure by glass reference electrode	117
Fig. 4-45	Transconductance curves of ENFET/REFET( $ZrO_2$ /PI-mix-NF) in differential mode measure by glass reference electrode	117
Fig. 4-46	Transconductance curves of ENFET/REFET( $ZrO_2$ /PI) in differential mode measure by glass reference electrode	118
Fig. 4-47	Transconductance curves of ENFET/REFET(ISFET) in differential mode measure by glass reference electrode	118
Fig. 4-48	The $I_{DS}$ - $V_{GS}$ curves of $ZrO_2$ /PR-mix-NF(1:1) REFET measure by bare Ti/Pd metal reference electrode	119
Fig. 4-49	Calibration curve of $ZrO_2$ /PR-mix-NF(1:1) REFET measure by bare Ti/Pd metal reference electrode	119
Fig. 4-50	Calibration curves of ENFET/REFET( $ZrO_2$ /PR-mix-NF) in differential mode measure by bare Ti/Pd metal reference electrode	120
Fig. 4-51	Calibration curves of ENFET and ENFET/REFET differential pair measure by different reference electrodes	120
Fig. 4-52	Calibration curves of ENFET and ENFET/REFET(ISFET) differential pair measure by different reference electrodes	121
Fig. 4-53	Summary of urea sensing range for different test structures	121
Fig. 4-54	Summary of urea sensitivity for different test structures	122

# Chapter 1

## Introduction

### 1.1 The importance of pH detection

pH is one of the most common measurement parameters because so many biological and chemical processes are dependent on pH. We can find the chemical characteristics of a substance by measuring pH. For example, the body fluid of living organisms usually has specific pH range. If the pH of the human blood changes by a little as 0.03 pH units or less the functioning of the body will be greatly impaired [1]. In our surroundings, the pH values of rivers, waters and soils affect the livability of fishes, animals and plants. In a word, a little change of the pH value will result in serious impact to these organisms. Hence, it is necessary to measure pH value accurately. Commonly used methods for pH detection will be introduced in the next section.

### 1.2 Techniques for pH detection

Traditionally, there are many methods for detecting pH value, such as (1) indicator reagents (2) pH test strips (3) metal electrode (4) glass electrode. The methods (1) and (2) are differentiated from colors and are impossible to reach high accuracy. The method (3) is difficult for daily use and reproducing. Because of some limitations in practical applications of the first three methods, the method (4) glass electrode becomes the most widely used method for pH measurement, and is considered to be the standard measuring method. Therefore we will have an

introduction for glass electrode in the next section.

### 1.3 The pH glass electrodes

In 1906, the first pH glass electrode was developed by M. Cremer with Fritz Haber and many efforts have been devoted to improve its application. The pH glass electrode consists of an electrode membrane that responds to pH, which only permits the passage of hydrogen ions in solution. Generally, a fixed concentration of HCl or a buffered chloride solution inside in contact with an internal reference electrode, which use of Ag/AgCl, as shown in Fig. 1-1.

When the glass electrode is immersed in the solution, the outer bulb surface will be hydrated (the thickness is about 0.3-0.6 nm) and exchanges sodium ions for hydrogen ions to build up a surface layer of hydrogen ions [2]. The build up of charges on the inside of the membrane is proportional to the amount of hydrogen ions in the outside solution. The potential difference between inside and outside the thin glass membrane is proportional to this difference in pH value in the external solution, and we can derive the potential difference from Nernst equation:

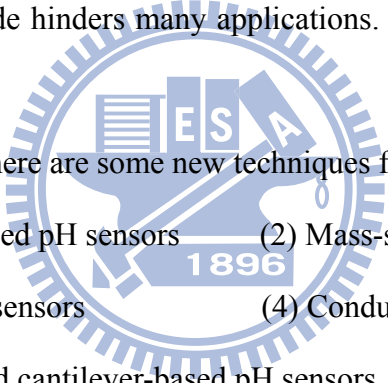
$$E = E_0 + \frac{RT}{nF} \ln a_{H^+} \quad (1-1)$$

where  $E$  = electrode potential,  $E_0$  = standard potential of the electrode,  $R$  = gas constant ( $8.31441 \text{ JK}^{-1} \text{ mol}^{-1}$ ),  $T$  = temperature (in Kelvin),  $n$  = valence ( $n = 1$  for hydrogen ions),  $F$  = Faraday constant and  $a_{H^+}$  = activity of hydrogen ions.

According to this equation, providing that at one side of the interface the activity of the ion of interest is kept constant, the electrode potential is direct logarithmic function of the ion activity on the other side. Because of its ideal Nernstian response independent of redox interferences, short balancing time of electric potential, high

selectivity, reliability and wide pH range, glass electrode is most widely used for pH measurement. However, glass electrode has several drawbacks for many industrial applications. Firstly, they are unstable in alkaline or HF solutions or at temperatures higher than 100°C. Also, they exhibit a sluggish response and are difficult to miniaturize. Moreover, they cannot be used in food or in vivo applications due to their fragility of the glass. Finally, due to the need for internal liquid reference solutions, the traditional glass electrode must be used at the vertical position for chemical reproducibility. Consequently, it is very inconvenient in applications. In order to overcome these drawbacks, the all-solid-state electrode sensors have been investigated for a long time. However, it is obvious that the unavailability of a reliable miniature reference electrode hinders many applications. There is an increasing need for alternative pH sensors.

According to Ref [2], there are some new techniques for pH detection:

- 
- (1) Optical-fiber-based pH sensors
  - (2) Mass-sensitive pH sensors
  - (3) Metal oxide pH sensors
  - (4) Conducting polymer pH sensors
  - (5) Nano-constructed cantilever-based pH sensors
  - (6) ISFET-based pH sensors**
  - (7) pH-image sensors

As mentioned above, the ISFET-based pH sensor is a new technique for pH detection. Due to the highly advanced IC fabrication techniques, a miniature ISFET-based pH sensor is of particular interest in the field of medical diagnostics for use in implantable devices or on catheter tips and shows a great potential for application in chemical and biological sensing devices.

#### **1.4 The ISFET-based pH sensors**

The ion sensitive field effect transistor (ISFET) was invented by P. Bergveld in

1970s [3] and has been introduced as the first miniaturized silicon-based chemical sensor. The ISFET structure is similar to the Metal Oxide Semiconductor Field Effect Transistor (MOSFET) except that metal gate. In other words, ISFET is a special type of MOSFET without a metal gate, in which the gate oxide is directly exposed to the buffer solution. When the sensing layer of the ISFET contacts with the electrolyte, it will induce a surface potential between the gate oxide and electrolyte. For the different pH value buffer solution, there are different surface potentials induced at the surface. Hence the electric field at the interface will be changed and the channel conductance that affects the drain current will also be modulated. Since the channel conductance and drain current can be modulated. For example, the general expression for the drain current of the ISFET in the linear region is

$$I_D = \frac{C_{ox}\mu W}{L} \left[ (V_{GS} - V_T) - \frac{1}{2}V_{DS} \right] V_{DS} \quad (1-2)$$

Therefore, in order to be able to measure the threshold voltage of the ISFET, it is necessary to bias it at constant drain current ( $I_D$ ) and constant drain to source voltage ( $V_{DS}$ ). In such situation there will be only two variables,  $V_G$  and  $V_T$ . When  $V_T$  varies, the gate voltage must adjust by an equal amount to compensate. The circuit to maintain constant  $I_D$  and constant  $V_{DS}$  can be carrying out by using feedback OP amplifiers and current sources and sinks [4]. Different pH concentrations will induce different voltage variation, so we can determine the pH value of the test solution from the potential difference. The more detailed operation mechanisms and theories are presented in Chapter 2. By these methods, we can plot a standard linear line between gate voltages and various pH values, and this standard can be taken to measure an unknown acid or alkaline solution [5].

The development of ISFET has been on going for more than 35 years, and the first ISFET sensing layer exploited was silicon dioxide ( $\text{SiO}_2$ ), which showed an

unstable sensitivity and a large drift. Recently, there are many materials that have been investigated and applied for the ion sensing layer. For instance, high dielectric constant insulator materials were used as pH-sensing layers because of their high sensitivity performance and long-term reproducibility. Table 1-1 shows the sensitivities and test ranges of different sensing layers. It is found that pH sensitivity is one of the important characteristic parameters of the ISFET devices and the response of the ISFET is mainly determined with the type of the sensing layer. Therefore, the sensing material plays a significant role. In the study, we use zirconium oxide ( $ZrO_2$ ) as the ion sensing layer. However, because of the poor interface between the high  $k$  sensing layer and silicon substrate, all sensing layers must be deposited on the thermally grown  $SiO_2$  to improve the interface properties [6], which are low density of interface state, small stress, and good adhesion. Hence, with the study of sensing layer, some materials are found that can detect different ions, for example,  $K^+$ ,  $Na^+$ ,  $Ca^+$ , and  $H^+$  ions.

To compare with the conventional pH-meter using glass electrode, ISFET has following features:

- (1) Small size and weight
- (2) Short response time
- (3) Potential of mass production at low cost
- (4) Compatible with the standard CMOS process
- (5) Small sample requirement

However, for most of the sensor devices, it is possible to fabricate a variety of chemical sensors with a small size down to the micrometer scale so that only a small amount of the test solution should be necessary, but this improvement is useless because of the lack of a miniaturized reference electrode [7]. Hence, how to reduce the scale of macroscopic commercial reference electrode is a major challenge. In this

study, the problems of the miniaturized solid-state reference electrodes are investigated for practical applications of urea-ENFET. We will discuss the importance of reference electrode in the next section.

## 1.5 The importance of reference electrode

The reference electrode is an important part of electrochemical measurement. The quality of the reference electrode is especially important in the direct potentiometric measurement of pH and blood electrolytes. For a material to be a good reference electrode, the desired parameters are high sensitivity, good linearity, fast response time, long life time, chemical and thermal independence.

An ideal reference electrode for use as the ISFET gate terminal should provide [4]:

- (1) An electrical contact to the solution from which to define the solution potential;
- (2) An electrode/solution potential difference ( $E_{ref}$ ) that does not vary with solution composition.

In other words, it is expected that it is sufficiently stable, that it is not fouled by a sample, and that the reference electrode itself does not contaminate a sample. It is advisable that a reference electrode is easy to manufacture and use, that it is service-free and cheap, and has a long life-time. The conventional silver chloride or calomel electrodes provide both of these functions by maintaining an electrochemical equilibrium with the solution. Such an electrode requires compartments filled with a reference solution and separated by a permeable membrane.

## 1.6 Solid-state reference electrode integrated with ISFET

Due to the lack of metal gate electrode for ISFET, the input gate voltage will be applied through a reference electrode, which provides a stable potential in the electrochemical measuring system, as shown in Fig. 1-2. The most simple and compact structure of ISFET is the all-solid-state reference electrode integrated with ISFET in a single chip. However, very few papers have been devoted to the miniaturization of the reference electrode, although hundreds of papers have been published concerning various sensing devices such as ISFET [8]. For some analytical applications, it is desirable to use all-solid-state pH sensor when the electrode has to work in a non-vertical position. All-solid-state electrodes have several advantages over glass electrode with internal filling solution, one of them being the minimization of the contribution from the liquid junction. Furthermore, all-solid-state electrodes may be exposed to higher temperatures and pressures than the liquid filling electrodes, and they need not be used in an upright position. They are miniaturizable, do not need refilling with internal solution and can be prepared in various shapes and sizes [9].

Today, due to the frequent applications of potentiometry with ion-selective electrodes in clinical and biological measurements, it is important that a reference electrode is necessary to miniaturize. Hence there has been a considerable effort to develop solid state reference electrodes over the past years. However, it is still a problem to create a long-term stable solid-state reference electrode. Because potential at the solid/liquid interface is thermodynamically undefined, it will lead to significant errors in pH measurement. The unstable problem may come from the redox reaction or other chemical reactions at the metal reference electrode and the liquid interface, i.e. the solid/liquid interface. Hence, providing a stable potential at the interface is a major challenge for miniaturized solid-state reference electrode integrated with ISFET.



## 1.7 The ISFET/REFET configuration in differential mode

Since the introduction of the ISFET by Bergveld [3], the use of a reference electrode (RE) has been a subject of discussion. One possibility is the on-chip fabrication of an Ag/AgCl electrode with IC-compatible techniques, including a gel filled cavity and a porous silicon plug [10]. This solution is problematic due to the leakage of the reference solution, which results in a limited device lifetime. Alternatively, another approach towards achieving this goal is to use a differential arrangement consisting of an ion-sensitive structure and an ion-insensitive structure (REFET) first introduced by Matsuo in 1978. As shown in Fig. 1-3 [11], with this ISFET/REFET arrangement, the conventional RE is replaced by a quasi-reference metal electrode (QRE) (typically of Pt or Au) [12]. The output signal of the system,  $V_{out}$ , obtained in a differential system where  $V_{GS}$  of the ISFET ( $V_{ISFET}$ ) and of the REFET ( $V_{REFET}$ ) are both measured versus the common QRE, is as follows:

$$V_{out} = V_{ISFET} - V_{REFET} \quad (1-3)$$

The metal/electrolyte interface is thermodynamically undefined, and therefore generates an unstable voltage, but this voltage is measured by the differential ISFET/REFET pair as a common mode voltage and does not result in a system output voltage. A change in the pH of the solution is, however, measured as a differential voltage, as the ISFET responds to the pH and the REFET does not [13]. The concept of an ISFET/REFET differential pair is not only applicable to pH sensing applications, but also to monitoring concentrations of other ions, such as  $\text{Na}^+$  and  $\text{K}^+$ , as well as other species, such as creatinine and urea, with the use of chemically and enzymatically modified field effect transistors (CHEMFET, ENFET, respectively) [14].

Several REFETs have been made based on different approaches, such as using a buffered hydrogel as insensitive membrane [15] or with an ion-blocking parylene gate [16]. However, the parylene REFET showed a number of operational problems [13]. According to the commonly accepted site-dissociation model for the pH-sensitivity of ISFETs with an inorganic gate material, its pH response can be described in terms of the number of reactive sites on the gate surface and their proton dissociation and association constants. Thus, a possible approach is the chemical modification of the ISFET surface to reduce the number of sites [17].

A commonly used material for polymeric membranes in ion selective electrodes (ISE) and CHEMFETs (modified ISFETs selective to ions other than  $H^+$ ) is poly(vinyl chloride) (PVC) [17]. This indicates that an ion-unblocking layer made by a PVC cocktail might be a good choice for REFET applications, since a reduced sensitivity to hydrogen ions for the REFET and a similar transconductance value for both the ISFET and REFET were obtained. However, the PVC-REFET still has some drawbacks, such as a small operation range, short lifetime, and high drift, which must be improved. In addition, PVC has usually not been considered for REFETs as it typically shows cation perm-selectivity [17]. This behavior is common to many polymeric membranes, and means that the membranes are permeable for cations. This results in an ionic strength dependence of the membrane potential, and thus of the REFET response. The source of the perm-selectivity seems to be the presence of immobile anionic sites in the membrane and a lower mobility of the anions in the membrane as compared to the cations. The perm-selectivity behavior can therefore be changed by adding lipophilic cations to the membrane, and thus it is affected by the membrane composition [17].

## 1.8 ISFET-based enzyme biosensors

Though Janata and Moss as early as in 1976 suggested the idea of using ISFETs as enzyme sensors, there were no publications about this up to 1980, when the first results were presented regarding ISFET practice for penicillin determination [18]. The device described by Caras and Janata consisted of two pH-ISFETs, one of which had on the top of its subgate part the membrane with covalently bound penicillinase and albumin, while the other had only the membrane with covalently bound albumin. This device is called an “enzyme field-effect transistor (ENFET)”. When penicillin was present in the solution, penicillinase in the membrane catalyzed penicillin hydrolysis that resulted in the production of protons and therefore in a local pH decrease in the gate area, registered by the ISFET. It was shown that these ENFETs needed only a small amount of the enzyme in the membrane and that they can be used repeatedly, which is certainly a serious ENFET advantage in comparison with the classical enzyme analysis [18].

At the first international conference on chemical sensors held in 1983 in Fukuoka, Japan, two pieces of research devoted to ISFET-based biosensors were reported: Miyahara et al. presented ENFET for urea and acetylcholine determination, Hanazato and Shiono—for glucose determination [18]. Since 1985 there has been a considerable increase of information on various aspects of ENFET development and operation.

Schematic representations of ENFETs from the R&D Institute of Microdevices (Kiev, Ukraine) are shown in Fig. 1-4 [18]. A differential pair of ISFETs (one covered with an enzyme-containing membrane and the other with a blank one) is usually employed to compensate for common interference, bulk pH and temperature changes. For both ISFETs, the “source and drain follower circuit” can be used, whereby the

output voltages are connected to an additional differential amplifier. The proposed differential mode of operation allows the use of a non-encapsulated substrate of the chip itself as a quasi-reference electrode [18]. This obviates the need for any conventional reference electrode or of a separate fabricated noble metal quasi-reference electrode to render the biosensor operational.

Some basic enzyme reactions, which we used for ENFET generate or consume protons, changing the pH inside the enzyme membrane registered by the ISFET. The data on the development of various ISFET-based enzyme biosensors are presented in Table 1-2. The practical application of ISFET-based sensors is complicated by the fact that their response is affected by the pH of the medium, buffer capacity, concentration of the substrate, and in some cases [18]. The buffer capacity of the solution tested depends on pH; therefore, the pH change in the matrix with the immobilized enzyme depends on the initial assay pH. Still more essential is the pH effect on the enzyme kinetics—the diagram of the pH effect on the enzymatic reaction rate is nearly bellshaped, so enzyme inhibition is probable when the matrix pH is much changed. The ENFET sensitivity limit, response time and value depend on a number of factors: an enzyme operation rate, outside mass transfer (i.e. substrate and buffer diffusion out of the solution value toward the membrane surface), membrane thickness and porosity, etc [18].

A very important option is the method used to immobilize the enzyme on the sensor surface [18]. On the one hand, all the principles and methods commonly used in the development of biosensors are appropriate. On the other hand, to realise the inherent potential of ISFETs as fully as possible, the enzyme biomembrane technology should:

- (a) provide membrane arrangement on the required part of the chip;
- (b) present proper adhesion of the membrane to the ISFET surface;

- (c) enable the development of a multisensor, which means the fabrication of a compact site for membranes with a different composition on the same chip surface;
- (d) be compatible with IC group technology.

From this point of view, the approach seems attractive—a thin layer of photopolymerized solution containing the enzyme is placed on the structure [18]. After exposition to ultrasonic irradiation through a photo pattern and washing non-polymerized solution, the matrix with the enzyme remains only on the surface area over the transistor gate. The albumin matrix with the enzyme is placed over the whole plate, then after polymerization the enzyme is deactivated by ultrasonic irradiation everywhere except for the required parts [18]. Membrane immobilization by modified photolithography is also a promising technique [18]. But these biosensors were not very stable. In paper [18] the authors try to enhance the enzyme immobilization platform to improve enzyme loading and stability by physically modifying the gate insulator surface. Prior work [18] indicated that immobilization onto porous silica beads increased enzyme stability and total activity relative to immobilization on non-porous surfaces, and a silica microsphere-modified surface is physically similar to that of porous silica beads. Therefore, silica microspheres of 20 or 200 nm diameter were formed on the basis of a catalyzed sol–gel process, then dip-coated onto the FET gates. Results indicate that the silica microsphere-modified gate did not affect device pH sensitivity and did enhance sensor performance indicating an increase in total enzyme activity. Results also indicate that sol–gel coatings were effective for improving enzyme stability [18].

## **1.9 Motivation of this work and thesis organization**

First of all, in order to get an available enzyme electrode applied to pH-ISFET based urea sensor, we seek for the proper ratio of urease to Nafion<sup>TM</sup> mixture membrane coated onto ZrO<sub>2</sub> of ENFET by Nafion<sup>TM</sup> entrapment as enzyme immobilization. As mentioned before, the enzyme immobilization methods are related to enzyme activity, urea sensing range, urea sensitivity, detection limit, response time, lifetime, linearity of dynamic range, and storage stability.

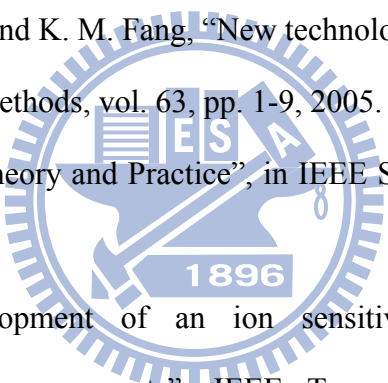
The presence of the commercial macro reference electrode is unwelcome in clinical and biological measurements. For miniaturization, many groups have been devoted to the development of miniature solid-state reference electrodes. However, these attempts do not seem to be successful with regard to the reproducibility and reliability in comparison with tradition reference electrodes having an internal solution, such as Ag/AgCl/aq.KCl and Hg/Hg<sub>2</sub>Cl<sub>2</sub>/aq.KCl. In this study, we will still focus on investigating the miniaturization of solid-state reference electrodes with no internal aqueous phase. By directly coating polymer-based materials such as PR and Nafion<sup>TM</sup> on the metal reference electrodes, new reference electrodes with no internal aqueous phase have been carried out. The protective membranes were deposited by using a drop-coating method.

According to our experimental results before, the unstable problem of the quasi-reference electrodes can be solved by co-fabricated REFET. The destination of fabricating a REFET is insensitive to the urea concentration. Based on the reference literatures, the sensing layer of a REFET is nothing more than the macromolecule, i.e. high polymer-based materials. In this thesis, a variety of polymer-based materials such as Nafion<sup>TM</sup>, photo resister (PR-FH6400) and polyimide were used as the sensing layers of REFETs. We find out that the urea sensitivity of the ZrO<sub>2</sub> pH-ISFET could be greatly decreased by these polymer-based materials, and it means that the surface potential is a constant value, i.e. the surface potential will be stable. In

differential measurement, the REFET can eliminate the unstable voltage from the quasi-reference electrode. The organization of the thesis is shown in Fig. 1-5.

In chapter 2, the basic theories of ISFET and ENFET are introduced. The entire fabrication process and measurement details will be described in chapter 3. After measuring the characteristics of the devices, we bring up some ideas about the experimental results and show the conclusions in chapter 4. At last, some works are presented in chapter 5 to investigate in the future.

## 1.10 References

- 
- [1] Y. Q. Miao, J. R. Chen and K. M. Fang, "New technology for the detection of pH", *J. Biochem. Biophys. Methods*, vol. 63, pp. 1-9, 2005.
- [2] P. Bergveld, "ISFET, Theory and Practice", in *IEEE Sensor Conference*, Toronto, Oct. 2003.
- [3] P. Bergveld, "Development of an ion sensitive solid-state device for neuro-physiological measurements", *IEEE Trans. Biomed. Eng. BME-17*, p.70-71, 1970.
- [4] Paul A. Hammond, Danish Ali, and David R. S. Cumming, "Design of a Single-Chip pH Sensor Using a Conventional 0.6-um CMOS Process.", *IEEE Sensors Journal*, vol. 4, no. 6, Dec, 2004.
- [5] Kow-Ming Chang, Kuo-Yi Chao, Ting-Wei Chou, and Chin-Tien Chang, "Characteristics of Zirconium Oxide Gate Ion-Sensitive Field-Effect Transistors", *Jpn. J. Appl. Phys.* 46, pp. 4333-4337, 2007.
- [6] Lin, Y-S., Puthenkovilakam, R., and Chang, J. P., "Dielectric property and thermal reproducibility of HfO<sub>2</sub> on silicon", *Applied Physics Letters*, 81(11), pp. 2041-2043, 2002.

- [7] A. Simonis, H. Luith, J. Wang, M.J. Schöning, New concepts of miniaturized reference electrodes in silicon technology for potentiometric sensor systems, *Sens. Actuators B* 103, pp. 429-435, 2004.
- [8] H. Suzuki, T. Hirakawa, S. Sasaki, I. Karube, "Micromachined liquidjunction Ag/AgCl reference electrode", *Sens. Actuators B* 46, pp. 146-154A, 1998.
- [9] Eine, et al., "Towards a Solid-State Reference Electrode," *Sensors and Actuators B*, 44, pp. 381-388, 1997.
- [10] R.L. Smith, D.C. Scott, "An integrated sensor for electrochemical measurements, *IEEE Trans. Biomed. Eng. BME* 33, pp. 83-90, 1986.
- [11] P. Bergveld, "Thirty years of ISFETOLOGY", *Sens. Actuators B* 88, pp. 1-20, 2003.
- [12] T. Matsuo, H. Nakajima, T. Osa, J. Anzai, "Parylene-gate ISFET and chemical modification of its surface with crown ether compounds, *Sens. Actuators* 9, pp. 115-123, 1986.
- [13] P. Bergveld, A. van den Berg, P.D. van der Wal, M. Skowronska-Ptasinska, E.J.R. Sudhóiter, D.N. Reinhoudt, "How electrical and chemical requirements for REFETs may coincide", *Sens. Actuators* 18, pp. 309-327, 1989.
- [14] Chao-Sung Lai, Cheng-En Lue, Chia-Ming Yang, Marek Dawgul and Dorota G. Pijanowska, "Optimization of a PVC Membrane for Reference Field Effect Transistors", *Sensors*, pp. 2076-2087, 2009.
- [15] P.A. Comte, J. Janata, "A field-effect transistor as a solid-state reference electrode", *Anal. Chim. Acta* 101, pp. 247-252, 1978.
- [16] T. Matsuo, H. Nakajima, "Characteristics of reference electrodes using a polymer gate ISFET", *Sens. Actuators* 5, pp. 293-305, 1984.
- [17] A. Errachid, J. Bausells, N. Jaffrezic-Renault, "A simple REFET for pH detection in differential mode", *Sens. Actuators B* 60, pp. 43-48, 1999.



- [18] Sergei V. Dzyadevych, Alexey P. Soldatkin, Anna V. El'skaya, Claude Martelet, Nicole Jaffrezic-Renault, “Enzyme biosensors based on ion-selective field-effect transistors”, *Analytica Chimica Acta* 568, pp. 248–258, 2006.



## Chapter 2

### Theory Description

#### 2.1 Definition of pH

The concept of pH was first introduced by Danish chemist S. P. L. Sørensen in 1909. Simply speaking, pH is a measurement of how acid or how basic a solution is. Solutions with pH more than 7 are considered basic, while those with pH less than 7 are considered acid. pH 7 is neutral because it is the pH of pure water at 25°C [1]. In formal, the definition of pH is expressed as

$$pH = -\log a_{H^+} = -\log \alpha [H^+] \quad (2-1)$$

where  $a_{H^+}$  is the hydrogen ion activity. The term  $\alpha$  is the activity coefficient which equals to 1 when diluted solution and  $[H^+]$  is the molar concentration of dissociated protons in units of moles per liter. From equation (2-1), we can know that pH reflects the amount of available hydrogen ions but not the concentration of hydrogen ions.

#### 2.2 Fundamental principles of ISFET

Since the Ion-selective field effect transistor (ISFET) was the first reported by P. Bergveld in 1970, research on new material of sensing film and fabrication process to improve the sensitivity and stability has been continuously proposed. At the same time, ISFET has developed into a new type of chemical sensing device. The structure of ISFET is similar to MOSFET (Metal Oxide Semiconductor Field Effect Transistor),

besides the metal gate electrode is replaced by a reference electrode and is inserted in an aqueous solution which is in contact with the sensing layer above the gate oxide. A schematic structures of MOSFET and ISFET are shown in Fig. 2-1. The following are the theoretical foundations which are mostly used to characterize the ISFET.

### 2.2.1 From MOSFET to ISFET

It is not difficult to find out the difference between ISFET and MOSFET. In general, the MOSFET is a Metal-Insulator-Semiconductor structure, and the ISFET is a Electrolyte-Insulator-Semiconductor structure. The difference in the ISFET is the replacement of the metal gate electrode of the MOSFET by the series combination of the reference electrode, electrolyte and chemically sensitive insulator or membrane. For this reason, the best way to comprehend the ISFET is to understand the operating principle of a MOSFET first.

The general expression for the drain current of the MOSFET and thus of the ISFET in the so-called ohmic or non-saturated region is

$$I_D = \frac{C_{ox}\mu W}{L} \left[ (V_{GS} - V_T) - \frac{1}{2}V_{DS} \right] V_{DS} \quad (2-2)$$

where  $C_{ox}$  is the gate insulator capacitance per unit area.  $L$  is the channel length and  $W$  is the channel width, respectively.  $\frac{W}{L}$  is the width-to-length ratio of the channel, and  $\mu$  is the electron mobility in the channel. We can see that if the fabrication process is controlled well and biased in well designed applied electronic circuits, the geometric parameter  $\beta = \mu C_{ox} \frac{W}{L}$ , as well as the drain-source voltage  $V_{DS}$ , and the threshold voltage  $V_T$  are constant, then the drain current  $I_D$  will be only the function of the gate to source voltage  $V_{GS}$  in MOSFET. Thus,  $V_{GS}$  is the only variable. In the ISFET, because the oxide/electrolyte interface will have a

chemical reaction and build up charges at the interface which produce an electrostatic potential distribution, then it will have a modification at  $V_T$ .

As well-known, the threshold voltage  $V_T$  of MOSFET is

$$V_T = \frac{\phi_M - \phi_{Si}}{q} - \frac{Q_{ox} + Q_{ss} + Q_B}{C_{ox}} + 2\phi_f \quad (2-3)$$

where the first term describes the difference in the workfunction between the gate metal ( $\phi_M$ ) and the silicon ( $\phi_{Si}$ ), the second term is due to the effect of accumulated charge in the oxide ( $Q_{ox}$ ), at the oxide-silicon interface ( $Q_{ss}$ ), and the depletion charge in the silicon ( $Q_B$ ), and the last term  $\phi_f$  is the potential difference between the Fermi levels of the doped and intrinsic silicon.

In the case of ISFET, when immersed in a liquid, two more differences have to be noted, the interfaces between the liquid and the gate oxide on the one side and between the liquid and the reference electrode at the other side. The interface potential at the gate oxide-electrolyte interface is determined by the surface dipole potential of the solution  $\chi_{sol}$ , which is a constant, and the surface potential  $\phi_o$  which results from a chemical reaction, usually governed by the dissociation of oxide surface group. And then the interface potential between the liquid and the reference electrode is the reference electrode potential relative to vacuum  $E_{ref}$ . Hence the expression of the ISFET threshold voltage becomes

$$V_T = E_{ref} - \phi_o + \chi_{sol} - \frac{\phi_{Si}}{q} - \frac{Q_{ox} + Q_{ss} + Q_B}{C_{ox}} + 2\phi_f \quad (2-4)$$

from the Equation (2-4), the work function of the metal gate  $\phi_M$  seems to be disappeared, but this is not true, because it is “buried” by definition in the term  $E_{ref}$  [2]. In addition, we can find that all terms are constant except  $\phi_o$ , and it dominates the sensitivity of ISFET to the electrolyte pH. The parameter  $\phi_o$  is a function of pH value with the specific solution and is determined by surface chemical

reaction at the sensing layer. According to the above-mentioned, we can know that the ISFET drain current  $I_D$  is a function of  $V_{GS}$  and  $V_T$ , i.e.  $I_D(V_{GS}, V_T)$ , and  $V_T$  is a function of surface potential  $\phi_o$ , i.e.  $V_T(\phi_o)$ , where  $\phi_o$  is a function of pH value with the specific solution. We can see these results obviously from Fig. 2-2. Therefore, detailed investigation of the electrode-electrolyte interface is necessary for designing a high pH sensitivity ISFET in order to obtain an accurate pH value.

In short, an ISFET is electronically identical to a MOSFET, and with one more feature: the possibility to chemically modify the threshold voltage via the interfacial potential at the oxide-electrolyte interface. So we will have a statement at the oxide/electrolyte interface in the next section, and that is the key point of ISFET.

### 2.2.2 The oxide-electrolyte interface

As mentioned in the preceding section, when we immerse the ISFET in the pH buffer solution, the oxide/electrolyte interface will build up charges and generate an electrostatic potential. The characteristics of the ISFET are completely controlled by the properties of the oxide-electrolyte interface, and protonation/deprotonation of the gate material is influenced by the pH solution, which controls the surface potential.

But what is the charging mechanism at the surface? The site-binding model introduced by Yate et al. is the most well-known method to describe the charging mechanism at the oxide/electrolyte interface as illustrated in Fig. 2-3 and Fig. 2-4. The surface of any metal oxide (the sensing layer) always contains hydroxyl groups, for example, in the case of silicon dioxide is SiOH groups. In this model, the oxide surface sites are assumed to be amphoteric, i.e. the amphoteric sites may donate or accept a proton from the solution, leaving a negatively charged or positively charged

surface group, respectively. The surface reactions are:



where  $A$  is the metal oxide component, such as Si, Al, Zr, Ta, and  $H_B$  represents the protons in the bulk of the solution. From these chemical reactions, it is obvious that an originally neutral surface hydroxyl site can be neutral, protonized or deprotonized depending on the pH value of the bulk solution. For this reason it is called an amphoteric site. We also have to know that there are a fixed number of surface sites per unit area,  $N_S$

$$N_S = \nu_{AOH} + \nu_{AOH_2^+} + \nu_{AO^-} \quad (2-7)$$

Based on some electrochemical knowledge and math derivation, we can get the surface charge density  $\sigma_o [C/m^2]$

$$\sigma_o = q(\nu_{AOH} - \nu_{AO^-}) = -qB \quad (2-8)$$

where  $B$  is the number of negatively charged groups minus the number of positively charged groups in mole per unit area. We can see that when the number of positively and negatively charged groups on the surface is equal and consequently there will be no net charge on the surface. Under this kind of situation, we say the pH value at the point of zero charge is  $pH_{pzc}$ . One more thing we have to know is that different operations of ISFETs (flat band condition and linear region) will yield different value of  $pH_{pzc}$  [3].

Then

$$\sigma_o = qN_S \left( \frac{a_{H_S^+}^2 - K_a K_b}{K_a K_b + K_b a_{H_S^+} + a_{H_S^+}^2} \right) \quad (2-9)$$

which  $K_a$  and  $K_b$  are intrinsic dissociation constants. A detailed derivation can see

the Ref. [4,5]. Equation (2-9) shows the relation between the activity of the protons at the oxide surface  $a_{H_s^+}$  and the surface charge density  $\sigma_o$  in terms of the total number of available sites  $N_s$  and the intrinsic dissociation constants  $K_a$  and  $K_b$ . After we get the surface charge density, we can find the intrinsic buffer capacity  $\beta_{int}$ , the capability of the surface to store charge as result of a small change in the  $H^+$  concentration, defined as

$$\frac{\partial \sigma_o}{\partial pH_s} = -q \frac{\partial B}{\partial pH_s} = -q \beta_{int} \quad (2-10)$$

From equation (2-9) and (2-10), we can get  $\beta_{int}$

$$\beta_{int} = N_s \frac{K_b a_{H_s^+}^2 + 4K_a K_b a_{H_s^+} + K_a K_b^2}{\left(K_a K_b + K_b a_{H_s^+} + a_{H_s^+}^2\right)^2} 2.3 a_{H_s^+} \quad (2-11)$$

It is called “intrinsic” buffer capacity, because it is only capable of buffering small changes in the surface pH ( $pH_s$ ) and not in the bulk pH ( $pH_b$ ). We can see that the value of  $N_s$ ,  $K_a$  and  $K_b$  are oxide dependent. More surface sites will lead to larger  $\beta_{int}$ . According to Ref. [4], Hydrolysis of the surface will create more surface sites and thus a rise in the intrinsic buffer capacity and the sensitivity.

Not only the surface reaction will affect the surface charge density, but also the background electrolyte will influence the surface charge density [4]. This dependence is ascribed to variations in the double layer capacitance. The surface charge  $\sigma_o$  is balanced by an equal but opposite charge in electrolyte,  $\sigma_{dl}$  as a result of charge neutrality. The two opposite charges,  $\sigma_o$  and  $\sigma_{dl}$ , is parallel to each other form the electrical double layer structure, and the integral electrical double-layer capacitance is named  $C_{dl,i}$ .

The relation between  $\sigma_o$ ,  $\sigma_{dl}$ ,  $C_{dl,i}$  and  $\phi_o$  is given by

$$\sigma_{dl} = -\sigma_o = -C_{dl,i} \phi_o \quad (2-12)$$

where the potential difference  $\varphi_o = \varphi_s - \varphi_B$ , the surface potential subtracts the bulk potential of the electrolyte.

But what is the detailed mechanism for the electrical double layer? The first double layer model is proposed by Helmholtz in 1879. He regards the double layer as a parallel plate capacitance structure as shown in Fig. 2-5. The plate distance “r” is taken as the ion radius and the double layer capacitance  $C_{dl} = \frac{Q}{V}$  will be a constant value, where Q is the surface charge and V is the potential difference of the double layer. But from the experiment, we can know the double layer capacitance is not a constant value, so the Helmholtz is not suitable to describe the exact double layer structure. Therefore the Helmholtz model is merely suitable for the high concentration electrolyte. Because the potential difference will be large in high concentration electrolyte, the double layer structure will be like the parallel plate capacitance.

Because the Helmholtz model only considers the electrostatic force, therefore it can not model the relation between the double layer capacitance and electrolyte concentration. In the beginning of 20th century, Gouy and Chapman proposed the idea of a diffuse layer to interpret the capacitive behavior of an electrode/electrolyte interface as shown in Fig. 2-6. This model made significant improvements by introducing a diffuse model of the electrical double layer, in which the potential at a surface decreases exponentially due to adsorbed counter-ions from the solution. They think that the ions in the solution are not only electrostatically attracted to the electrode surface but also the attraction is consumed by the random thermal motion which acts to equalize the concentration through the solution. The ions concentration in the electrolyte will obey the Boltzmann equation:

$$C_i(x) = C_i^o \exp\left(\frac{-z_i q \phi_x}{kT}\right) \quad (2-13)$$

where  $\phi_x$  is the potential at any distance x with respect to the bulk of the solution,



$C_i(x)$  and  $C_i^o$  are the molar concentration of species  $i$  at a distance  $x$  and in the bulk of the solution, respectively.  $Z_i$  is the magnitude of the charge on the ions. The relation between ionic activity ( $a_i$ ) and ions concentration ( $c_i$ ) is  $a_i = f_i \times c_i$ , where  $f_i$  is activity coefficient. In diluted electrolyte  $f_i$  will be approached unity. However, the Gouy-Chapman model has one major drawback. The ions are considered as point charge that can approach the surface arbitrarily close in this model. This will cause unrealistic high concentrations of ions near the surface at high values of  $\phi_o$  [4]. Hence, the Gouy-Chapman model is only suitable for low concentration electrolyte. This implies that the electrical double layer structure have to combine the Helmholtz and Gouy-Chapman model in certain way.

In 1924, Stern combined these two double layer models, named Gouy-Chapman-Stern model. The Gouy-Chapman-Stern model, which combines the Helmholtz single adsorbed layer with the Gouy-Chapman diffuse layer, is most widely used to describe the electrical double layer structure in ISFET literature. The model describes that some of the ions in the electrolyte are next to the electrode surface and because of the finite ions size, the ions couldn't approach the surface arbitrarily close. The other ions are distributed in the electrolyte according to the Boltzmann equation and form a charge diffuse layer in the electrolyte. There is a distance,  $x_H$ , which is the closest plane for the centers of the ions. Hence, the diffuse layer is starting from  $x_H$ , and will possess the same amount of charge  $\sigma_{dl}$  (of opposite sign) as oxide surface charge  $\sigma_o$ , because the Helmholtz layer is not containing any charge, as shown in Fig. 2-7 and Fig. 2-8. In Gouy-Chapman-Stern model, the double layer capacitance consists of a series network of a Helmholtz layer capacitance (Stern capacitance) and a diffuse layer capacitance. The difference between  $\phi_o$  and  $\phi_1$  is the potential difference across the Stern capacitance and the

Stern capacitance has a value of  $\frac{\epsilon_r \epsilon_o}{x_H} [F/m^2]$ . By the Gouy-Chapman-Stern model, we can get the critical parameter : differential double layer capacitance  $C_{dif}$ , the ability of the double layer to store charge in response to a small change in the potential, defined as

$$C_{dif} = \frac{\partial \sigma_o}{\partial \phi_o} = - \frac{\partial \sigma_{dl}}{\partial \phi_o} \quad (2-14)$$

According to Ref. [3], for reasons of simplicity, not the expression for  $C_{dif}$  is stated here, but of its inverse. The derived inverse  $C_{dif}$  is made up of two components in series:

$$\frac{1}{C_{dif}} = \frac{\partial \phi_o}{\partial \sigma_o} = \frac{1}{C_{stern}} + \frac{1}{\sqrt{\frac{2\epsilon_r \epsilon_o z^2 q^2 n_o}{kT} \cosh\left(\frac{zq\phi_1}{2kT}\right)}} \quad (2-15)$$

where  $\phi_1$  is the potential at  $x_H$ , and  $n_o$  is the concentration of each ion in the bulk solution in number/liter, and  $z$  is the valence of the ions. The parameters  $\epsilon_r$ ,  $\epsilon_o$ ,  $k$ ,  $q$ , and  $T$  have their usual meaning.

### 2.2.3 Theory for the pH sensitivity of ISFET

From above discussions, the sensitivity of the pH ISFET is related to the intrinsic buffer capacity  $\beta_{int}$  and the differential capacitance  $C_{dif}$ . By site-binding model and Gouy-Chapman-Stern model, we can get the values of  $\beta_{int}$  and  $C_{dif}$ , respectively. The pH sensitivity is the change of the insulator-electrolyte potential,  $\phi_o$ , on the change of the bulk pH,  $\frac{\partial \phi_o}{\partial pH_B}$ . This expression is derived from a separate treatment of both sides of the double layer, i.e., the gate insulator and the electrolyte [8]. Combining equation (2-10) and equation (2-14), we can get the effect of a small

change in the surface pH ( $pH_S$ ) on the change in the surface potential  $\varphi_o$ ,

$$\frac{\partial \varphi_o}{\partial pH_S} = \frac{\partial \varphi_o}{\partial \sigma_o} \cdot \frac{\partial \sigma_o}{\partial pH_S} = -\frac{q\beta_{\text{int}}}{C_{\text{dif}}} \quad (2-16)$$

Combining equation (2-16) with the Boltzmann equation, the activity of the bulk protons  $a_{H_B^+}$  can be related to the activity of the protons in the direct vicinity of the oxide surface  $a_{H_S^+}$ , that is

$$a_{H_S^+} = a_{H_B^+} \cdot \exp\left(\frac{-q\varphi_o}{kT}\right) \quad (2-17)$$

or in the form of pH

$$pH_S - pH_B = \frac{q\varphi_o}{2.3kT} \quad (2-18)$$

then equation (2-16) can be written in the form

$$\frac{\partial \varphi_o}{\partial \left( pH_B + \frac{q\varphi_o}{2.3kT} \right)} = -\frac{q\beta_{\text{int}}}{C_{\text{dif}}} \quad (2-19)$$

rearrangement of equation (2-19), we can get a general expression for the sensitivity of the electrostatic potential to changes in the bulk pH,

$$\frac{\partial \varphi_o}{\partial pH_B} = -2.3 \frac{kT}{q} \alpha \quad (2-20)$$

with

$$\alpha = \frac{1}{\frac{2.3kTC_{\text{dif}}}{q^2\beta_{\text{int}}} + 1}, \quad 0 < \alpha < 1 \quad (2-21)$$

the parameter  $\alpha$  is a dimensionless sensitivity parameter that varies between 0 and 1 depending on  $\beta_{\text{int}}$  and  $C_{\text{dif}}$ . When  $\beta_{\text{int}}$  is high and  $C_{\text{dif}}$  is small enough,  $\alpha$  will approaches 1. If  $\alpha = 1$ , the ISFET has a so-called Nernstain sensitivity of precisely -59.2 mV/pH at 298K, which is also the maximum achievable sensitivity.

It appears that the usual SiO<sub>2</sub> from the MOSFET process does not fulfill the requirements of a high value  $\beta_{\text{int}}$ . The pH sensitivity of SiO<sub>2</sub> sensing film ISFET is

only about 30mV/pH. In order to find high sensitivity sensing film, many sensing layers have been investigated such as  $\text{Si}_3\text{N}_4$  [9,10],  $\text{Al}_2\text{O}_3$  [9,11],  $\text{Ta}_2\text{O}_5$ [9,12],  $\text{HfO}_2$  [12],  $\text{SnO}_2$  [13].

The ISFET has many advantages over the conventional glass electrode such as small size, strong robustness, high input impedance, low output impedance, and rapid response [6,9]. It seems to attractive for biomedical applications.

## **2.3 Basic principles of ENFET**

The enzyme field-effect transistor (ENFET) is a bioelectronic device which belongs to a class of chemical potentiometric sensors that take advantage of the high selectivity and sensitivity of biologically active materials. In this device, the enzyme is immobilized on the insulator if the ISFET. In literature, a dual-gate is often proposed, where one of the FETs can act as a reference system and is assembled in the same way as the sample FET , but it contains a blank enzyme-free gel membrane. This arrangement allows some automatic compensation of fluctuations in solution pH and temperature [14].

The enzyme-substrate system controls the specificity of the ENFET operation, and the reaction kinetics that take place in the biologically active materials (enzyme) determine how fast the substrate is converted into the product. To get an understanding of the ENFET operation, the reaction kinetics of the biological-recognition processes must be considered, together with the mass transport theory (Fig. 2-9) [14].

### **2.3.1 The definition of system configuration**

Consider the system consisting of a sensor surface, lying at  $x = 0$ , coated with an immobilized enzyme layer of thickness  $L$ . Beyond this lies the transport boundary layer. Beyond the transport boundary layer, the concentration of analyte, the enzyme's substrate  $S$ , has a defined value  $[S]$  and that of the product  $[P]$  is taken to be zero (see Fig. 2-10). Notice that these bulk concentrations of substrate and product represent two basic boundary conditions of the system. Enzyme-catalyzed reaction takes place in the immobilized enzyme layer. This reaction depletes the substrate and generates the product in the enzyme layer, causing the concentration gradients which drive the mass transport process. The product is measured potentiometrically, without being consumed, at the sensor surface. A steady state is reached when the rate of reaction in the immobilized enzyme layer is balanced by mass transport of reactant and product to and from it [14].

### 2.3.2 Enzyme-catalyzed reaction of substrate

Let us consider a single enzyme acting on a substrate molecule, where any other reactants are assumed to be in excess so as not to limit the reaction. The reaction then follows the Michaelis-Menten kinetics



where  $E$  is the enzyme,  $S$  is the substrate,  $ES$  is the bound intermediate enzyme-substrate complex,  $P$  is the product and  $k_1, k_{-1}, k_2$  are the reaction-rate constants for the enzyme-substrate binding reaction, the unbinding of the enzyme-substrate complex, and the formation of the product, respectively.

The rate of product formation is given by

$$v_f = \frac{\partial [P]}{\partial t} = k_2 [ES] \quad (2-23)$$

where the rate  $v_f$  has units of mol/l-s and  $t$  is the time. To relate the rate of product formation with the substrate concentration, it is assumed that the reaction is in steady state; that is, by assuming that the rates of formation and breakdown of the complex are equal. This assumption leads us to write the rate equation for the intermediate complex as

$$\frac{\partial[ES]}{\partial t} = k_1[E][S] - k_{-1}[ES] - k_2[ES] = 0 \quad (2-24)$$

Since the total concentration of enzyme  $[E]_0$  present at all times will be the sum of concentrations in free and complexed forms  $[E] + [ES]$ , we substitute  $[E] = [E]_0 - [ES]$  into equation (2-24), solve it for  $[ES]$ , and substitute into Eq. (2-23), obtaining

$$v_f = \frac{k_2[ES]_0[S]}{([S] + K_M)} = k_2[ES] \quad (2-25)$$

where we have introduced the Michaelis constant defined as

$$K_M \equiv \frac{(k_{-1} + k_2)}{k_1} \quad (2-26)$$

$K_M$  is not a true equilibrium constant but is the ratio of rate constants for complex formation and disappearance, the latter comprising both simple dissociation back to reactants plus decomposition into products.

Few enzymes follow the Michaelis-Menten kinetics over a wide range of experimental conditions. Most enzyme-substrate interactions have more complex kinetics. However,  $K_M$  is still a useful measure of the enzyme-substrate interaction.

When the enzyme is brought in contact with a substrate, a complex concentration profile develops, which is a function of both diffusion and reaction processes. In the reaction region of the enzyme, the product concentration is achieved by mass transfer given by Fick's second law as well as by enzyme kinetics [14].

### 2.3.3 Enzyme-modified ISFET

For a gel membrane-immobilized system, the coupled mass transport and kinetic reaction for the depletion of substrate across the gel layer must be considered.

The enzyme reaction rate follows the Michaelis-Menten kinetics, Eq. (2-22), and the concentration of the substrate and the product in the enzyme membrane are described by the diffusion-reaction equation, which is just Fick's second law with a term added to account for the consumption or production of a species, i.e.,

$$\frac{\partial C}{\partial t} = D \frac{\partial^2 C}{\partial x^2} \pm R(C) \quad (2-26)$$

where  $D$  is the diffusion coefficient of the species,  $R(C)$  is the reaction term, and the sign depends on whether species is produced (product) or consumed (substrate). Considering the steady-state response, the time derivative will be set to zero. Using the Michaelis-Menten kinetics, Eq. (2-25), as the reaction term, Eq. (2-26) becomes, for the *substrate*,

$$D_s \frac{\partial^2 [S]}{\partial x^2} - \frac{k_2 [E]_0 [S]}{K_M + [S]} = 0 \quad (2-27)$$

and for the *product*,

$$D_p \frac{\partial^2 [P]}{\partial x^2} + \frac{k_2 [E]_0 [S]}{K_M + [S]} = 0 \quad (2-28)$$

where  $D_s$  and  $D_p$  are the diffusion coefficients of the substrate in the gel layer and of the product, respectively.

Analytical solutions to Eqs. (2-27) and (2-28) can be found when we consider the two limiting cases,  $[S] \ll K_M$  and  $[S] \gg K_M$ . The first case represents enzyme kinetics that are much faster than the transport through the membrane, the substrate

concentration being the limiting factor. The second case accounts for very high substrate concentration that saturates the enzyme.

$[S] \ll K_M$ , Eq. (2-27) becomes

$$\frac{\partial^2 [S]}{\partial x^2} - \alpha [S] = 0 \quad (2-29)$$

where

$$\alpha = \frac{k_2 [E]_0}{K_M D_S} \quad (2-30)$$

is the enzyme loading factor or diffusion modulus, which represents the effective concentration of the enzyme, including the concentration of enzyme in the membrane, the kinetics of the enzyme reaction, and the mass transport of the substrate molecules through the membrane. The boundary conditions to solve Eq. (2-29) are

$$\left. \frac{\partial [S]}{\partial x} \right|_{x=0} = 0 \quad (2-31a)$$

$$[S] \Big|_{x=L} = [S]_L \quad (2-31b)$$

where  $[S]_L$  is the substrate concentration at the outer surface of the immobilized enzyme layer at  $x = L$ . The solution for the substrate concentration is

$$[S] = \left( \frac{\cosh(x\sqrt{\alpha})}{\cosh(L\sqrt{\alpha})} \right) [S]_L \quad (2-32)$$

where  $x$  defines the distance across the gel-membrane layer, which extends from the interface between the gel and the transducer's surface at  $x = 0$ , to the gel-solution interface at  $x = L$ . To find a relationship of product concentration from the substrate concentration, we add Eqs. (2-27) and (2-28), i.e.,

$$D_S \frac{\partial^2 [S]}{\partial x^2} + D_P \frac{\partial^2 [P]}{\partial x^2} = 0 \quad (2-33)$$

In this way the kinetic term due to the enzyme catalyzed reaction disappeared. Eq. (2-33) can be integrated once to give



$$D_s \frac{\partial [S]}{\partial x} + D_p \frac{\partial [P]}{\partial x} = \text{const.} \quad (2-34)$$

Eq. (2-34) represents the diffusion fluxes in the enzyme layer. At the membrane's outer surface ( $x = L$ ), the product and substrate fluxes must balance in the steady state, since no material is being created or destroyed. Thus, the value of the constant must be zero throughout the membrane. Integrating Eq. (2-34) between  $x = 0$  and  $x = L$ ,

$$D_s [S]_L + D_p [P]_L = D_s [S] + D_p [P] = \text{const.} \quad (2-35)$$

Combining Eq. (2-35) and (2-32), then

$$[P] = \frac{D_s}{D_p} \left[ 1 - \frac{\cosh(x\sqrt{\alpha})}{\cosh(L\sqrt{\alpha})} \right] [S]_L + [P]_L \quad (2-36)$$

Setting  $x = 0$  in Eq. (2-36) gives the surface concentration of product, which is proportional to the transducer's output signal in an ENFET, then

$$[P]|_{x=0} = \frac{D_s}{D_p} \left[ 1 - \frac{1}{\cosh(L\sqrt{\alpha})} \right] [S]_L + [P]_L \quad (2-37)$$

Eq. (2-37) indicates that, for  $[S] \ll K_M$ , the surface concentration is directly proportional to the substrate concentration at the enzyme layer outer surface.

If  $[S] \gg K_M$ , Eqs. (2-27) and (2-28) become

$$D_s \frac{\partial^2 [S]}{\partial x^2} - k_2 [E]_0 = 0 \quad (2-38)$$

$$D_p \frac{\partial^2 [P]}{\partial x^2} + k_2 [E]_0 = 0 \quad (2-39)$$

Eqs. (2-38) and (2-39) can be integrated, and both are subject to the boundary conditions of Eqs. (2-31), then

$$[S] = [S]_L + \frac{k_2 [E]_0}{2D_s} (x^2 - L^2) \quad (2-40)$$

and

$$[P] = [P]_L + \frac{k_2 [E]_0}{2D_p} (L^2 - x^2) \quad (2-41)$$

From Eq. (2-41), we can notice that the product concentration at the surface ( $x=0$ ) of the transducer is a constant that depends on the immobilized enzyme concentration, the reaction kinetics, the diffusion mass transport, and it is independent of substrate concentration. Therefore the output of the biosensor is constant. In this case the substrate concentration is so large that it has saturated the enzyme. Then there is no sufficient amount of enzyme in the membrane to detect changes in such a large substrate concentration [14].

The above analysis shows that, for a given amount of enzyme in the membrane, the response of the sensor will go from an approximately linear dependence on the analyte concentration to a saturation value for an increase of the analyte concentration.

We now consider the response of an ISFET, modified by an immobilized enzyme layer  $E$  that catalyzes the reaction of the substrate  $S$ , leading to formation of the acid  $HA/(H^+ + A^-)$ , according to the reaction



In the steady state, a balance between the rates of mass transport of the substrate from bulk solution to the enzyme layer, production of the acid by the enzyme layer and transport of the product acid into the bulk solution will be achieved, leading to a stable local pH change in the region of the immobilized enzyme layer.

The mass transport of product acid from the surface of the immobilized enzyme layer into bulk solution is a complex problem because of proton association and dissociation reactions in solution. First, the proton dissociation and association reactions of the acid itself must be taken into account, i.e.,



Second, the reaction of any buffer system,  $B^-/BH$ , must be considered, i.e.,



Complete analytical solution of the set of differential equations describing mass transport coupled with the kinetics of acid protonation and deprotonation reactions is not possible, either in the presence or absence of buffer [14].

## 2.4 Summary

In this chapter, we have introduced the basic concepts and theories of ISFET and ENFET. The ISFET operational mechanism is similar to the MOSFET. In a constant drain to source voltage  $V_{DS}$ , the drain current will only controlled by  $V_G$ . Furthermore, in ISFET, the drain current will also controlled by different pH values. Because there will be a chemical reaction at the oxide/electrolyte interface, and build up charges and potential to change the drain current  $I_D$ . We introduce the charging mechanism at the surface layer by site-binding model introduced by Yate et al.. We also describe the background electrolyte will also influence the surface charge density, and use the Gouy-Chapman-Stern model to describe this mechanism. By these two models, we can get the critical parameters  $\beta_{int}$ ,  $C_{dif}$  and derive the expression equation of sensitivity  $\frac{\partial \psi_o}{\partial pH_B} = -2.3 \frac{kT}{q} \alpha$ .

## 2.5 References

[1] Y. Q. Miao, J. R. Chen and K. M. Fang, "New technology for the detection of pH",

- J. Biochem. Biophys. Methods, vol. 63, pp. 1-9, 2005.
- [2] P. Bergveld, "Thirty years of ISFETOLOGY What happened in the past 30 years and what happen in the next 30 years", Sensors and Actuators B, vol. 88, pp. 1-20, 2003.
- [3] H.K. Liao, et al. , "Study on  $pH_{pzc}$  and surface potential of tin oxide gate ISFET", Materials Chemistry and Physics, vol. 59, pp. 6-11, 1999.
- [4] P. Bergveld, "ISFET, Theory and Practice", in IEEE Sensor Conference, Toronto, Oct. 2003.
- [5] R.E.G. van Hal et al. , "A general model to describe the electrostatic potential at electrolyte oxide interface", Advance in Colloid and Interface Science, vol.69, pp.31-62, 1996.
- [6] Miao Yuqing , Guan Jianguo, Chen Jianrong, "Ion sensitive field transducer-based biosensors", Biotechnology Advances, vol. 21, pp. 527-534, 2003.
- [7] W. M. Siu, R. S. C. Cobbold, "Basic Properties of the Electrolyte-SiO<sub>2</sub>-Si System: Physical and Theoretical Aspects", IEEE Transactions on Electron Device, vol. ED-26, NO. 11, Nov., 1979.
- [8] R.E.G. van Hal, J.C.T. Eijkel, P. Bergveld, "A novel description of ISFET sensitivity with the buffer capacity and double layer capacitance as key parameters", Sensors and Actuators B, vol. 24, pp. 201-205, 1995.
- [9] Tadayuki Matsuo, Masayoshi Esashi, "Methods of ISFET Fabrication", Sensors and Actuators, vol. 1, pp. 77-96, 1981.
- [10] Imants R. Lauks, Jay N. Zemel, "The Si<sub>3</sub>N<sub>4</sub>/Si Ion-Sensitive Semiconductor Electrode ", IEEE Transactions on Electron Devices, vol. ED-26, no.12, pp. 1959- 1964, Dec., 1979.
- [11] J.C. Chou, C.Y. Weng, "Sensitivity and hysteresis effect in Al<sub>2</sub>O<sub>3</sub> gate pH-ISFET ", Materials Chemistry and Physics, vol. 71, pp. 120-124, 2001.

- [12] P.D. van der Wal et al. , "High-K Dielectrics for Use as ISFET Gate Oxide", in Sensors, Proceedings of IEEE, 2004.
- [13] H.K.Liao et al. , " Study of amorphous tin oxide thin films for ISFET applications", Sensors and Actuators B, vol.50, pp. 104-109, 1998.
- [14] Massimo Grattarola, Giuseppe Massobrio, "BIOELECTRONICS HANDBOOK : MOSFETs, Biosensors, and Neurons", McGRAW-HILL, pp. 294-299, 1998.



## Chapter 3

### Experiment and Measurement

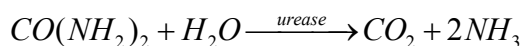
#### 3.1 Introduction

To investigate the properties of the PR-mix-Nafion<sup>TM</sup> as well as Polyimide-mix-Nafion<sup>TM</sup> as REFET sensing layer and PR-mix-Nafion<sup>TM</sup> as protective membrane above solid-state reference electrode which are both with urease-mix-Nafion<sup>TM</sup> membrane-based urea-ENFET, the miniaturized reference electrodes for urea-ENFET and REFET are fabricated in this chapter. The organization of the chapter 3 is as follows. We first will introduce the characteristics of urease, Polyimide, Nafion<sup>TM</sup> and PR materials. The fabrication process flow of urea-ENFET and REFET will be described in section 3. The section 4 contains illustration of key steps in this experimental process. Section 5 is the measurement system setup which is used for investigating the characteristics of different ratio of urease-mix-Nafion<sup>TM</sup> urea-ENFET and of different polymer-based structural REFET as well as PR-mix-Nafion<sup>TM</sup> membrane-based solid-state reference electrode.

#### 3.2 The characteristics of the Urease, Polyimide, Nafion<sup>TM</sup> and PR

##### 3.2.1 Urease

Urease (EC 3.5.1.5) is an enzyme that catalyzes the hydrolysis of urea into carbon dioxide and ammonia. The reaction occurs as follows:



In 1926 James Sumner showed that urease is a protein. Urease is found in bacteria, yeast and several higher plants. The multi-subunit enzyme usually has a 3:3 (alpha:beta) stoichiometry with a 2-fold symmetric structure (note that the image above gives the structure of the asymmetric unit, one third of the true biological assembly). An exceptional urease is found in *Helicobacter pylori*, which combines four of the regular six subunit enzymes in an overall tetrahedral assembly of 24 subunits ( $\alpha_{12}\beta_{12}$ ). Fig. 3-1 shows its chemical structure. This supra-molecular assembly is thought to confer additional stability for the enzyme in this organism, which functions to produce ammonia in order to neutralise gastric acid. The presence of urease is used in the diagnosis of *Helicobacter* species [1].

Urease conductometric biosensors for detection of heavy metal ions consisting of interdigitated gold electrodes and enzyme membranes formed on their sensitive parts have been used for a quantitative estimation of general water pollution with heavy-metal ions. The measurements of the urease residual activity have been carried out in Tris-HNO<sub>3</sub> buffer after preincubation in model metal-salt solution. The detection limits, depending on preincubation time and dynamic ranges, have been determined in model solutions of heavy-metal ions [1].

### 3.2.2 Polyimide

Polyimide (PI) is widely used in electronics and aerospace because of their excellent thermal, electrical, chemical, and mechanical properties. It consists of an organic dianhydride and a diamine [2]. These two components react to a polyadduct with high viscosity and high density. In this study, we employ polyimide as sensing

membrane above sensing layer ( $ZrO_2$ ) of REFET because it exhibits several advantages, such as thermal reproducibility, good chemical resistance, high viscosity, excellent mechanical properties, and characteristic orange/yellow color. Therefore we use polyimide membrane to gate lower sensitivity to different concentration of urea tested solutions from chemical reaction of REFET.

### 3.2.3 Nafion

According to the lectures, Nafion<sup>TM</sup> is a perfluorinated polymer that contains small proportions of sulfonic or carboxy ionic functional groups and with these functional groups, Nafion has the features of unique equilibrium ionic selectivity and the ionic transport. Fig. 3-2 shows its chemical structure and model, and we can see that Nafion<sup>TM</sup> can be divided into three parts: (A) a hydrophobic fluorocarbon backbone C-F (B) an interfacial region of relatively large fractional void volume (C) the clustered regions where the majority of the ionic exchange sites, counter ions, and absorbed water exists [3-6]. Because of the high concentration  $SO_3^-$  ion clusters, Nafion<sup>TM</sup> exhibits a high conductivity to cations, i.e. high cation exchange. Furthermore, Nafion<sup>TM</sup> is modified from Teflon, so Nafion<sup>TM</sup> is extremely resistant to chemical attack and high working temperature. According to the above introduction, we mix Nafion<sup>TM</sup> with urease, PR, and polyimide onto  $ZrO_2$  or Pd to be the protective membrane and to improve the adhesion of them with  $ZrO_2$  or metal reference electrode. Generally speaking, we call those an entrapment method.

### 3.2.4 PR

Positive photo resistor (FH6400) is also a test polymer material in our



experiment. FH6400 is composed of three parts: (1) resin (2) sensitizer, DNQ (3) solvent. Among them, resin is a polymer with heat-resistant property and is widely used as the etching protective film.

### 3.3 Fabrication process flow of co-fabricated ENFET and REFET

All procedures of experiment were accomplished in NDL (National Nano Device Laboratory) and NFC (Nano Facility Center). In this study, the ENFET and REFET devices were made on a p-type Si (100) wafer. The fabrication procedures are listed as follows and the process is illustrated in Fig. 3-3:

(a)

1. RCA clean
2. Wet oxidation of silicon dioxide ( $6000 \text{ \AA}$ ,  $1050^\circ\text{C}$ , 65mins)

(b)

3. Defining Source/Drain region (Mask#1)
4. BOE wet etching of silicon dioxide
5. Dry oxidation of silicon dioxide as screen oxide ( $300 \text{ \AA}$ ,  $1000^\circ\text{C}$ , 20mins)
6. Source/Drain implantation (Dose= $5\text{E}15(1/\text{cm}^2)$ , Energy= $25\text{KeV}$ )
7. Source/Drain annealing ( $950^\circ\text{C}$ , 60mins)

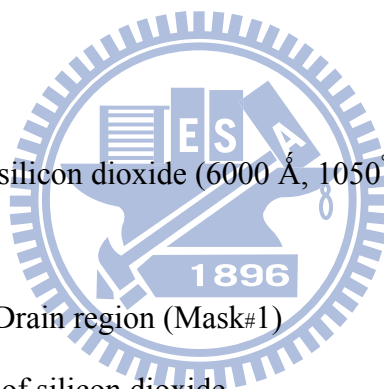
(c)

8. PECVD oxide deposition ( $1 \mu\text{m}$ )

(d)

9. Defining contact hole and gate region (Mask#2)
10. BOE wet etching of silicon dioxide
11. Dry oxidation of gate oxide ( $100 \text{ \AA}$ ,  $850^\circ\text{C}$ , 60mins)

(e)



12. Defining of Sensing layer (Mask#3) and sensing layer ( $ZrO_2$ ) deposition by Sputtering (300 Å).

13.  $ZrO_2$  sintering (600°C, 30mins)

(f)

14. Define the contact and solid state reference electrode region (Mask#4)

15. Ti/Pd deposition (200 Å /350 Å) by sputtering or Al evaporation (5000 Å)

(g)

16. Backside Al evaporation (5000 Å)

17. Pd and Al sintering 400°C, 30mins

(h)

18. The urease (EC 3.5.1.5, 5 U/mg)-mix-Nafion<sup>TM</sup> membrane-based material was coated onto gate region ( $ZrO_2$ ) of ENFET

19. The PR-mix-Nafion<sup>TM</sup> membrane-based material was coated onto metal electrode surface for solid-state reference electrode

20. The PR-mix-Nafion<sup>TM</sup> or Polyimide-mix-Nafion<sup>TM</sup> membrane-based material was coated onto gate region ( $ZrO_2$ ) as REFET's sensing layer

### 3.4 Key steps illustration

#### 3.4.1 Gate region formation

In step 1, RCA clean is a standard process of wafer cleaning steps which needs to be performed before high temperature processing steps (oxidation, diffusion, CVD) of silicon wafers in semiconductor manufacturing. The purpose of the RCA clean is to reduce the possible pollution (such as dust particles, grease, organics, diffusion ions, and native oxide) from the wafer surface. Careful RCA clean will ensure the integrity

of device electricity. In step 2, 6000 Å thickness wet oxide is deposited as barrier layer for S/D implantation. The energy and the density of S/D implantation parameters are 25 (KeV) and  $5E15$  ( $1/cm^2$ ) with phosphorous dopant, respectively. After S/D implanting, we have to activate the dopant by following a 950°C, 60 mins  $N^+$  annealing. Then, we must deposit 1 μm thickness oxide by PECVD. In standard MOSFET process, we don't need to deposit it. However, it is necessary to perform for protecting the pH-ISFET device. During a long period of electrolyte immersing, ions may diffuse and affect the electrical characterization of ISFET, so a thicker oxide can eliminate the effect. It is a significant difference compared with standard MOSFET processes. After oxide depositing by PECVD, we grow dry oxide with thickness 100 Å as gate oxide.

### 3.4.2 Sensing layer deposition



In step 12, we deposit  $ZrO_2$  sensing layer by sputtering. Various sensing material with different deposition techniques decides the characteristics of response time and sensitivity. It has been proved the  $ZrO_2$  film deposited by sputtering has good characteristics as a pH-ISFET sensing layer. Therefore, in this study, we still use  $ZrO_2$  as the sensing layer and research the suitable solid-state reference electrode as well as REFET for it. Table 3-1 is the sputtering parameters. On the other hand, seeking for the proper ratio of urease to Nafion<sup>TM</sup> membrane onto  $ZrO_2$  of ENFET is one of main purposes for us. Under general situation, we call this procedure immobilization of the enzyme. Following is our process flow:

1. Dropping the mix composition of urease (EC 3.5.1.5 from Jack beans, 5 U/mg, lyophilized, Merck corp.) and Nafion<sup>TM</sup> (5 wt.%) both in 5mM phosphate buffer solution (PBS) with the ratio 1:1, 5:1, and 20:1 (Nafion<sup>TM</sup> not in PBS)

onto the sensing layer ( $ZrO_2$ ) of ENFET at room temperature. (10 mg urease/100  $\mu l$  5mM PBS; 100  $\mu l$  Nafion<sup>TM</sup>/100  $\mu l$  5mM PBS)

2. Dried under a 4°C environment as well as a dust-free ambient air condition for 12 hours, and the solution became colloid.

### 3.4.3 PR-mix-Nafion<sup>TM</sup> membrane-based reference electrodes

In step 15, we have to deposit titanium (Ti) as the adhesion layer before depositing Pd because the adhesion between Pd/SiO<sub>2</sub> is very poor. The Ti layer can improve the surface adhesion and Pd layer can protect the titanium from oxidation and corrosion. In step 19, this procedure is the most important part in our experiment. PR-mix-Nafion<sup>TM</sup> membrane-based reference electrodes have been fabricated by combining silicon fabrication and drop-coating method. To investigate the PR-mix-Nafion<sup>TM</sup> membrane-based material on the improvement of reference electrode performance, two types of reference electrodes (Ti/Pd and polymer-based Ti/Pd) were prepared. Then the mix composition of PR (FH6400) and Nafion<sup>TM</sup> was coated onto an exposed area of metal electrode to produce a solid-state reference electrode as one of the two types of reference electrodes. The test structures are listed in Table 3-2. Following is our process flow:

1. Dropping the mix composition of PR (FH6400) and Nafion<sup>TM</sup> (5 wt.%) solution with the ratio 1:1 onto the metal electrode at room temperature.
2. Dried under a dust-free ambient air condition for 12 hours, and the solution became colloid.

### 3.4.4 PR-mix-Nafion<sup>TM</sup> and Polyimide-mix-Nafion<sup>TM</sup> membrane-based sensing layer

In step 20, this procedure is also important in our experiment. We coated the mix composition of Nafion<sup>TM</sup> and PR as well as the mix composition of Nafion<sup>TM</sup> and Polyimide with different ratios as the REFET sensing layer. The test structures are listed in Table 3-2. Following is our process flow:

1. Dropping the mix composition of PR (FH6400) and Nafion<sup>TM</sup> (5 wt.%) solution with the ratio 1:1 or the mix composition of Polyimide and Nafion<sup>TM</sup> (5 wt.%) with the ratios 3:1 and 1:0 onto the sensing layer (ZrO<sub>2</sub>) at room temperature.
2. Dried under a dust-free ambient air condition for 12 hours, and the solution became colloid.

### 3.5 Packing and measurement system



Before executing measurement, a container is bonded to the gate region of ENFET and REFET using epoxy resin. Entire sensing region and solid-state reference electrode must be included in the opening under the container. In order to investigate the characteristics of different ratio of urease and Nafion<sup>TM</sup> as ENFET gate structure and of different polymer-based sensing layer as REFET sensing layer in addition to PR-mix-Nafion<sup>TM</sup> membraned-based reference electrodes, we measure the  $I_{DS}$ - $V_{GS}$  curves for the urea-ENFET and REFET by using HP4156A as measurement tool and the measurement setup is shown in Fig. 3-4. In the setup of HP-4156A, substrate voltage is grounded to avoid the body effect and the reference electrode sweeps to different voltage.

For getting accurate result of measurement, all measuring conditions of the experiments were carried out at a constant temperature of 25°C using a temperature

control system, and the entire measurement procedures were executed in a dark box because light will produce serious influence on the urea-ENFET or REFET [8]. The measured urea concentrations are 1.25 mg/dl, 10 mg/dl, 40 mg/dl, 80 mg/dl, 120 mg/dl, 240 mg/dl, and the urea reagent [ $CO(NH_2)_2$ , Merck corp.] was supplied by Merck corp. Preparation of phosphate powder [phosphate ( $KH_2PO_4$ ), Merck corp.] is needed mixing for the urea-buffer testing solutions. All reagents are analytical grade and phosphate buffer solution (PBS) is prepared in DI water with 10mM (pH = 6). The quantity takes 240 grams urea to join in 100 milliliter phosphate buffer solutions to treat as 240 mg/dl the urea-buffer testing solution. Then, we can use the similar method to mix 120 mg/dl again, 80 mg/dl, 40 mg/dl, 10 mg/dl and 1.25 mg/dl and so on different concentrations urea-buffer testing solutions. All sample solutions were vigorously stirred. In addition, we must put in before the measurement the urea-buffer testing solutions in 4°C environment to preserve for guaranteeing the experimental accuracy.



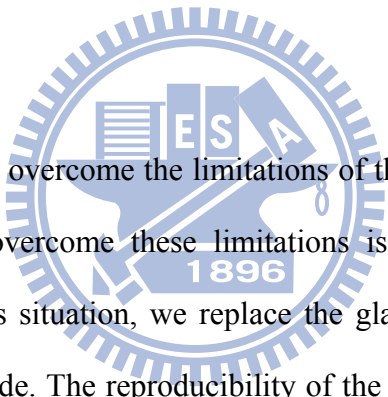
### 3.5.1 Current-Voltage (I-V) measurement set-up

In our measurement, a HP-4156A semiconductor parameter analyzer system was set up to measure the I-V characteristic curves, in which include  $I_{DS}-V_{GS}$  and  $I_{DS}-V_{DS}$  curves at controlled temperature. We have to take care when dropping the urea-buffer solution at the sensing region. Because the sensing region is small, we have to pay attention to preventing generation of air bubbles at the interface. In order to make sure that the devices are under a steady state, every concentration of urea-buffer solution is immersed for 60s before measuring.

From  $I_{DS}-V_{GS}$  curves, we can extract the response voltage of different concentration of urea-buffer testing solution by  $ZrO_2$  with urease-mix-Nafion<sup>TM</sup>

membrane-based urea-ENFET and  $\text{ZrO}_2$  with polymer-based REFET. At first, we find the point of maximum transconductance, i.e. the maximum slope of  $I_{\text{DS}}\text{-}V_{\text{GS}}$  curves, and get the corresponding current value ( $I_{\text{DS}}$ ). At the constant  $I_{\text{DS}}$  of maximum transconductance, we can find that with different concentration of urea-buffer testing solutions the reference electrode voltage ( $V_{\text{G}}$ ) will shift and the shifted voltage between the reference electrode voltage ( $V_{\text{G}}$ ) of phosphate buffer solution (PBS) and specific concentration of urea-buffer solution is the response voltage, as illustrated in Fig. 3-5.

### 3.5.2 Current-Voltage (I-V) measurement set-up with solid-state reference electrodes




In this study, we try to overcome the limitations of the glass reference electrode, and one of the ways to overcome these limitations is through the all-solid-state reference electrodes. In this situation, we replace the glass reference electrode with solid-state reference electrode. The reproducibility of the output voltage ( $V_{\text{G}}$ ) is what we concern about in this study first. Hence, as the same with measuring for response voltage, every concentration of urea-buffer testing solution is immersed for 60 seconds before  $I_{\text{DS}}\text{-}V_{\text{GS}}$  measurement. Then the reproducibility of output voltage is measured with two tested structures. One is with metal reference electrode of bare Pd and the other is with PR-mix-Nafion<sup>TM</sup> membrane-based solid-state reference electrode. From the reproducibility of output voltage, we can observe the sensing scope and sensing tendency of test structures for different concentration of urea-buffer testing solutions.

### 3.5.3 Reaction time measurement set-up with glass reference electrodes

The reaction rate characteristics were measured with 1.25 mg/dl, 10 mg/dl, 40 mg/dl, 80 mg/dl, 120 mg/dl, and 240 mg/dl urea-buffer solutions and the period of 20 seconds as the second measuring point and 10 seconds as the other seven measuring points by same condition samples. Nine measuring points in the time frame of 90 seconds were measured by urease/PBS-mix-Nafion<sup>TM</sup>/PBS with the ratio 5:1 enzymatic membrane-based ENFETs using glass reference electrodes. The detection principle is in a similar manner to that of the urea response voltage measurement and is shown in Fig. 3-6.

### 3.6 References

- 
- [1] <http://en.wikipedia.org/wiki/Urease>
- [2] M. Sato, T. Yamamoto, M. Takeuchi, K. Yamanouchi, "Humidity sensitivity of Lamb waves on composite polyimide:ZnO:Si<sub>3</sub>N<sub>4</sub> structure, Jpn. J. Appl. Phys. 32 Part 1, pp. 2380-2383, 1993.
- [3] John Payne, "Nafion® - Perfluorosulfonate Ionomer", April, 2005 from <http://www.psrc.usm.edu/mauritz/nafion.html> .
- [4] David T.V. Anh, W. Olthuis, P. Bergveld, "Hydrogen peroxide detection with improved selectivity and sensitivity using constant current potentiometry", Sensors and Actuators B, vol. 91, pp. 1-4, 2003.
- [5] Patrick J. Kinlen, John E. Heider, David E. Hubbard, "A solid-state pH sensors based on a Nafion-coated iridium oxide indicator electrode and a polymer-based silver chloride reference electrode", Sensors and Actuators B, vol. 22, pp. 13-25, 1994.
- [6] J.P. Tsao, C.W. Lin, "Preparations and Characterizations of the Nafion/SiO<sub>2</sub> Proton



Exchange Composite Membrane”, *Journal of Materials Science and Engineering*, vol. 34, No. 1, pp. 17-26, 2002.

[7] K. M. Chang, K. Y. Chao, T. W. Chou, and C. T. Chang, “Characteristics of Zirconium Oxide Gate Ion-sensitive Field-Effect Transistors”, *Japanese Journal of Applied Physics* Vol. 46 No. 7A, pp. 4334-4338, 2007.

[8] Paik-Kyun Shin, “The pH-sensing and light-induced drift properties of titanium dioxide thin films deposited by MOCVD”, *Applied Surface Science*, vol. 214, pp. 214-221, 2003.



## Chapter 4

### Results and Discussions

#### 4.1 Introduction

There are two main aims of this research. One is to investigate the pH-ISFET based urea sensors by means of Nafion<sup>TM</sup> entrapment as enzyme immobilization method. The other is to study the urea-ENFET integrated with miniaturized solid-state reference electrode as well as polymer membrane-based REFET by applying a differential measurement. In this chapter, Section 2 begins with background on the history and development of the different enzyme immobilization methods. The experimental results and discussion of the pH-ISFET based urea sensors are described in the section 3, 4, and 5. Finally, conclusion is reported in the section 6.

#### 4.2 Enzyme immobilization methods

A urea biosensor has urease (EC 3.5.1.5) as its biocomponent which catalyzes the hydrolysis of urea to ammonium and bicarbonate ions.



An important aspect in the practical application of a biosensor is the operational life of the biological component. When an enzyme is immobilized for the purpose of biosensing, there is loss of activity due to denaturation and deactivation of the enzyme that ultimately reduces the life of the biosensor. Therefore, techniques to enhance the operational and storage stability of the biocomponent are important in the application of biosensors.

An amperometric urea biosensor has been developed in which urease and glutamate dehydrogenase were immobilized on the nylon nets coupled with the platinum electrode. The glutamate dehydrogenase along with sodium hydroxide enhanced the reproducibility and stability of the sensor. The biosensor was used for clinical purposes [1]. A urea biosensor was developed in which urease was covalently immobilized in a film of electroinactive polypyrrole (PPy) with polyions polyacrylate (PAA) and poly l-lysine (PLL) to make a composite PPy/PAA-urease-PLL film. The doping of PPy with anions rendered enhanced stability to the electrode and the PPy/PAA electrode showed a selective Nernstian response to change in  $H^+$  ions (pH), which forms the potentiometric basis of the biosensor. A potentiometric urea biosensor has been developed in which  $NH_4^+$  ISE is used as a transducer in double matrix membrane (DMM) technology. This DMM prevented the interference of  $Na^+$  and  $K^+$  ions towards urea estimation. Urease was immobilized on the ion selective membrane in a hydrogel of poly (carbamoylsulfonate) [1]. A solid-state urea biosensor has been developed in which urease is immobilized on neutral poly (3-cyclohexyl thiophene) which is assembled over a platinum disc electrode. The polymer made the platinum electrode sensitive to pH and it showed a Nernstian response. The biosensor had a stability of 3 months when stored at  $4^\circ C$  under dry conditions [1]. The Langmuir–Blodgett technique has been exploited to facilitate better adsorption of urease enzyme. This technique involves the formation of monolayer film of poly (*N*-vinyl carbazole)/stearic acid on which urease has been immobilized by physical adsorption [1]. A potentiometric urea biosensor based on the immobilization of urease on carboxylic poly (vinyl chloride), a pH sensitive membrane, through electrostatic adsorption has also been developed. Here urease was immobilized through self-assembly technique which was found to be better than the

conventional technique of covalent binding in terms of better response, selectivity and ease of regeneration. Like the previous study, this biosensor too was regenerable [1]. A urea biosensor has been developed in which urease is immobilized on the triacetylcellulose membrane. Here two approaches are used (1) membrane with immobilized pH indicator (neutral red) and free urease (2) membrane with immobilized pH indicator and immobilized urease. Various parameters like pH optima, stability and rate of urea decomposition were studied [1]. A portable urea biosensor based on extended gate field effect transistors (EGFET) as the potentiometric transducer has been reported. Urease enzyme was immobilized by covalent entrapment in photocrosslinkable polyvinylalcohols bearing styrylpyridinium groups (PVA-SbQ). The EGFET comprised of a sensitive membrane of SnO<sub>2</sub> formed on indium titanium oxide (ITO) glass by sputtering, on which the urease immobilized PVA-SbQ film was polymerized [1]. A potentiometric biosensor based on the immobilization of urease on polyethylenimine film has been developed and four different methods of urease immobilization on the polyethylenimine film have been tested. These methods are physical adsorption, entrapment, physical adsorption, followed by reticulation with dilute aqueous solution of glutaraldehyde and glutaraldehyde activation of film followed by direct contact with urease solution. Out of all these methods, the physical adsorption of urease on the film followed by reticulation was observed the best method of urease immobilization because of low diffusional limitations, strong binding force between the enzyme and the matrix, reduced loss of enzyme from the matrix and a high stability of 4 weeks [1]. A study was carried out to analyse the response time taken by covalently immobilized urease on inorganic supports. Three different supports were chosen for the study namely silica gel, controlled pore glass and Poraver®. The assembly was in the form of a reactor and used a conductometric approach to evaluate the enzyme reactors column

for change in conductivity. This change in conductivity was provided by the hydrolysis of urea by urease which was then measured using a conductivity cell. Immobilization of enzyme on the inorganic support followed a three-step procedure, which included preparing the support material by drying and washing followed by derivatization of the surface with organosilane and finally coupling of enzyme to support using glutaraldehyde [1]. A urea biosensor based on polyaniline (PANi)-urease-Nafion/Au composite electrode has been reported which exploits the doping of the  $NH_4^+$  ions released as a result of urea hydrolysis, to cause reduction of PANi giving an elicit response on a cyclic voltammogram. Urease was immobilized onto the composite film by electrodeposition and casting methods, both bearing different response characteristics. The sensor had a detection range of 3–30 mg/dl and 6–60 mg/dl using glutaraldehyde and Nafion, respectively in the electrode [1]. In a further study the characteristics of urea biosensor has been compared by immobilizing urease on latex polymer functionalized by hydroxyl groups; acetate and lactobionate groups; imparting neutral and cationic character, respectively to these polymers [1]. With the recent approaches in nanotechnology, a urea biosensor using nanocomposite fibres has been developed. The fibres were prepared by electrospinning urease with polyvinylpyrrolidone. Urease encapsulated in electrospun membrane offered a large surface area which improved adsorption rate and response characteristics of the sensor [1]. An array-based optical biosensor based on sol–gel immobilization has been reported for the simultaneous determination of pH, urea, acetylcholine and heavy metals [1]. Urea biosensors have been developed by immobilizing urease through ionic interaction in a polyvinylferrocenium matrix based on potentiometric and amperometric transducers [1]. A recent report on urea biosensor explains the development of the sensor by immobilization of urease onto piezoelectric alumina

membranes based on conductometric response [1]. A potentiometric biosensor has been developed with urease immobilized in polyelectrolyte microcapsules [1].

### **4.3 Enzyme immobilization of the pH-ISFET based urea sensor**

#### **4.3.1 pH sensitivity and linearity of the pH-ISFET and urea-ENFET**

In this experiment, for the reason of the urea-ENFET based on pH-ISFET, we first measure the sensitivity of ZrO<sub>2</sub> pH-ISFET by glass reference electrode. In chapter 1, we have introduced the potential of glass electrode is very stable and accurate. The sensitivity of the ZrO<sub>2</sub> pH-ISFET in buffer solutions with pH = 1, 3, 5, 7, 9, 11, and 13 at a constant temperature of 25°C is obtained using a HP4156A semiconductor parameter analyzer. We also used the linear fit program to fit our experimental data. Fig. 4-1 shows that the sensitivity and sensitivity linearity of ZrO<sub>2</sub> pH-ISFET measured by glass reference electrode is about 55 mV/pH and 0.9996. Furthermore, we can observe that I<sub>DS</sub>-V<sub>GS</sub> curves are shifted parallel with the pH concentration of the buffer solutions in the non-saturation region with V<sub>DS</sub> = 1.5V. It is obviously that the threshold voltage shift towards positive values with increasing pH values.

Then, for the purpose of enzyme immobilization, the mixture of urease/PBS-mix-Nafion<sup>TM</sup>/PBS with the ratio 1:1 is dropped onto the ZrO<sub>2</sub> sensing layer of pH-ISFET as the urea-ENFET. Following that we still measure the sensitivity of ZrO<sub>2</sub> urease-mix-Nafion<sup>TM</sup> urea-ENFET by glass reference electrode. Fig. 4-2 shows that the sensitivity and sensitivity linearity of ZrO<sub>2</sub> urease-mix-Nafion<sup>TM</sup> urea-ENFET measured by glass reference electrode is about 43 mV/pH and 0.9922. From Fig. 4-1, Fig. 4-2, and Table 4-1, the discussions of the measuring results of H<sup>+</sup>

sensitivity and linearity are listed as follows:

- (1) The  $H^+$  sensitivity and linearity of  $ZrO_2$  urease-mix-Nafion<sup>TM</sup> urea-ENFET are similar to those of  $ZrO_2$  pH-ISFET. It is because pH variations are detected by the  $ZrO_2$  sensing layer, not the urease-mix-Nafion<sup>TM</sup> structure. To the urea-ENFET, the urease just plays a role as the catalyst for the hydrolysis of urea.
- (2) From Fig. 4-2, there has been a little decrease in the  $H^+$  sensitivity as a result of the urease molecular groups blocking effect, so the  $H^+$  ions are difficult to diffuse toward the  $ZrO_2$  surface. In other words, the numbers of the surface sites of  $ZrO_2$  regarded as sensing layer are reduced because of urease component contained.

#### 4.3.2 The proper immobilization method of enzyme membranes

In the section 4.3.1, we have prepared a  $ZrO_2$  urease-mix-Nafion<sup>TM</sup> enzymatic membrane with the ratio 1:1 urea-ENFET. The urea measurement of that urea-ENFET in the urea solutions with concentrations of 1.25 mg/dl, 10 mg/dl, 40 mg/dl, 80 mg/dl, 120mg/dl, and 240 mg/dl respectively at a constant temperature of 25°C is obtained by glass reference electrode using a HP4156A semiconductor parameter analyzer. Fig. 4-3 and Fig. 4-4 show the urea sensitive characteristics of  $ZrO_2$  urease-mix-Nafion<sup>TM</sup> enzymatic membrane with the ratio 1:1 urea-ENFET. From the experimental results of Fig. 4-3 and Fig. 4-4, we can observe that the  $I_{DS}$ - $V_{GS}$  curves and gate voltages under constant drain current condition are irregular and unstable. From the other point of view, the presence of the urea is difficult to be detected between the urea concentrations of 1.25 mg/dl and 240 mg/dl. In short, there are almost no detection range and linear part of dynamic range with this structure in spite of the longer

lifetime (more than one week) of the urease-mix-Nafion<sup>TM</sup> enzymatic membrane.

In order to carry out an available urea sensor, we have to enhance the content of the urease in the urease-mix-Nafion<sup>TM</sup> membrane by adjusting the ratio of the components. The urease diluted with the 5 mM PBS is twenty times to the Nafion<sup>TM</sup> without diluting both coated onto the ZrO<sub>2</sub> sensing layer. Similarly, we measure the urea detection properties under the same condition. The results are shown in Fig. 4-5 and 4-6, and it is clear that the threshold voltage shift towards positive values with increasing urea concentrations. Apparently, it means that increasing urea concentrations represent more OH<sup>-</sup> ions produced because of the hydrolysis of urea. As shown in Fig. 4-6, every gate voltage of each urea concentration stands for the response voltage based on the gate voltage of phosphate buffer solution (without incorporating urea), and the events include pH 6.98, 7.7, 8.75, 10.6, 11.48, and 12.77 for each experimental point of different concentrations of urea solutions. In addition, we also found that the detection limitation is 1.25 mg/dl, and the urea sensitivity is 1.33 mV/(mg/dl) of dynamic range. In other words, the sensing range of this structure is from 1.25 mg/dl to 240 mg/dl. Unfortunately, the lifetime of the urease/PBS-mix-Nafion<sup>TM</sup> membrane is smaller than 30 minutes. Consequently, we still should search for the proper enzymatic membrane by adjusting the ratio of the components.

Finally, we choose the moderate proportion of urease to Nafion<sup>TM</sup> between 1:1 and 20:1 used in the previous paragraph and regard it as our new structure. The enzymatic membrane in the urease/PBS-mix-Nafion<sup>TM</sup>/PBS structure with ratio 5:1 was coated onto the ZrO<sub>2</sub> sensing layer of the urea-ENFET. The urea detection characteristics with different concentrations of urea buffer solutions are obtained under the same condition once more. The results are shown in Fig. 4-7 and 4-8. The events include pH 6.23, 6.92, 7.76, 8.19, 8.57, and 9.6 for each experimental point of

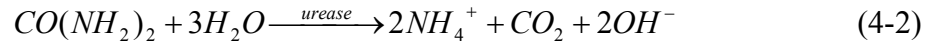


different concentrations of urea solutions under constant drain current situation. In Fig. 4-8, the consequences are observed that the detection limitation is 8 mg/dl, and the urea sensitivity is 0.64 mV/(mg/dl) of dynamic range. In other words, the sensing range of this structure is from 8 mg/dl to 240 mg/dl. Compare with Fig. 4-6 and It is noteworthy that the urea sensitivities such as response voltages are quite all lower than those applying the urease/PBS-mix-Nafion<sup>TM</sup> components with the ratio 20:1 (about 50% thereabouts of the response voltage) when the urea concentration surpasses 40 mg/dl specially. Luckily, the lifetime of urease/PBS-mix-Nafion<sup>TM</sup>/PBS membrane with the ratio 5:1 is more than seven days. According to the above experimental results, we have chosen the urease/PBS-mix-Nafion<sup>TM</sup> membrane with the ratio 5:1 which possesses balanced characteristics such as urea sensitivity and linearity in the various aspects as well as availability treated as ENFET's enzyme layer in our following research. The overall performances for urea detection by three kind of different proportion combinations are summarized in Table 4-2. From Fig. 4-3 to Fig. 4-11, and Table 4-2, the discussions of the measuring results of urea sensitivity and lifetime of enzymatic membranes are listed as follows:

- (1) The urea sensing properties and the enzymatic membrane's lifetime are more possibly related to the proportion of the composition which includes urease and Nafion<sup>TM</sup>.
- (2) When the proportion of urease to Nafion<sup>TM</sup> achieves 1:1, the enzymatic membrane is unable to provide enough urease regard as catalyst for urging the hydrolysis of urea.
- (3) Based on our previous experimental results, when the proportion of urease to Nafion<sup>TM</sup> achieves 1:1 or 5:1, the Nafion<sup>TM</sup> element is effective truly to entrap the urease component completely on the ZrO<sub>2</sub> surface preventing the urease from hydrolyzing in tested urea buffer solutions. That is to say it need

to supply sufficient Nafion<sup>TM</sup> for enzyme immobilization and to advance the lifetime and availability of ENFETs.

- (4) Firstly, we quote the theoretical expression referring to the hydrolysis of urea from the reference [2] :



$$[NH_4^+]_p = [OH^-]_p = \frac{at}{V} \quad (4-3)$$

Where  $a$  is the urease activity, and  $t$  is the time.  $V$  is the volume of testing urea solution. It is evident that in a given volume  $V$  and time  $t$ , the concentrations of produced ammonia ions and hydroxyl ions are as a function of the urease activity  $a$ . In other words, the more urease activity  $a$  results in the more  $OH^-$  ions generated, so the response voltage of specific urea concentration is much higher. In addition, when an enzyme is immobilized for the purpose of biosensing, there is loss of activity due to denaturation and deactivation of the enzyme that ultimately reduces the life of the biosensor [1]. At last, we can conclude that the urea sensitivity measured by means of the urease/PBS-mix-Nafion<sup>TM</sup> enzymatic membrane with the ratio 20:1 is surely higher than those measured by the urease/PBS-mix-Nafion<sup>TM</sup>/PBS enzymatic membrane with the ratio 5:1 because the less Nafion<sup>TM</sup> component permits the enzyme molecules in a much free configuration and leads to higher activity.

- (5) According to reference [3] and our study, when the enzyme is brought in contact with a substrate, a complex concentration profile develops, which is a function of both diffusion and reaction processes. In the reaction region of the enzyme, the product concentration is achieved by mass transfer given by Fick's second law as well as by enzyme kinetics. The effective concentration

of the enzyme, including the concentration of enzyme in the membrane, the kinetics of the enzyme reaction, and the mass transport of the substrate molecules through the membrane. The product concentration at the surface of the transducer is a constant that depends on the immobilized enzyme concentration, the reaction kinetics, the diffusion mass transport, and it is independent of substrate concentration. The substrate concentration is so large that it has saturated the enzyme. Then there is no sufficient amount of enzyme in the membrane to detect changes in such a large substrate concentration [3]. Based on our experimental results in Fig. 4-6 and 4-8, the difference of the response voltages between 40 mg/dl and 240 mg/dl as well as 1.25 mg/dl of urea concentrations can be explained by considering reaction kinetics. For high urea concentration, the detection range and the urea sensitivity can be promoted by applying the urease-mix-Nafion<sup>TM</sup> enzymatic membrane with higher concentration and activity of urease.

#### 4.3.3 The response time of urea-ENFET

The reaction rate characteristics were measured with 1.25 mg/dl, 10 mg/dl, 40 mg/dl, 80 mg/dl, 120 mg/dl, and 240 mg/dl urea-buffer solutions and the period of 20 seconds as the second measuring point and 10 seconds as the other seven measuring points by same condition samples. Nine measuring points in the time frame of 90 seconds were measured by urease/PBS-mix-Nafion<sup>TM</sup>/PBS with the ratio 5:1 enzymatic membrane-based ENFETs using glass reference electrodes.

The experimental results are shown in Fig. 4-12 ~ Fig. 4-18, and it is obvious that all the response voltages are reached 90 % as a steady state response after 25 seconds. Hence, the response time of the urease/PBS-mix-Nafion<sup>TM</sup>/PBS with the

ratio 5:1 enzymatic membrane-based ENFET for different concentrations of urea buffer solutions is indicated between 25 seconds and 60 seconds. This phenomenon can be interpreted by thinking of enzyme reaction kinetics. The reaction rate is controlled by the enzyme characteristics. Generally speaking, higher concentrations for urea buffer solutions require longer response time to react completely. On the other hand, higher concentrations for urea buffer solutions result in larger response voltages in our case. In brief, we can certainly conclude that it may obtain a rapid reaction characteristic by way of the structure like MOSFET and the proper urease/PBS-mix-Nafion<sup>TM</sup>/PBS with the ratio 5:1 enzymatic membrane.

#### 4.3.4 The influence of the titration by high concentration urea solution

In order to investigate the affection of a trace of high concentration urea buffer solution, we add one to three drops of the 240 mg/dl concentration urea buffer solution respectively into 1.25 mg/dl concentration urea buffer solution whose volume is about 5 ml. The results are presented in Fig. 4-19 and Fig. 4-20. Clearly, we can see that the threshold voltage shift towards positive values with increasing 240 mg/dl concentration urea drops. The pH variations include 0.98, 1.64, and 1.83, respectively. In other words, the variations in gate voltages are proportional to dripped 240 mg/dl concentration urea buffer solution drops. It is noteworthy that there is nearly a saturated effect when adding more and more drops of 240 mg/dl concentration urea buffer solution. As discussed above, the urea-ENFET by urease/PBS-mix-Nafion<sup>TM</sup>/PBS enzymatic membrane with the ratio 5:1 has a micro-sensing property for detecting few variations of urea concentrations in human blood for practical applications.

#### 4.3.5 The effect of concentration of the phosphate buffer solution

The performance of the enzyme sensor depends on the activity of an immobilized enzyme, which is strongly affected by the environmental conditions, especially by the pH value of the aqueous measurement medium. Therefore as a first step, an optimal pH value for the urea sensitive sensor was determined. According to reference [4, 5], an optimal pH value for the sensor response is observed at pH 6, so we choose it as our phosphate pH value with the concentration 10 mM in the measurement background. Additionally, the influence of buffer capacity is discussed as follows [4, 6]. For an increase in the buffer concentration 5 mM to 10 mM the sensor response decreases slightly. Furthermore, for an increase in the buffer concentration, the linear part of the sensor dynamic range extends too. The results are presented in Fig. 4-21 by measuring the 5 mM and 10 mM phosphate buffer solutions with urease/PBS-mix-Nafion<sup>TM</sup>/PBS enzymatic membrane (5 : 1) urea-ENFET. It is clear that the shifted voltage 47.79 mV represents the pH value 6.87 of 5 mM phosphate buffer solution. Above all, we select the 10 mM concentration with pH 6 as our phosphate buffer solution because of the larger linear part of the sensing dynamic range.

#### 4.3.6 Storage stability

The lifetime of enzymatic membranes constitutes a limiting factor for biosensor applications. In this context, an attempt was made to compare the storage conditions for immobilized enzyme. An amount of the urea biosensors were fabricated and then were stored in the dark at 4°C. During 7 days, the urea measurement of that urease/PBS-mix-Nafion<sup>TM</sup>/PBS enzymatic membrane (5 : 1) urea-ENFET in the urea

solutions with concentrations of 1.25 mg/dl, 10 mg/dl, 40 mg/dl, 80 mg/dl, 120mg/dl, and 240 mg/dl respectively at a constant temperature of 25°C is obtained by glass reference electrode using a HP4156A semiconductor parameter analyzer. The results are shown in Fig. 4-22 and summarized in Table 4-3. After 7 days, the response voltages of every urea concentrations have no diminution obviously except 1.25 mg/dl and 10 mg/dl urea concentrations, and it represents that the sensor responses of urea concentrations exceeding 40 mg/dl all reach 92 % at least compared with the sensor responses measured at first. In other words, when the biosensor were stored in dry and dark, at 4°C, 90 % of the initial enzymatic activity for urease/PBS-mix-Nafion<sup>TM</sup>/PBS enzymatic membrane (5 : 1) can be kept after 7 days. The noticeable decreases in the responses of lower concentrations are probably due to the desorption of the enzyme that is weakly held by the surface. One drawbacks of the entrapping method is the possibility of losing enzyme activity, since some pore sizes permit escape of the enzyme. In conclusion, the lifetime of the urea biosensor is larger than 7 days.

#### **4.4 Solid-state reference electrode integrated with ENFET**

##### **4.4.1 Solid-state reference electrode**

D. haramé was first to incorporate a silver/silver chloride (Ag/AgCl) structure on the ISFET chip [7]. In microelectrochemical sensors, thin-film Ag/AgCl electrodes without any internal reference electrolyte are often referred as “quasi-reference electrodes”. Most investigations have been focused on the miniaturization of the Ag/AgCl electrode. However, several factors limit the durability of the Ag/AgCl electrode. Foremost is the well-known non-negligible diffusion of the chlorine ions when the Ag/AgCl electrode directly contacts to the electrolyte solution. Moreover,

the electrode is susceptible to changing activity of its primary ion [e.g.  $a(\text{Cl}^-)$  in Ag/AgCl system] and the existence of interfering redox materials. Hence, the lifetime of such structure is very short and the potential reproducibility is very poor. In other words, the potential at the solid/liquid interface is thermodynamically undefined and will lead to significant errors in pH measurement. In addition, its use is thus severely restricted. To solve these problems of bare Ag/AgCl electrode as mentioned above, another approach was attempted and devoted to miniaturize and scale down the mature macro liquid-junction reference electrode, yet preserving its basic structure and operation principle. This approach was carried out to incorporate the liquid-filled solid-state reference electrode as an integrated part of the ISFET chip, using IC technology and micro-machining. However, to seal a small volume of saturated potassium chloride (KCl) electrolyte is still a mass production challenge [8]. Recently, various modifying methods have been proposed to improve the Ag/AgCl electrode, such as KCl membrane and Nafion<sup>TM</sup> coating [9], where chloride ions were trapped within the KCl membrane.

According to previous experiment in our group, it showed that the polymer-based materials can make REFET have low sensitivity. It means that the surface potential maintains almost a constant value, i.e. the surface potential will be stable. On the basis of the experimental results, we applied the PR-mix-Nafion<sup>TM</sup> structure as the protective membrane of the metal reference electrode. Comparing with the Ag/AgCl reference electrode, such solid-state reference electrode will not have the problem of chloride diffusion.

As described in the previous section, an electrochemical sensor needs a reference electrode to define a stable accurate electrochemical potential as the measurement reference. It is therefore important that the potential of the reference electrode to be constant and invariant with solution composition. Hence, we can observe the behavior

of these solid-state reference electrodes.

#### 4.4.2 The bare metal reference electrode

A good reference electrode is a prerequisite for providing a stable reference potential. An unstable reference electrode potential results in the shift of the working electrode potential and affects the output current. To get a chemical-resistant electrode, we deposit noble metal, Pd, as the reference electrode by sputtering. Comparing with the Ag/AgCl reference electrode, the Pd reference electrode will not have the problem of chloride diffusion.

The urea measurement of the urease/PBS-mix-Nafion<sup>™</sup>/PBS enzymatic membrane with the ratio 5:1 urea-ENFET in the urea solutions with concentrations of 1.25 mg/dl, 10 mg/dl, 40 mg/dl, 80 mg/dl, 120mg/dl, and 240 mg/dl respectively at a constant temperature of 25°C is obtained by bare metal reference electrode (Ti/Pd) using a HP4156A semiconductor parameter analyzer. Fig. 4-23 and Fig. 4-24 show the experimental results. The discussions of the measuring results of urea sensitivity and linearity of enzymatic membranes are listed as follows:

- (1) As shown in Fig. 4-23 and Fig. 4-24, it is not difficult to find out that the  $I_{DS}$ - $V_{GS}$  curves are unstable as a result of bare metal reference electrode. In addition, the linearity is also poor as a matter of course. The unstable phenomenon is caused by solid/liquid interface and other chemical reactions.
- (2) According to Fig. 4-24, we also found that the detection limitation is 5 mg/dl. In other words, the sensing range of this structure is from 5 mg/dl to 120 mg/dl.
- (3) What the special is that the response voltage appears a slight decrease phenomenon when the urea concentration exceeds 120 mg/dl as a result of



voltage vibration.

#### 4.4.3 The PR-mix-NF coated solid-state reference electrode

PR-mix-Nafion<sup>TM</sup> membrane-based reference electrodes have been fabricated by combining silicon fabrication and drop-coating method. To investigate the PR-mix-Nafion<sup>TM</sup> membrane-based material on the improvement of reference electrode performance, the mix composition of PR (FH6400) and Nafion<sup>TM</sup> with the ratio 1:1 was coated onto an exposed area of Pd metal electrode to produce a solid-state reference electrode as the reference electrode. Next, the urea measurement of the urease/PBS-mix-Nafion<sup>TM</sup>/PBS enzymatic membrane with the ratio 5:1 urea-ENFET in the urea solutions with concentrations of 1.25 mg/dl, 10 mg/dl, 40 mg/dl, 80 mg/dl, 120mg/dl, and 240 mg/dl respectively at a constant temperature of 25°C is obtained by Ti/Pd/PR-mix-Nafion<sup>TM</sup> membrane solid-state reference electrode using a HP4156A semiconductor parameter analyzer. The results are shown in Fig. 4-25 and Fig. 4-26. The overall performances for urea detection by three kind of different reference electrodes such as glass reference electrode, bare Ti/Pd metal reference electrode, and Ti/Pd/PR-mix-NF solid-state reference electrode are summarized in Fig. 4-27, Fig. 4-28, Table 4-4, and Table 4-5. The discussions of the measuring results of urea sensitivity and linearity for urea-ENFET with different reference electrodes are listed as follows:

- (1) According to Fig. 4-26, we found that the detection limitation is 10 mg/dl, and the urea sensitivity is 0.47 mV/(mg/dl) of dynamic range. In other words, the sensing range of this structure is from 10 mg/dl to 240 mg/dl.
- (2) As shown in Fig. 4-27, compare the urea detection characteristics measured by Ti/Pd/PR-mix-NF solid-state reference electrode with those measured by

bare Ti/Pd metal reference electrode, and it is obvious that the linearity between 10 and 240 mg/dl is improved greatly due to PR-mix-NF polymer-based material. Moreover, the response voltage maintains the tendency of increment as surpassing 120 mg/dl by Ti/Pd/PR-mix-NF solid-state reference electrode, so we can conclude that the detection range extends to 240 mg/dl as a result of PR-mix-NF structure.

(3) From Fig. 4-27, although the urea sensitivity for each concentration fall a little, the gate voltage vibration is decreased by means of applying PR-mix-NF polymer-based material. It means that the low sensitivity sensing layer of REFET also work at the solid-state reference electrodes. The PR-mix-NF structure with different ratio seems to have the potential to solve the unstable problem of the solid-state reference electrode.

(4) To enhance the lifetime of PR-mix-NF membrane and improve the interface adhesion between PR-mix-NF membrane and Pd metal layer, we can coat with HMDS on Pd metal layer by spin coating fabrication before dropping PR-mix-NF mixture.

(5) As presented in Fig. 4-28, compare the urea detection characteristics measured by Ti/Pd/PR-mix-NF solid-state reference electrode with those measured by glass reference electrode, and it is apparent that the linearity of the former is better than that of the latter between 10 mg/dl and 120 mg/dl. By chance, the normal level of urea is from 8 mg/dl to 23 mg/dl in human blood as well as from 15 mg/dl to 40 mg/dl in serum, so we consider that the urea-ENFET with Ti/Pd/PR-mix-NF solid-state reference electrode is possible in clinical application based on the discussion (1) and (5) of section 4.4.3.

(6) From Fig. 4-28, the little reduction of the urea sensitivity for every

concentration measured by Ti/Pd/PR-mix-NF solid-state reference electrode is because of the non-uniform mixture of PR and Nafion<sup>TM</sup> and the poor interface adhesion between PR-mix-NF membrane and Pd metal layer.

## **4.5 The ENFET/REFET configuration in differential mode**

### **4.5.1 ENFET/REFET differential pair with different polymer-based material**

For solving the problem of unstable output voltage measured by bare metal reference electrode and achieving the miniaturization purpose, a REFET (Reference ion-sensitive Field Effect Transistor) co-fabricated with ISFET is applied. The REFET is identical with ISFET but it is not sensitive to the ions which are measured. By applying a differential measurement with ISFET/REFET arrangement, the unknown and unstable electrode potential manifests itself as common mode signal and is thus suppressed by the CMRR (common-mode-rejection-ratio) of the system.

According to the commonly accepted site-dissociation model for the pH-sensitivity of ISFETs with an inorganic gate material, its pH response can be described in terms of the number of reactive sites on the gate surface and their proton dissociation and association constants, i.e., the more numbers of surface sites the larger sensitivity it has. For the sake of reducing sensitivity, we need to find an effective diffusion barrier for protons, thus reducing the pH sensitivity of the device. In this study, we want to build up a REFET which is suitable for the ZrO<sub>2</sub> urea-ENFET, so to find a REFET with low urea sensitivity is our main object.

First of all, in order to look for the proper polymer-based material with low urea sensitivity regarded as sensing layer of REFET, and we prepare PR-mix-Nafion<sup>TM</sup> mixture with the ratio 1:1 as well as Polyimide-mix-Nafion<sup>TM</sup> mixture with the ratio

3:1 and 1:0 coated onto the ZrO<sub>2</sub> sensing layer of ISFET by drop-coating method. According to the experimental results previously in our laboratory, the film structure by drop-coating process is not in order, and Nafion<sup>TM</sup> has many voids in its chemical structure. If we mix PR with Nafion<sup>TM</sup>, the voids will be filled with PR. And then it will become a more regular and stronger structure. Next, the urea measurement of the PR-mix-Nafion<sup>TM</sup> and Polyimide-mix-Nafion<sup>TM</sup> polymer-based membrane as well as ZrO<sub>2</sub> sensing layer without polymer-based material above it all treated as REFET's sensing layer in the urea solutions with concentrations of 1.25 mg/dl, 10 mg/dl, 40 mg/dl, 80 mg/dl, 120mg/dl, and 240 mg/dl respectively at a constant temperature of 25°C is obtained by glass reference electrode using a HP4156A semiconductor parameter analyzer. The results of urea insensitive characteristics measured by four kinds of different structure for REFET are shown in Fig. 4-29 ~ Fig. 4-37. For implementing the mechanism of ENFET/REFET in the differential mode, then we integrate the urease/PBS-mix-Nafion<sup>TM</sup>/PBS enzymatic membrane with the ratio 5:1 urea-ENFET with one of four kinds of diverse sensing layer as REFET both measured by glass reference electrode in the differential ENFET/REFET measurement respectively. The results are presented from Fig. 4-38 to Fig. 4-42 and summarized in Table 4-6 and Table 4-7. At last, it is the most important of all that the electrical conductivity such as transconductance of ENFET must be similar to that of REFET so that the same feedback circuit and the smaller differential amplifier can be designed available to achieve the goal for low cost and simple fabrication. In other words, the more similar transconductance leads to the easily matched ENFET/REFET differential pair as well as the peripheral circuit loop. In theory, the transconductance which symbolized by  $g_m$  is also named transistor gain, and the definition of  $g_m$  is expressed as  $\frac{\partial I_{DS}}{\partial V_{GS}}$ . Due to the statement discussed previously, we extract the  $g_m$

curve of ENFET as well as REFET and then combine the  $g_m$  curve of ENFET with that of REFET to compare the matching extent for ENFET and REFET with different sensing layer. The results are shown in Fig. 4-43 ~ Fig. 4-47. In terms of Fig. 4-29 ~ Fig. 4-47, Table 4-6 and Table 4-7, the discussions of the measuring results of urea sensitivity and linearity for ENFET/REFET pair in differential mode with different structure as REFET's sensing layer are listed as follows:

- (1) According to Fig. 4-37, it is obvious that all the response voltages for various urea concentrations of tested urea buffer solutions are nearly below 15 mV except the  $ZrO_2$  ISFET regarded as REFET, so it is surely proved that PR-mix-Nafion<sup>TM</sup>, Polyimide-mix-Nafion<sup>TM</sup>, and Polyimide polymer-based membranes have possession of properties related to insensitive to urea.
- (2) From Fig. 4-30 and Fig. 4-38, we can see that the  $ZrO_2$  ISFET is sensitive to urea in the urea concentration range of 80 mg/dl to 120 mg/dl and the variations are similar to those of ENFET in the same range. In theory, since buffer solutions have been used to prevent variations, this phenomenon is not easy to understand. On the other hand, the  $ZrO_2$  ISFET has no urease looked on as catalyst above sensing layer. It can be assumed that, since the urease activity is globally responsible for a constant consumption of  $H^+$  ions in the Nafion<sup>TM</sup> film, a pH increase is confined near the  $ZrO_2$ /urease-mix-Nafion<sup>TM</sup> gate structure. This increase should be responsible for a pH gradient, i.e. for  $H^+$  ion diffusion phenomena, in the urea-ENFET proximity. Finally, these diffusion phenomena could be detected by the  $ZrO_2$ -ISFET.
- (3) As shown in Fig. 4-42, we found that the detection limitations are about 8 mg/dl, and the urea sensitivity is about 0.63 mV/(mg/dl) of dynamic range by each ENFET/REFET pair with different materials as sensing layers in the differential measurement. In other words, the sensing range of all differential

ENFET/REFET configurations is from 8 mg/dl to 240 mg/dl. Evidently, the urea sensitivity and linearity of dynamic range based on ENFET/REFET differential pair with PR-mix-Nafion<sup>TM</sup> membrane as REFET's sensing layer are better than others, even though the performance of ENFET/REFET differential pair with Polyimide-mix-Nafion<sup>TM</sup> and Polyimide membranes as REFET's sensing layer are also excellent in our study. It is noteworthy that there is a little decrease in urea sensitivity for each urea concentration measured by ENFET/ISFET differential pair with ZrO<sub>2</sub> as ISFET's sensing layer as a result of H<sup>+</sup> ion diffusion phenomena detected by ZrO<sub>2</sub>-ISFET.

(4) In theory,  $CMRR = \frac{|A_{dM}|}{|A_{cM}|} = \frac{\text{differential mode gain}}{\text{common mode gain}}$  and  $g_m$  is proportional to

$|A_{dM}|$ . If  $g_m \rightarrow \infty$ , then  $|A_{dM}| \cdot CMRR \rightarrow \infty$ . As described previously, we expect that  $g_m$  values of ENFET and REFET are both larger and equal at linear region, so the unstable voltages from quasi-reference electrode/electrolyte can be suppressed by the CMRR of the ENFET/REFET differential system. In the ENFET/REFET system, the urea response can be obtained with a differential measurement set-up. Therefore, given the common mode rejection ratio (CMRR) in the differential system, the transconductance operated in linear region ( $g_m \equiv \partial I_{DS} / \partial V_{GS} = W\mu_n C_{ox} V_{DS} / L$ ) of the ENFET and REFET(ISFET) should be the same. As shown in Fig. 4-47, similar transconductance were measured at  $V_{DS}$  as 1.5V and prove that the PR-mix-Nafion<sup>TM</sup> layer, urease-mix-Nafion<sup>TM</sup> layer, and ZrO<sub>2</sub> layer have some electrical conductivity and behave as ion-unblocking membranes. Sum up the discussions narrated previously such as urea sensitivity, linearity of dynamic range as well as transconductance

characteristics, and we obtain a conclusion that the  $ZrO_2/PR\text{-mix-Nafion}^{TM}$  structure and  $ZrO_2$  both regarded as REFET's sensing layer is suitable for ENFET in the differential measurement.

#### 4.5.2 Coplanar ENFET/REFET differential pair with quasi-reference electrode

According to section 4.5.1, we choose the  $PR\text{-mix-Nafion}^{TM}$  polymer-based membrane with the ratio 1:1 as REFET's sensing layer, and then we integrate ENFET with REFET in the differential mode which is measured by bare metal electrode Ti/Pd as quasi-reference electrode. The differential measurement of the urease/PBS-mix-Nafion<sup>TM</sup>/PBS enzymatic membrane with the ratio 5:1 urea-ENFET and  $PR\text{-mix-Nafion}^{TM}$  polymer-based membrane REFET in the urea solutions with concentrations of 1.25 mg/dl, 10 mg/dl, 40 mg/dl, 80 mg/dl, 120mg/dl, and 240 mg/dl respectively at a constant temperature of 25°C is obtained by quasi-reference electrode (Ti/Pd) using a HP4156A semiconductor parameter analyzer. The results are shown in Fig. 4-23 ~ Fig. 4-24, Fig. 4-48 ~ Fig. 4-50, and Table 4-8. In addition, for the sake of comparing the performance of ENFET/REFET differential pairs measured by quasi-reference electrode and glass reference electrode with that of ENFETs measured by glass reference electrode and  $PR\text{-mix-Nafion}^{TM}$  polymer-based membrane solid-state reference electrode, we present the comparative results in Fig. 4-51 ~ Fig. 4-54 and summarized in Table 4-9 and Table 4-10. Based on Fig. 4-23 ~ Fig. 4-24, Fig. 4-48 ~ Fig. 4-50, Fig. 4-51 ~ Fig. 4-54, Table 4-9 and Table 4-10, the discussions of the measuring results of urea sensitivity and linearity for ENFETs and ENFET/REFET differential pairs by different measuring manners are listed as follows:

- (1) As shown in Fig. 4-50, we found that the detection limitation is 8 mg/dl, and

the urea sensitivity is 0.6 mV/(mg/dl) of dynamic range by ENFET/REFET pair with PR-mix-Nafion<sup>TM</sup> polymer-based membrane as sensing layer in the differential measurement. In other words, the sensing range of this differential ENFET/REFET configurations biased by quasi-reference electrode is from 8 mg/dl to 240 mg/dl. The potential difference between liquid and quasi-reference electrode results in the voltage vibration, so the response voltages measured by PR-mix-Nafion<sup>TM</sup> polymer-based membrane REFET become more and more unstable.

- (2) According to Fig. 4-51 and Table 4-9, the performance for sensing range, linearity of dynamic range, and urea sensitivity measured by quasi-reference electrode in a differential mode is extremely close to the ENFET measured by glass reference electrode.
- (3) On the basis of comparative results discussed in this chapter which contain ENFETs and ENFET/REFET differential pairs by different structures and reference electrodes, the applicable ENFETs and ENFET/REFET differential pairs are concluded in Fig. 4-52 and Table 4-10. We verify that the ENFET (urease/PBS-mix-Nafion<sup>TM</sup>/PBS enzymatic membrane with the ratio 5:1) can be applied in clinical domain by modifying the troublesome solid-state reference electrode with PR-mix-Nafion<sup>TM</sup> membrane. Besides, ZrO<sub>2</sub>/PR-mix-Nafion<sup>TM</sup> structure and ZrO<sub>2</sub> without polymer-based material above it both have the potential being the sensing layers of REFETs.

## 4.6 Conclusions

In this study, the biosensor of urea-ENFET with urease/PBS-mix-Nafion<sup>TM</sup>/PBS (5:1) enzymatic membrane was successfully fabricated by Nafion<sup>TM</sup> entrapment



method for enzyme immobilization. It exhibits wide sensing range of between 8 and 240 mg/dl, low detection limit of 8 mg/dl, high sensitivity of 0.64 mV/(mg/dl), fast response time of from 25 to 60 seconds, long lifetime, linear response, and good storage stability.

Furthermore, for the purpose of miniaturization, we successfully apply the PR-mix-Nafion<sup>TM</sup> polymer-based material for REFET as the sensing layer and for solid-state reference electrode as the protective membrane. The structure of PR-mix-Nafion<sup>TM</sup> polymer-based membrane for solid-state reference electrode and for REFET as the sensing layer is simple and easy to fabricate by drop-coating method. Our analysis indicated the PR-mix-Nafion<sup>TM</sup> polymer-based membrane can work at the solid-state reference electrodes and the unstable voltage problems of solid-state reference electrode are greatly solved by Ti/Pd/PR-mix-Nafion<sup>TM</sup> structure. The ZrO<sub>2</sub>/urease-mix-Nafion<sup>TM</sup> urea-ENFET measured by the solid-state reference electrode has good sensing range of between 10 and 240 mg/dl and low detection limit of 10 mg/dl as well as excellent linear response of dynamic range. On the other hand, in differential ENFET / REFET measurement, the urea sensitivity can achieve 0.63 mV/(mg/dl) because of the ultra low sensitivity REFET treated by PR-mix-Nafion<sup>TM</sup> structure. In addition, the sensing range of urea is from 8 to 240 mg/dl and the detection limit is 8 mg/dl. The performance is extremely close to those of glass reference electrode. Further, the ENFET / REFET differential pair with quasi-reference electrode (Ti/Pd) performs excellent sensing range of between 8 and 240 mg/dl and high sensitivity of 0.6 mV/(mg/dl). The results are similar to those of glass reference electrode, and it is proved that PR-mix-Nafion<sup>TM</sup> membrane has the potential being as the REFET's sensing layer for REFET implementation.

From the experimental results, we confirm the kind of polymer-based materials have a big potential to integrate a miniaturized solid-state reference electrode into

ENFET chip and for surface modifying of REFET's sensing layer in order to implement ENFET / REFET differential measurement. The cheap and simple production of miniaturized all-solid-state reference microelectrodes and ENFET / REFET differential pairs with quasi-reference microelectrodes could substitute classical reference electrodes in practical applications.

#### 4.7 References

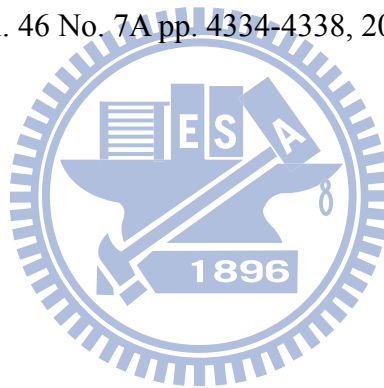
- [1] Minni Singh, Neelam Verma, Arun Kumar Garg, Niha Redhu, "Urea biosensors", Sens. Actuators B 134, pp. 345-351, 2008.
- [2] W. Sant, M.L. Pourciel, J. Launay, T. Do Conto, A. Martinez, P. Temple-Boyer, "Development of chemical field effect transistors for the detection of urea", Sens. Actuators B 95, pp. 309-314, 2003.
- [3] Massimo Grattarola, Giuseppe Massobrio, "BIOELECTRONICS HANDBOOK : MOSFETs, Biosensors, and Neurons", McGRAW-HILL, pp. 294-299, 1998.
- [4] Jia-Chyi Chen, Jung-Chuan Chou, Tai-Ping Sun, Shen-Kan Hsiung, "Portable urea biosensor based on the extended-gate field effect transistor", Sens. Actuators B 91, pp. 180-186, 2003.
- [5] Filiz Kuralay, Haluk Ozyoruk, Attila Yildiz, "Amperometric enzyme electrode for urea determination using immobilized urease in poly(vinylferrocenium) film", Sens. Actuators B 114, pp. 500-506, 2006.
- [6] A.P. Soldatkin, D.V. Gorchkov, C. Martelet, N. Jaffrezic-Renault, "Application of charged polymeric materials as additional permselective membranes for modulation of the working characteristics of penicillin sensitive ENFETs", Materials Science and Engineering C 5, pp. 35-40, 1997.
- [7] I-Yu Huang, Ruey-Shing Huang, "Fabrication and characterization of a new planar

solid-state reference electrode for ISFET sensors”, *Thin Solid Films*, vol. 406, pp.255-261, 2002.

[8] I-Yu Huang, Ruey-Shing Huang, Lieh-Hsi Lo, “Improvement of integrated Ag/AgCl thin-film electrodes by KCl-gel coating for ISFET applications”, *Sensors and Actuators B*, vol. 94, pp. 53-64, 2003.

[9] Chen Dong-chu, et al., ”Preparation of Nafion Coated Ag/AgCl Reference Electrode and Its Application in the pH Electrochemical Sensor”, *Journal of Analysis Science*, vol. 21, pp. 432-434, Aug., 2005.

[10] K. M. Chang, K. Y. Chao, T. W. Chou, and C. T. Chang, ”Characteristics of Zirconium Oxide Gate Ion-sensitive Field-Effect Transistors” *Japanese Journal of Applied Physics* Vol. 46 No. 7A pp. 4334-4338, 2007.



## Chapter 5

### Future Work

In our experiment, characteristics of various sensing materials and structures are studied. Based on the observed results, PR-mix-Nafion<sup>TM</sup> polymer-based membrane is a good candidate for solid-state reference electrode and REFET. But the coating process is not optimized in this experiment. For the purpose of mass manufacture, the yield and reliability are the most important issues. In our experiment, the performance sometimes will fail and unstable during coating and measurement. So, the optimized coating method, including the influence of dropping manners, needs to be studied further. The properties of these polymer materials and other new polymer stuffs are also need to be more understood.

In addition, the optimized enzyme immobilization method by Nafion<sup>TM</sup> entrapment, including the mixture ratio of urease to Nafion as well as coating manners both related to activity and thickness, needs to be studied further.

At last, the phosphate buffer solution will be replaced with bovine blood serum or human serum to investigate the urea detection properties for clinical application. Hence, the device will become a useful tool in the future.

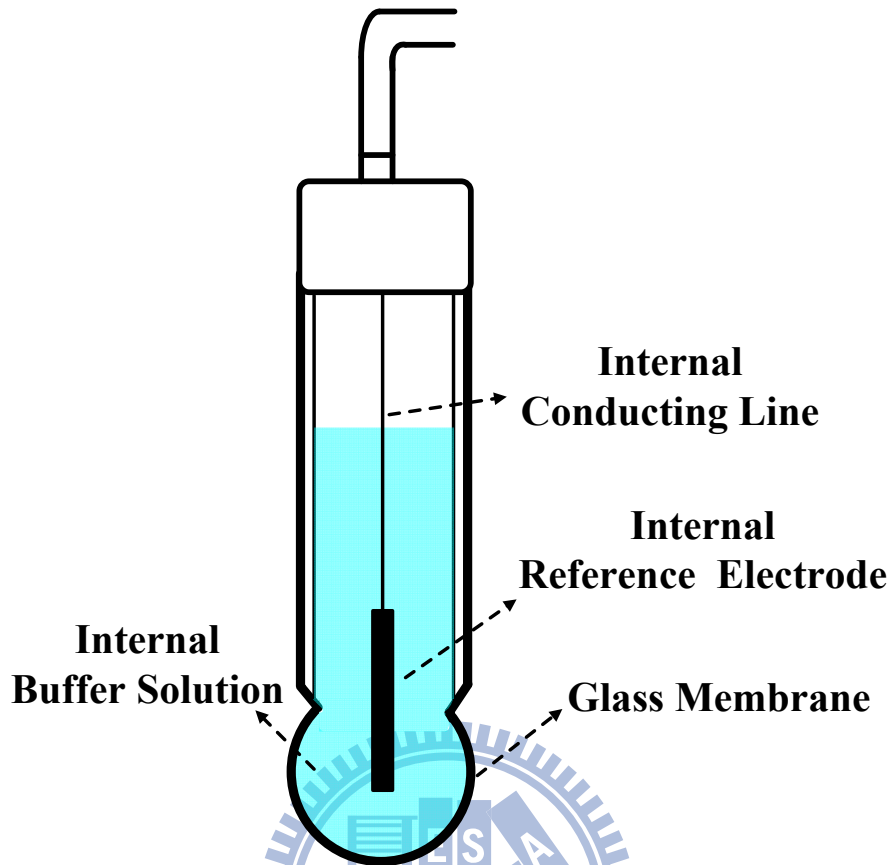


Fig. 1-1 Conventional pH glass electrode

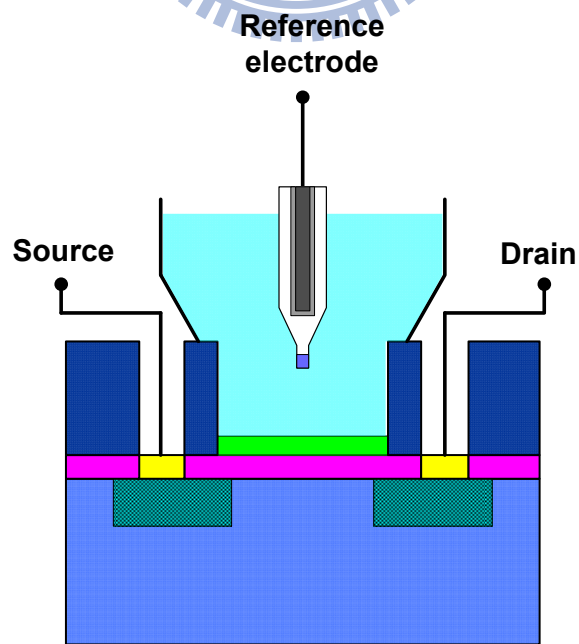


Fig. 1-2 Cross-Section Structure of ISFET

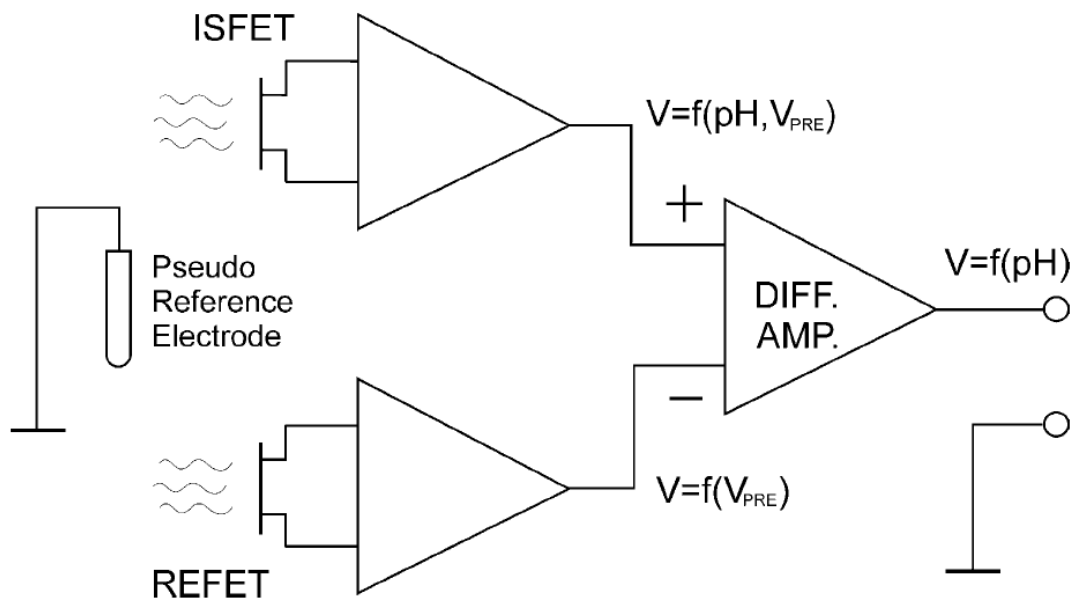


Fig. 1-3 Block diagram of a differential ISFET/REFET measuring system [11]

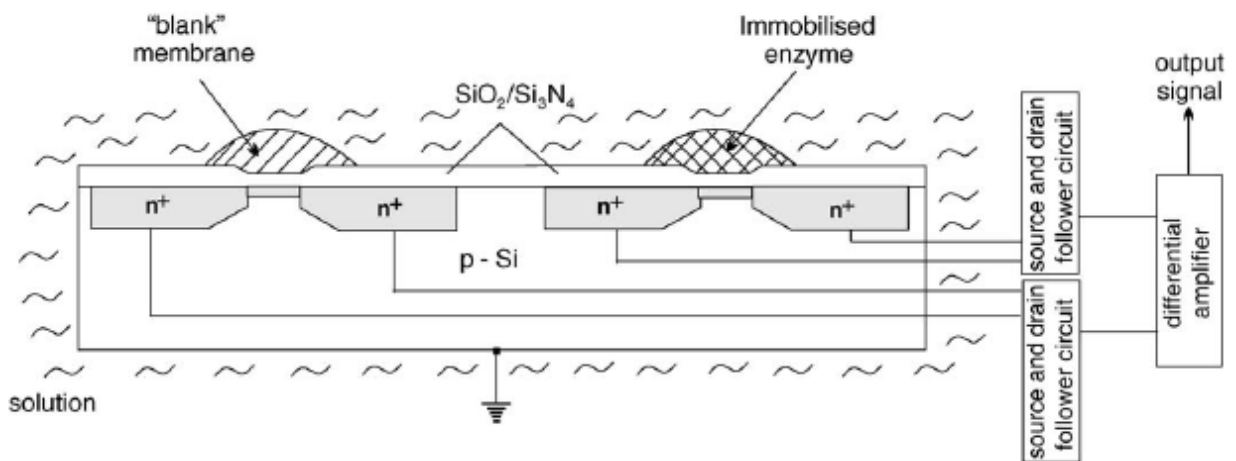


Fig. 1-4 Schematic representation of ENFET from R&D Institute of Microdevices [18]

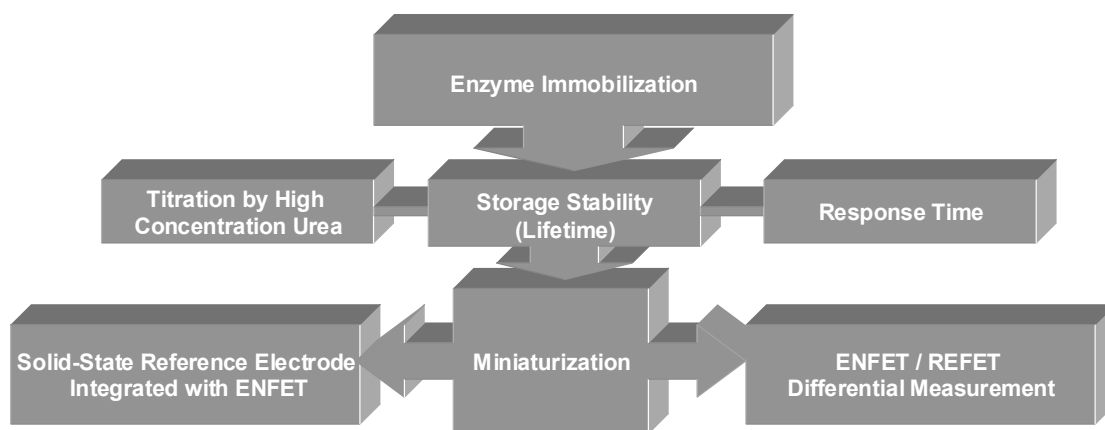


Fig. 1-5 Organization of thesis



Table 1-1 Sensitivity for different sensing layers

Sensing layer	Test range (pH)	Sensitivity (mV/pH)	Reference
ZrO <sub>2</sub>	1-13	57.5	5
SiO <sub>2</sub>	4-10	25-48	6
Si <sub>3</sub> N <sub>4</sub>	1-13	46-56	6
Al <sub>2</sub> O <sub>3</sub>	1-13	53-57	6
Ta <sub>2</sub> O <sub>5</sub>	1-13	56-57	6
SnO <sub>2</sub>	2-10	58	7

Table 1-2 Data on ENFETs developed [18]

	Substance tested	Enzyme
1	Glucose	Glucose oxidase
2	Urea	Urease
3	Penicillin	Penicillinase Penicillin G acylase
4	Acetylcholine	Acetylcholinesterase
5	Creatinine	Creatinine deiminase
6	4-Chlorophenol	Tyrosinase
7	Formaldehyde	Alcohol oxidase Aldehyde dehydrogenase
8	Hypochlorite	Acetylcholinesterase
9	Organophosphorous pesticides	Acetylcholinesterase Organophosphate hydrolase Organophosphorus acid anhydrolase
10	Heavy metal ions	Urease
11	Glycoalkaloids	Butyrylcholinesterase
12	Lactic acid	Lactate dehydrogenase
13	Lactose	Glucokinase/galactosidase
14	Threonine	Threoninedeiminase
15	L-glutamine acid	Glutamine synthetase
16	Total protein	Trypsin
17	Cyanide	Peroxidase



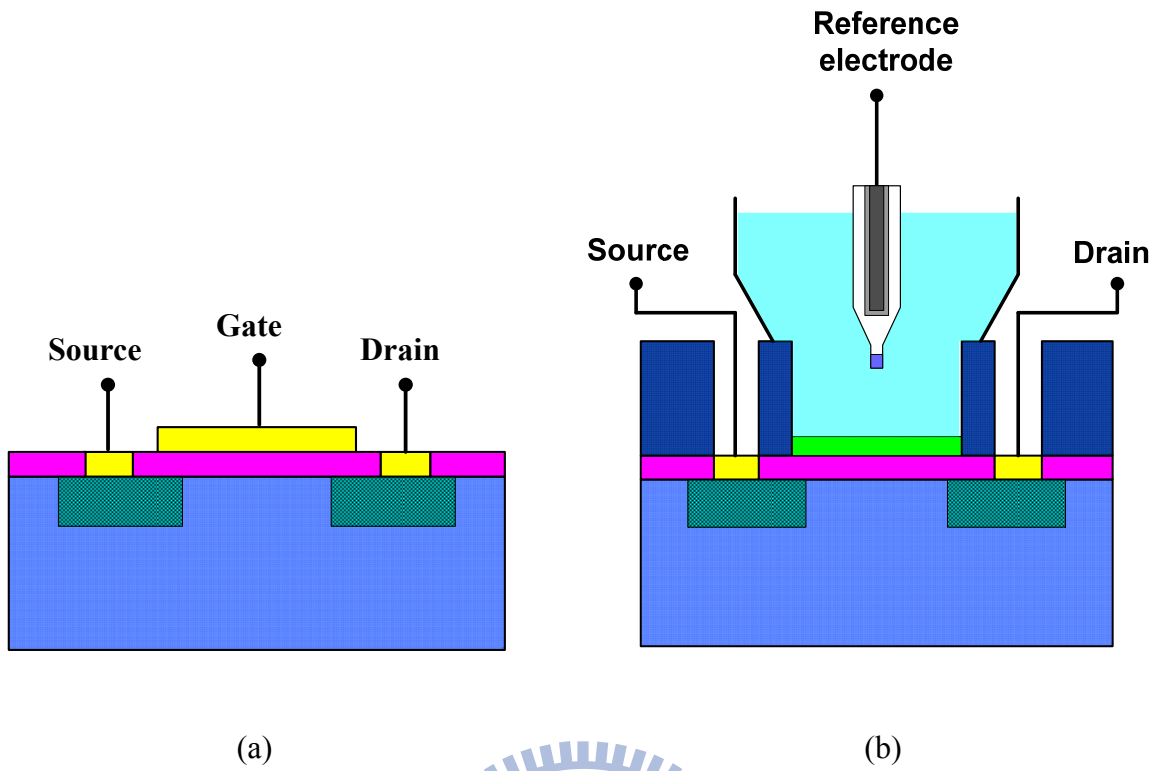


Fig. 2-1 Schematic representation of a MOSFET (a) and an ISFET (b) cross-section

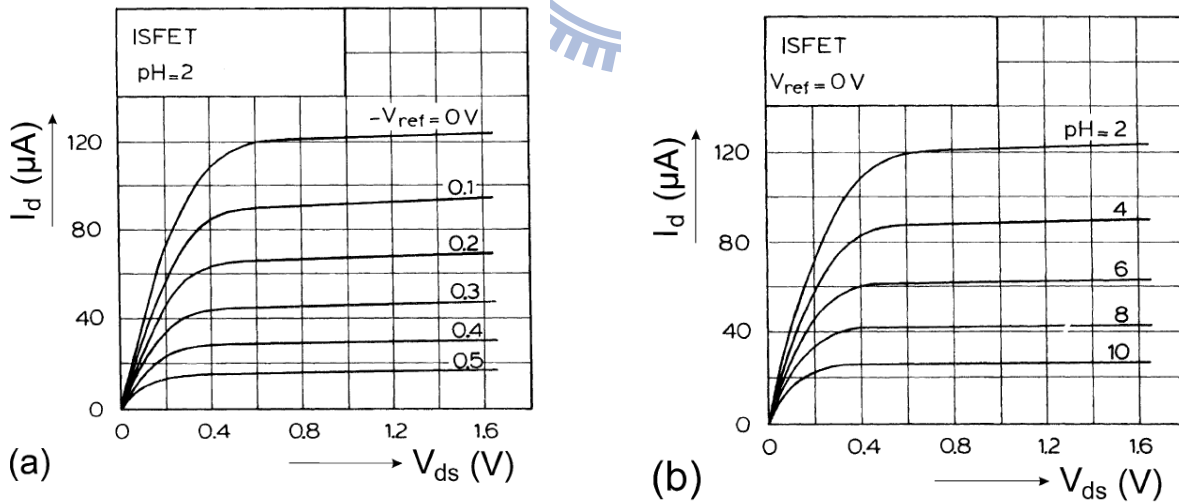


Fig. 2-2  $I_D$ - $V_{DS}$  curve of an ISFET with  $V_{gs}$ (a), and pH (b) as a parameter

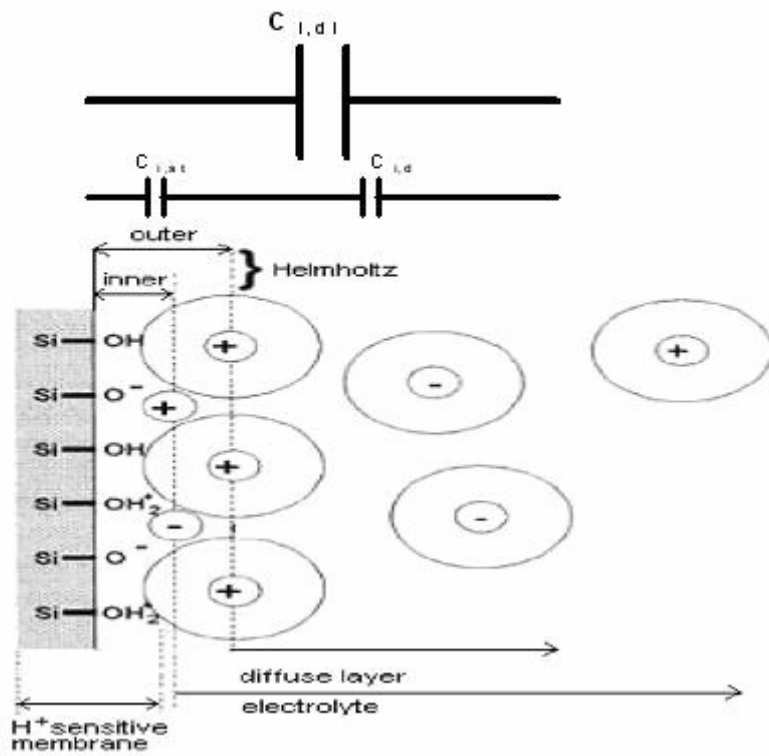


Fig. 2-3 Electrode and electrolyte interface

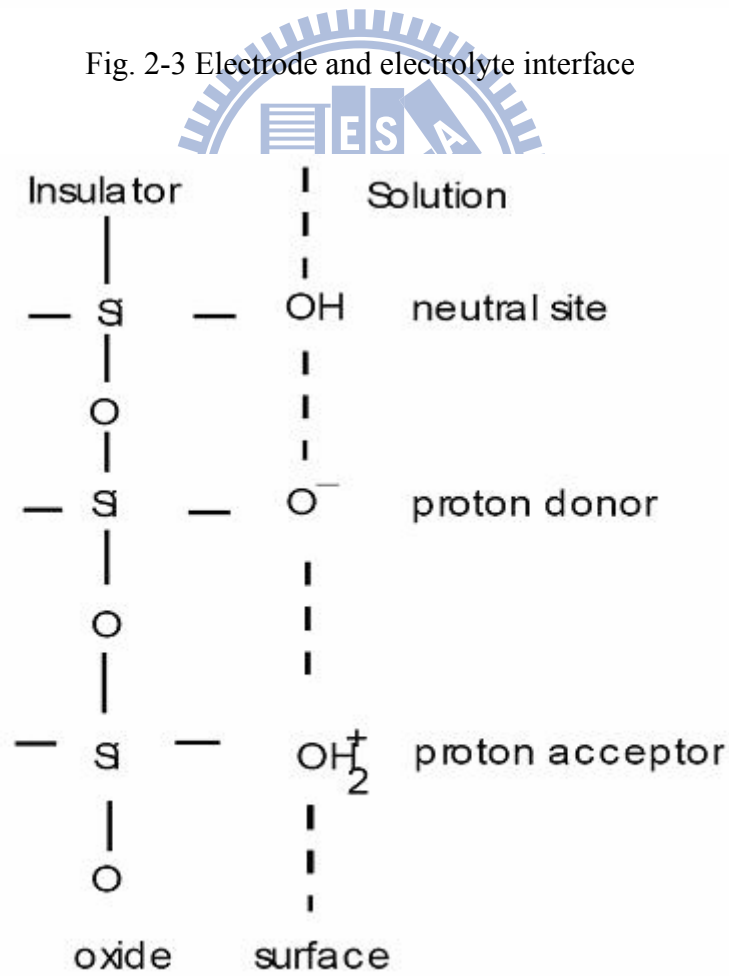


Fig. 2-4 Schematic representation of site-binding model

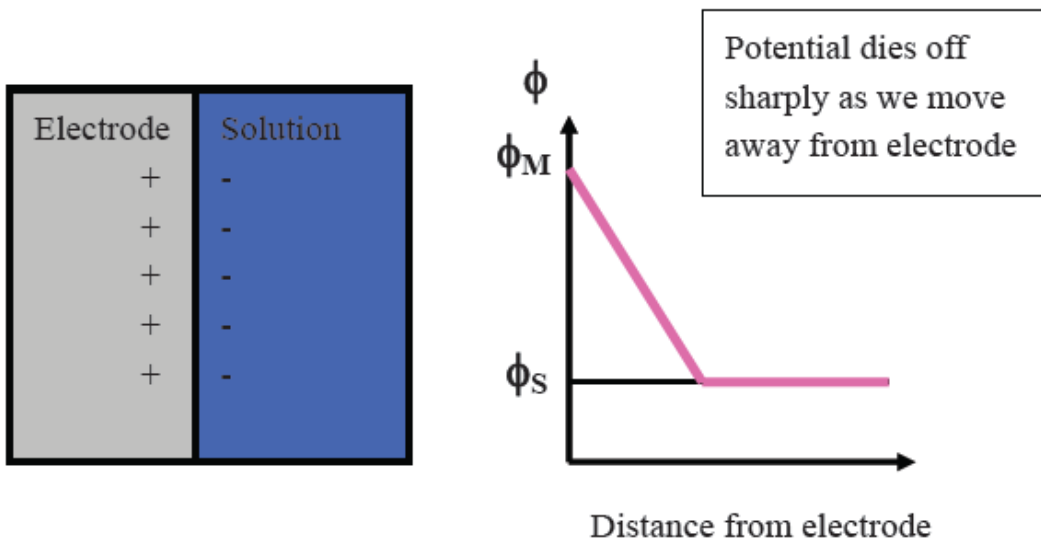


Fig. 2-5 Helmholtz model

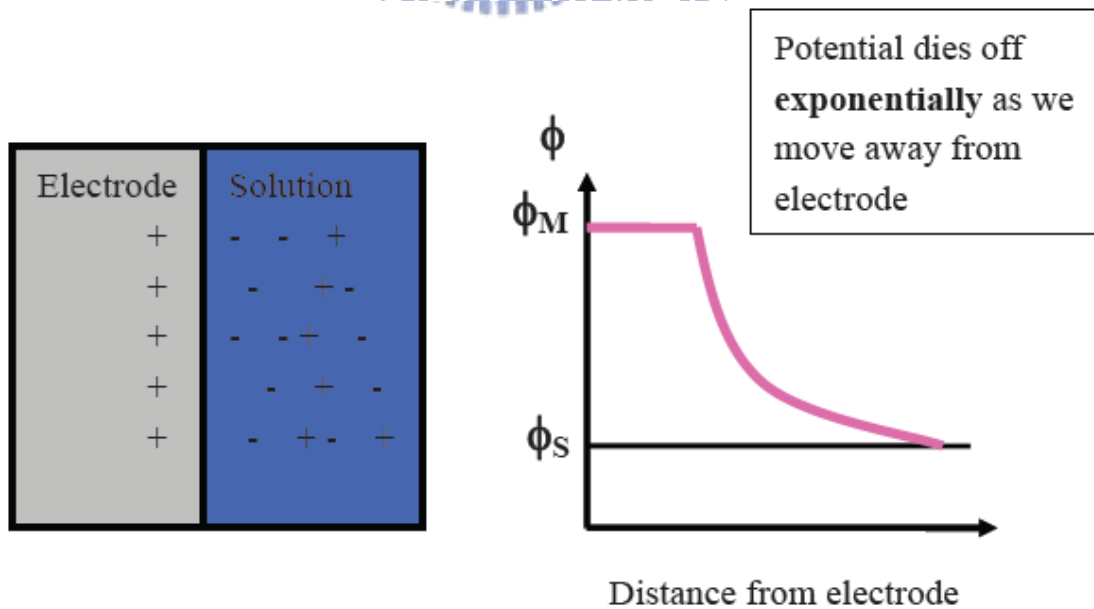


Fig. 2-6 Gouy-Chapman model

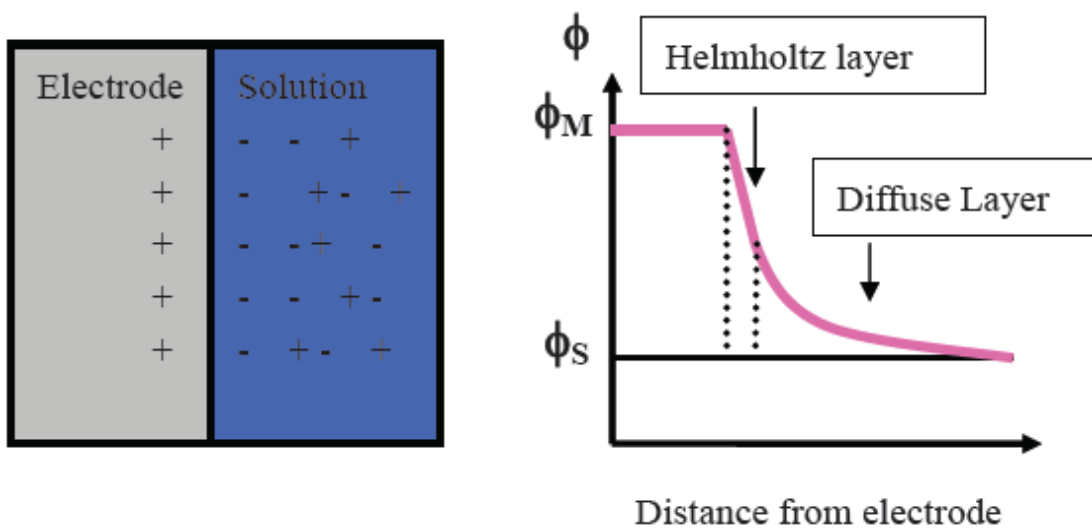


Fig. 2-7 Gouy-Chapman-Stern model

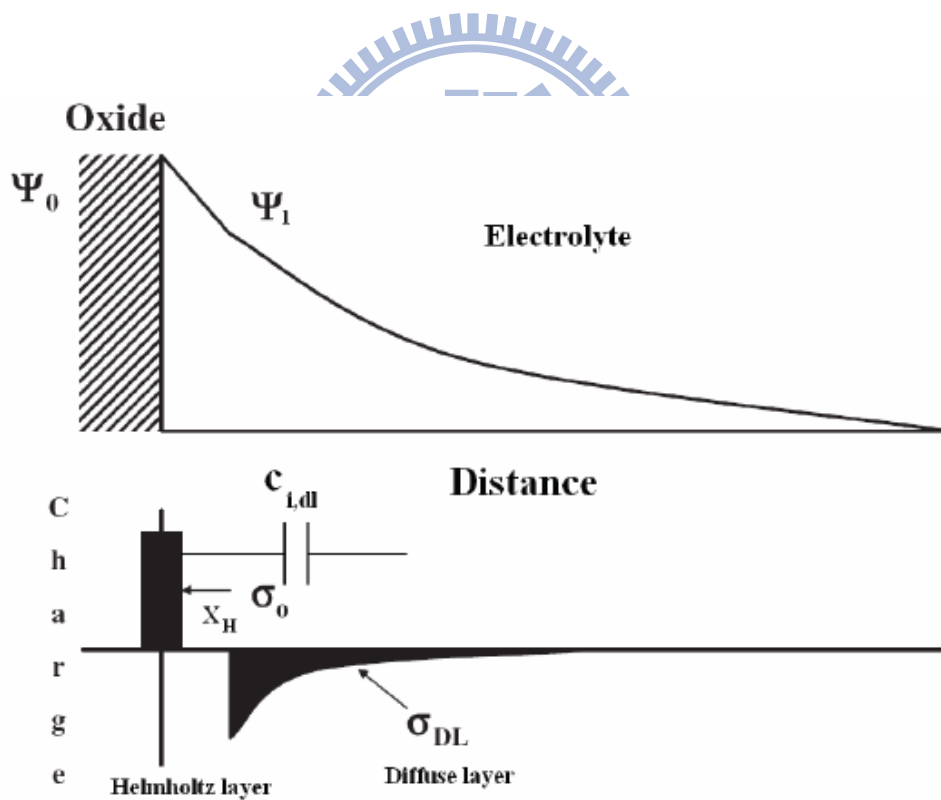


Fig. 2-8 Potential profile and charge distribution at an oxide/electrolyte solution interface

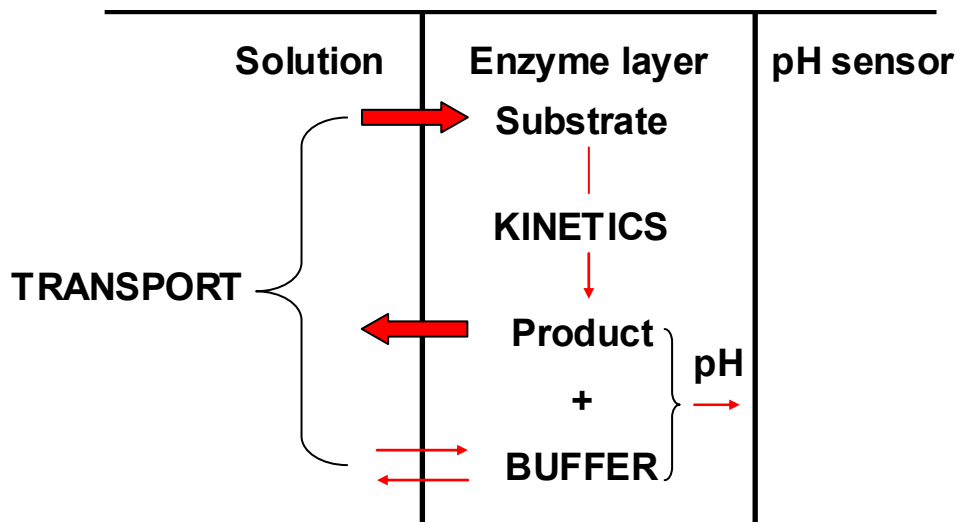


Fig. 2-9 Mechanisms involved in the response of pH-based enzyme sensors [14]

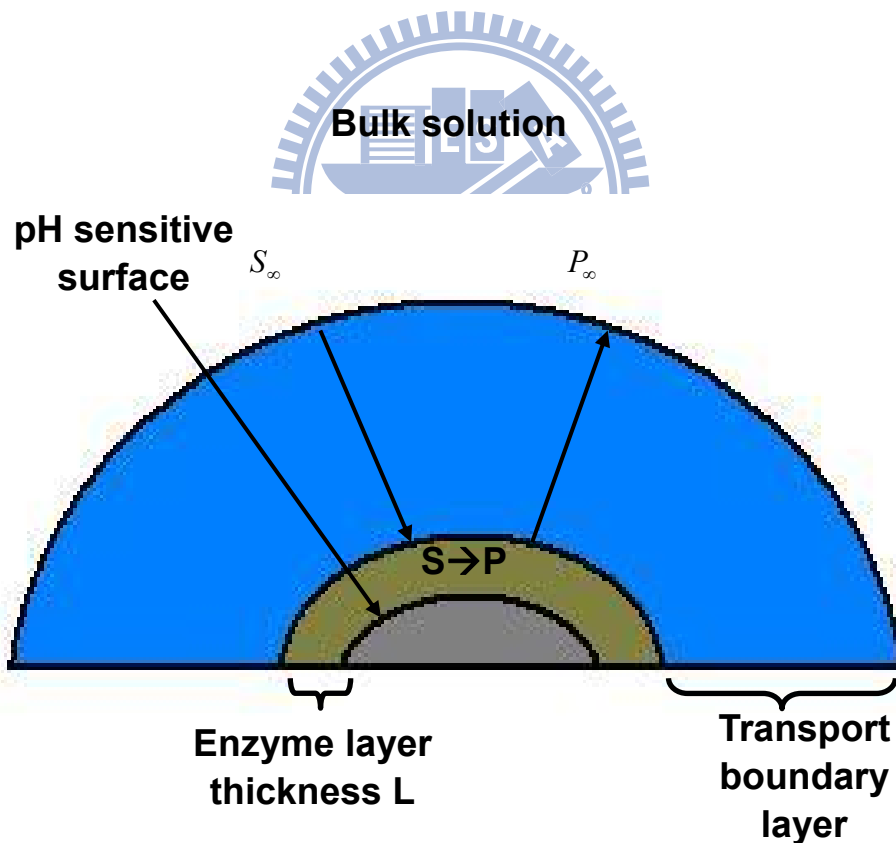


Fig. 2-10 Schematic representation of the potentiometric biosensor using an immobilized enzyme layer [14]

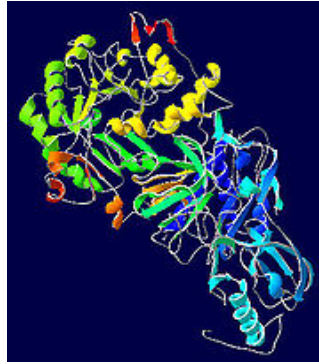


Fig. 3-1 The chemical structure of Helicobacter Pylori urease [1]

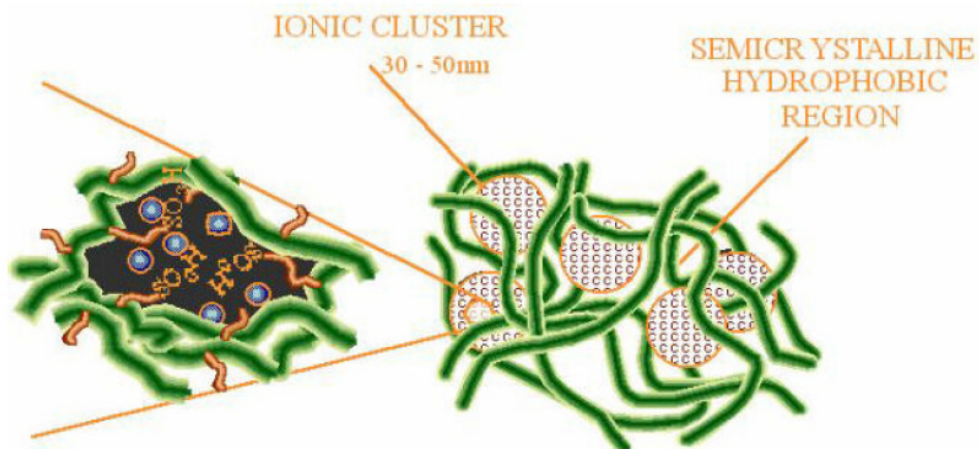
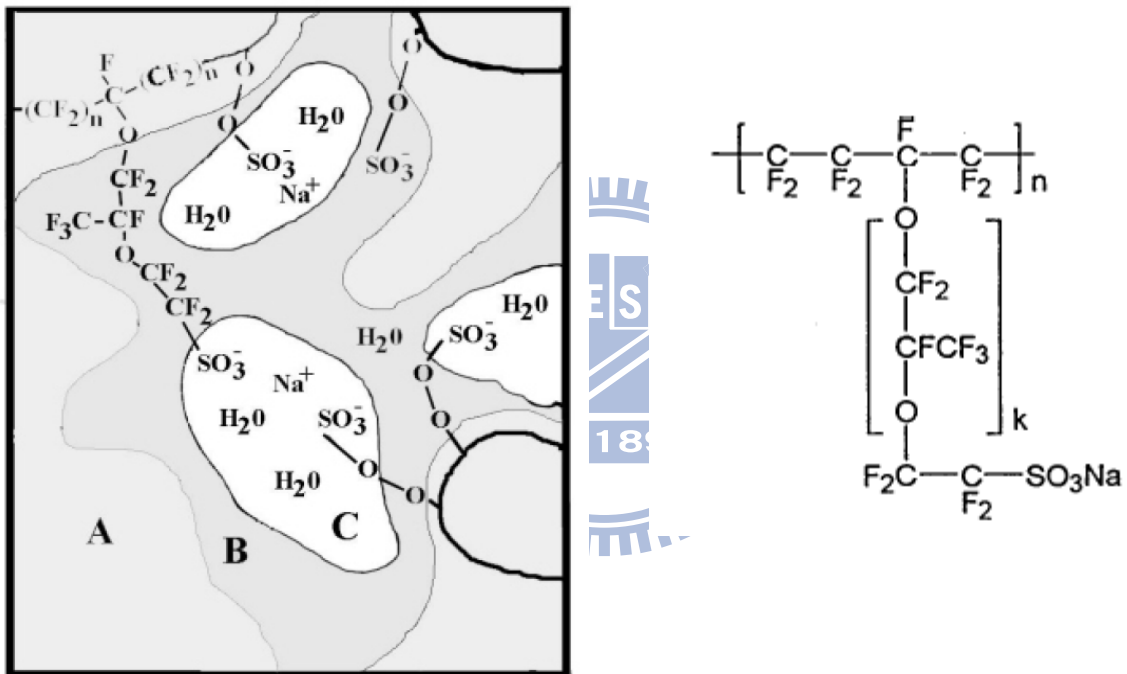
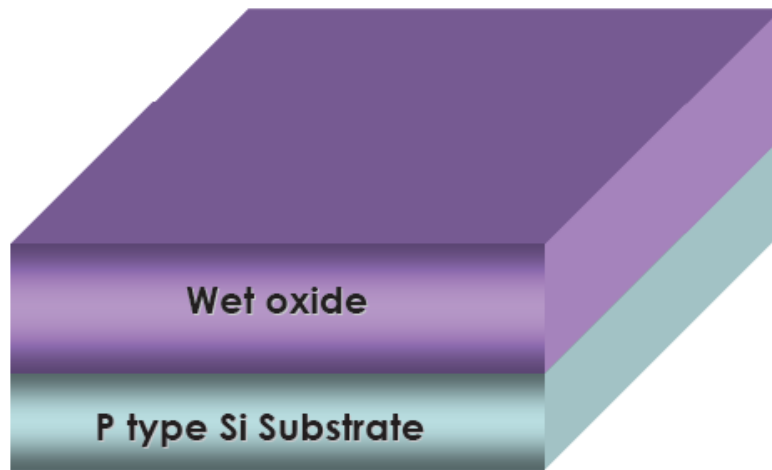
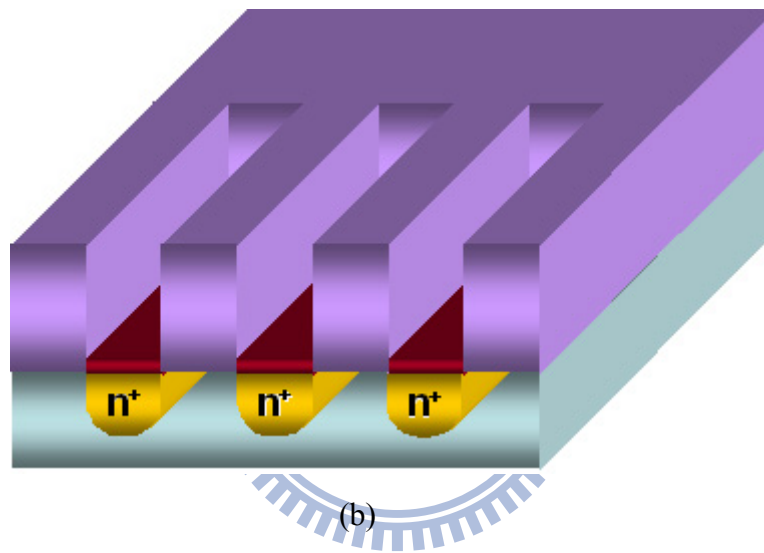


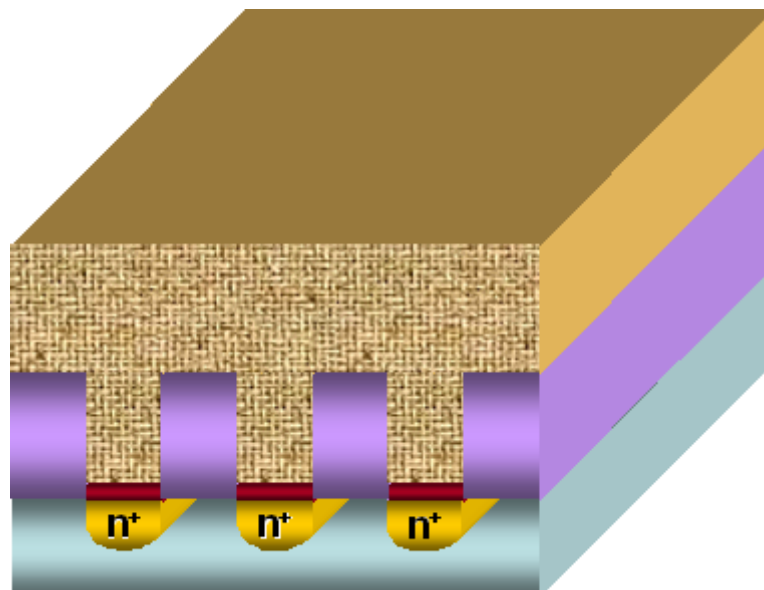
Fig. 3-2 Chemical structure and model of Nafion<sup>TM</sup>



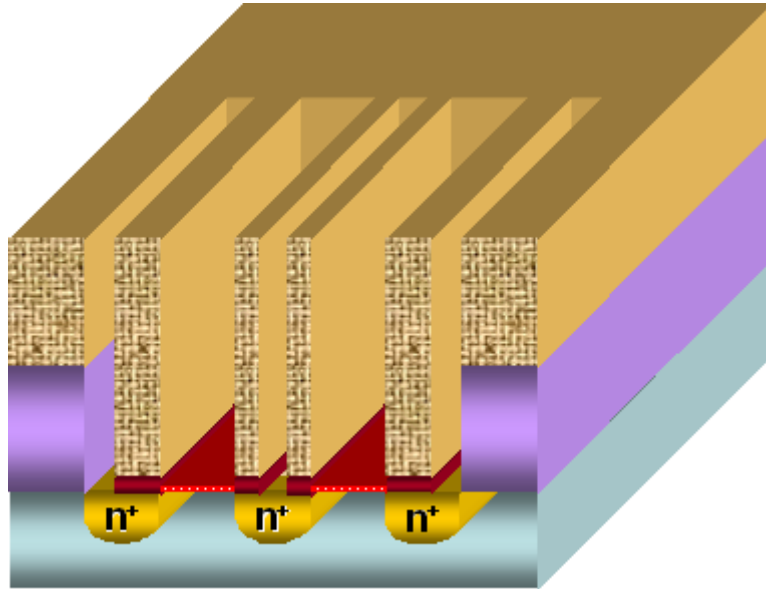
(a)



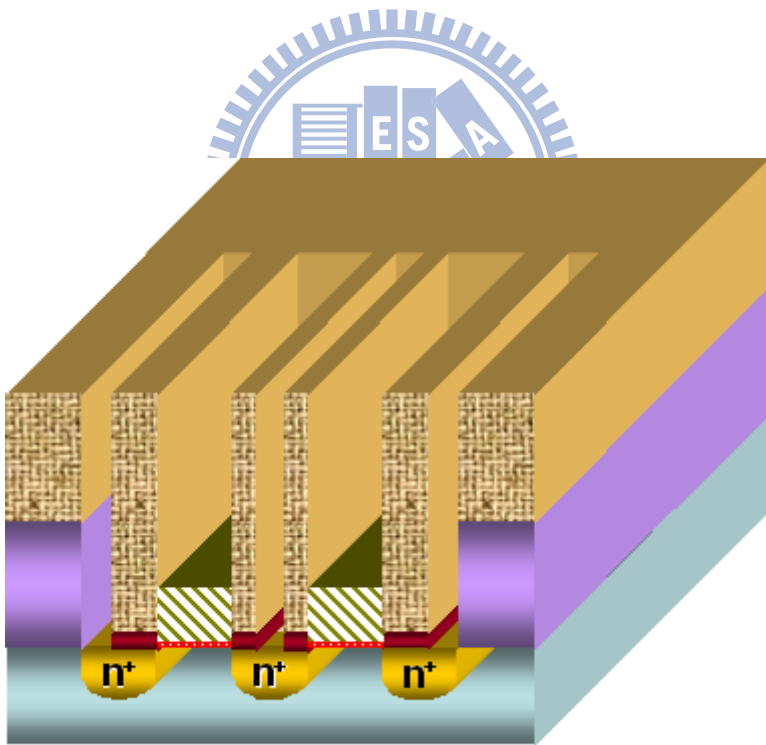
(b)



(c)

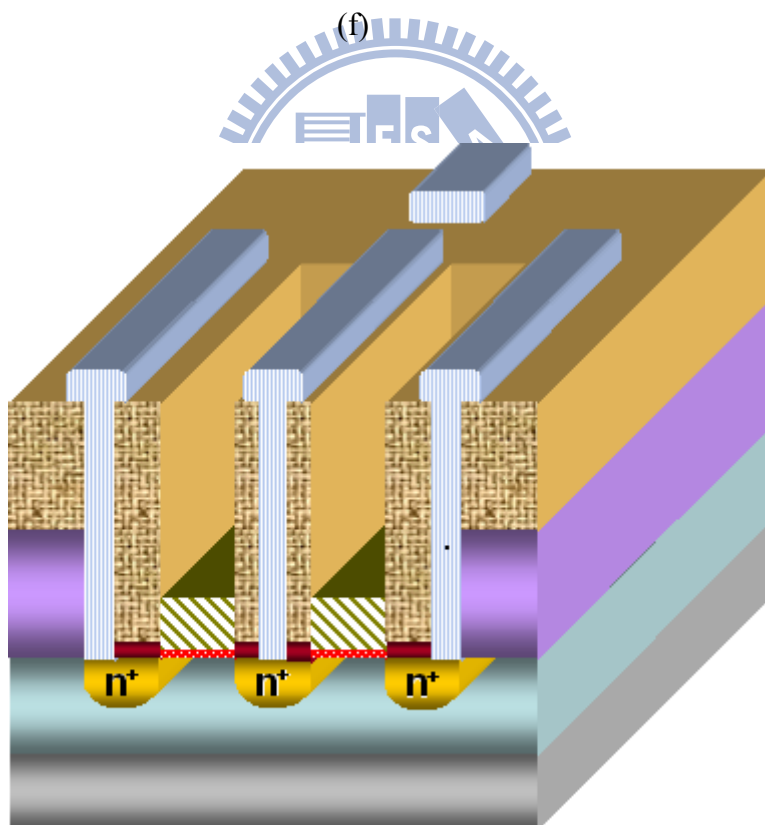
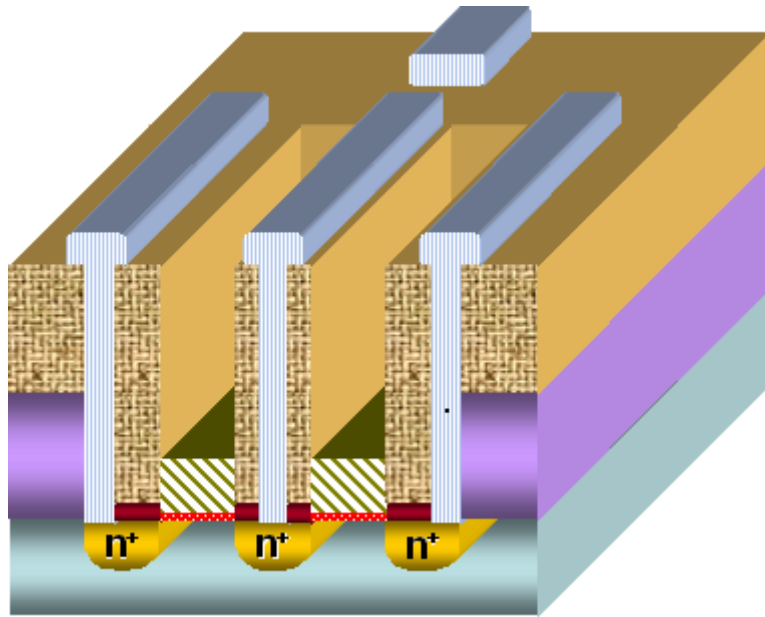


(d)



(e)





(g)

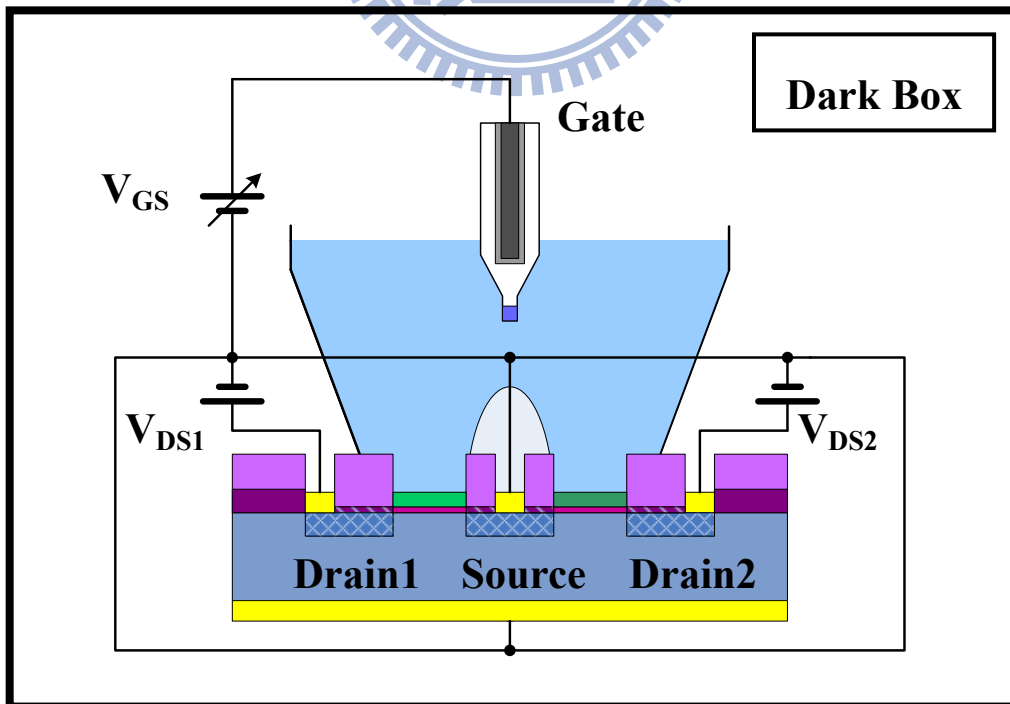
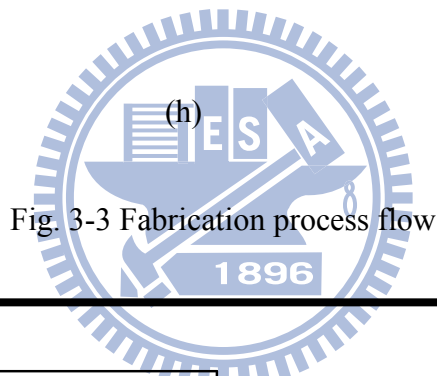
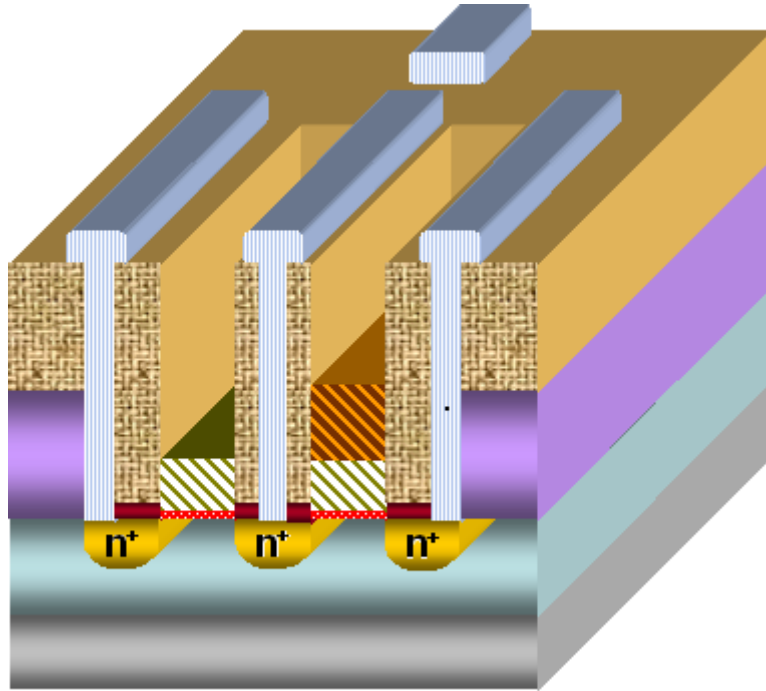


Fig. 3-4 Measurement set-up

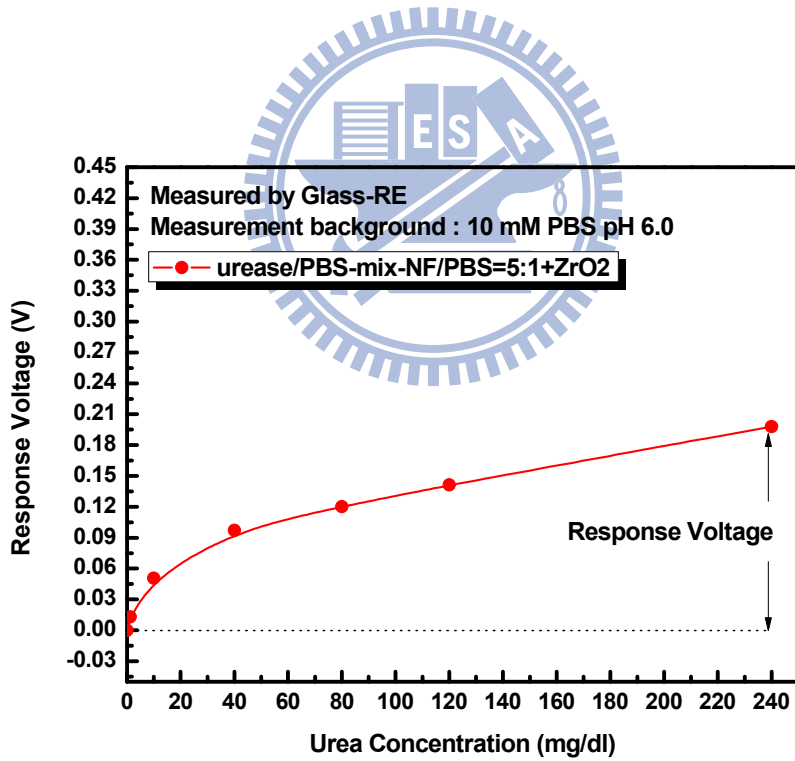
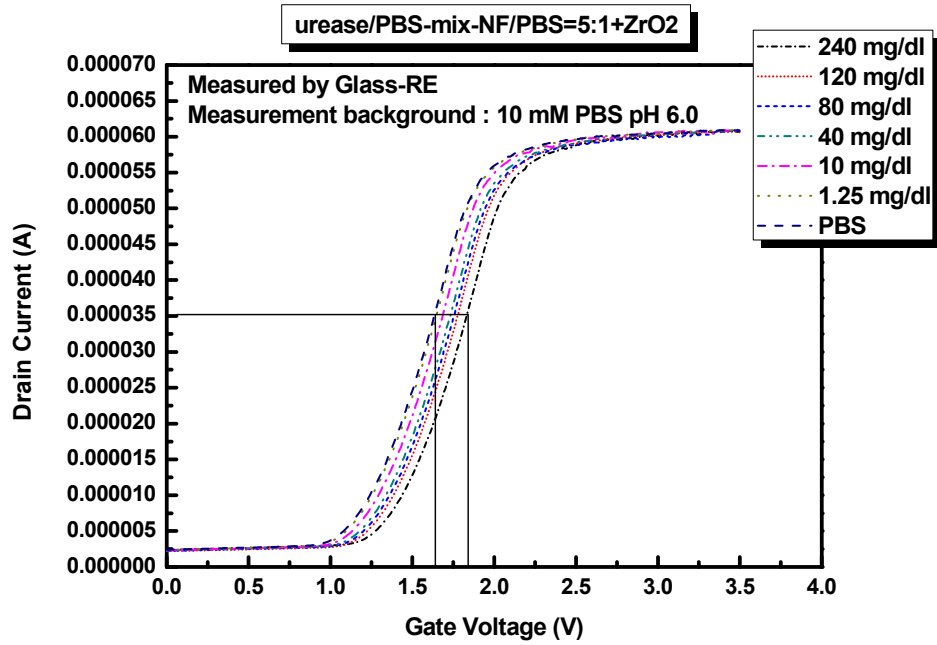


Fig. 3-5 Extraction method of sensing range and sensitivity

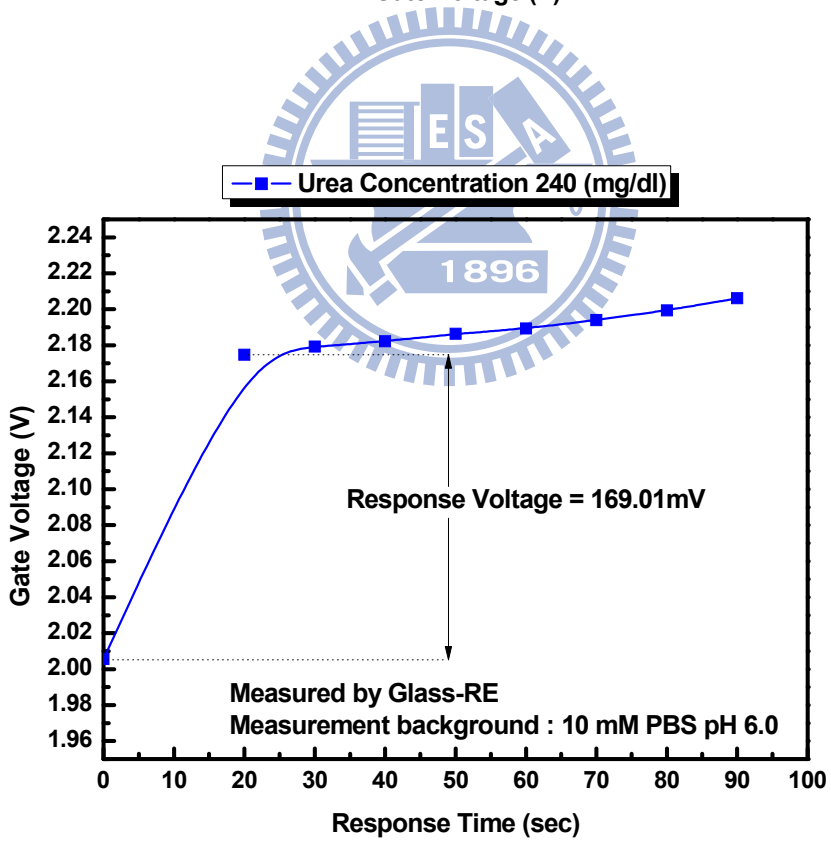
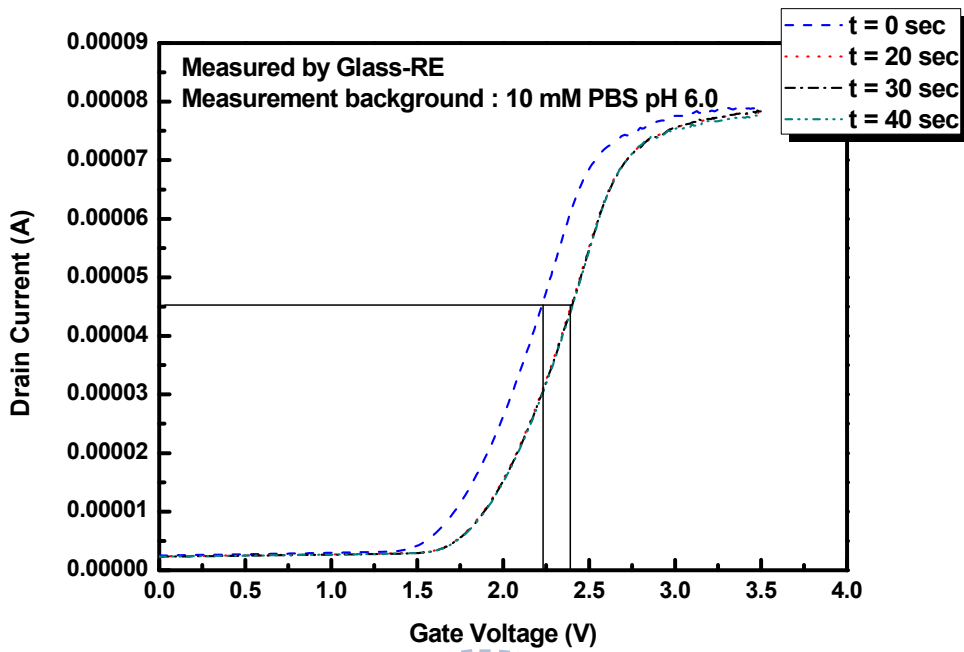


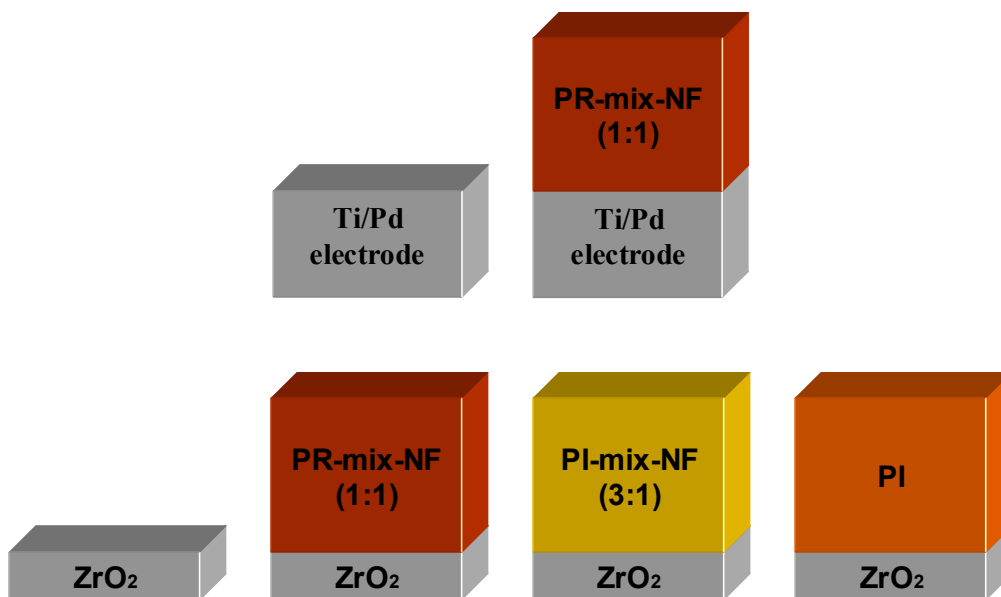
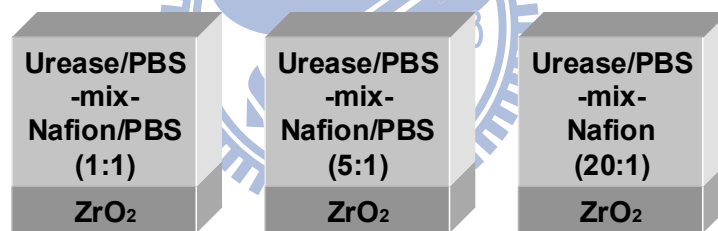
Fig. 3-6 Extraction method of response time

Table 3-1 ZrO<sub>2</sub> Sputtering parameters

parameters of ZrO <sub>2</sub> sputter
power : 110 W
Ar / O <sub>2</sub> flow rate : 24 / 8 ( sccm )
Density : 6.51
Acoustic impedance : 14.72
Tooling factor : 0.533
Rate : 0.2 Å / s
Pre-sputter 60W for 10 min
Pressure : $7.6 \times 10^{-3}$ torr

Table 3-2 Summary of test structures

	Test Structures		
<b>Enzyme Immobilization</b>	<b>Urease/PBS -mix- NF/PBS (1:1)</b>	<b>Urease/PBS -mix- NF/PBS (5:1)</b>	<b>Urease/PBS -mix- NF (20:1)</b>
<b>Solid-RE</b>	<b>Bare Ti/Pd Metal-RE</b>	<b>Ti/Pd/ PR-mix-NF Solid-RE</b>	
<b>ISFET</b>	<b>ZrO<sub>2</sub></b>		
<b>REFET</b>	<b>ZrO<sub>2</sub>/PR-mix-NF (1:1)</b>	<b>ZrO<sub>2</sub>/PI-mix-NF (3:1)</b>	<b>ZrO<sub>2</sub>/PI</b>



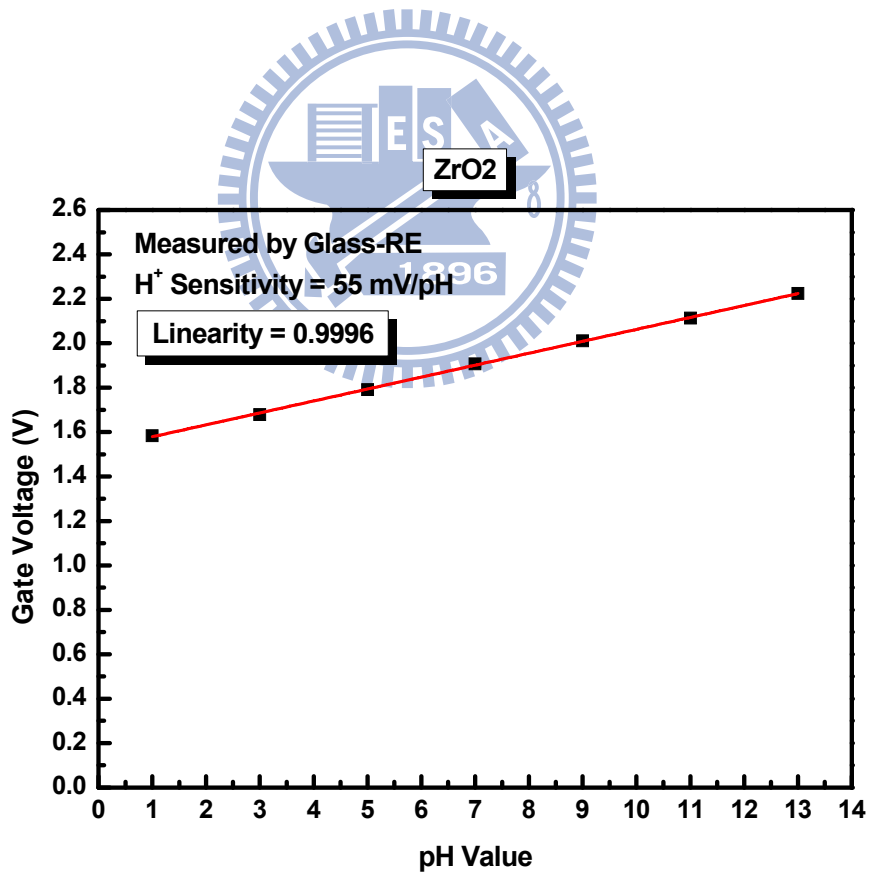
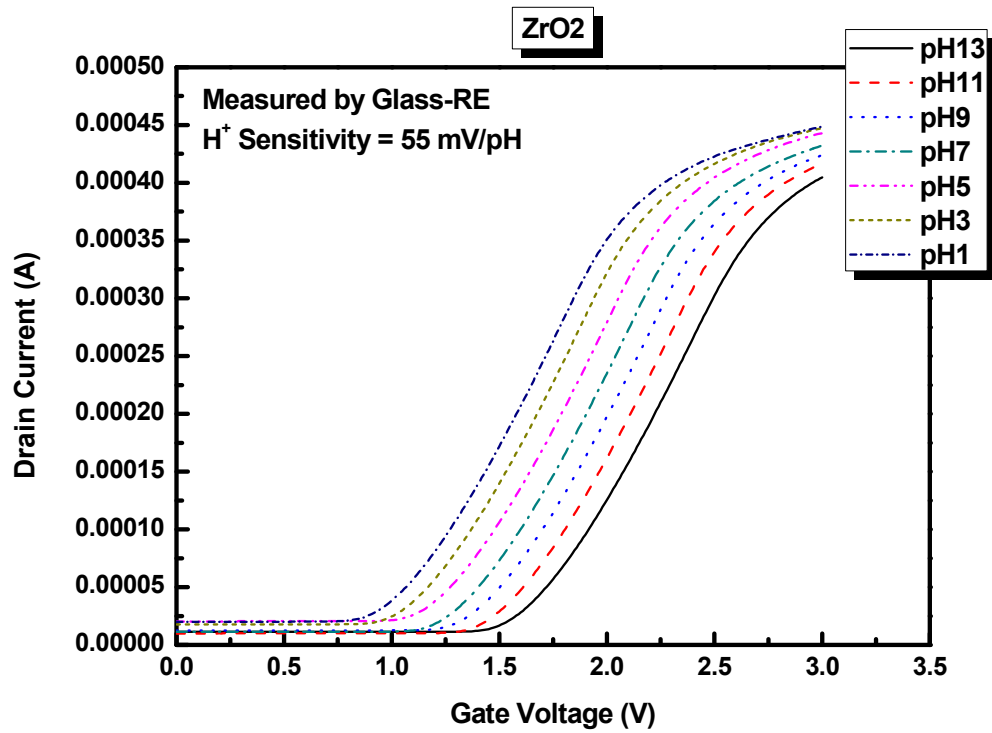


Fig. 4-1 The  $I_{DS}$ - $V_{GS}$  curves and sensitivity linearity of  $ZrO_2$ -pH-ISFET measure by glass reference electrode

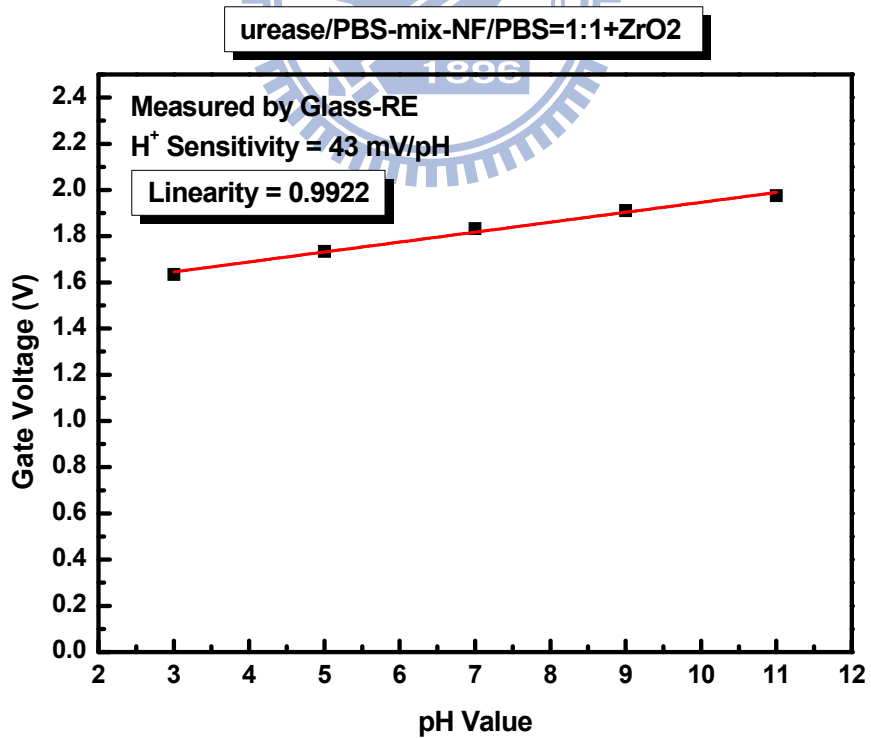
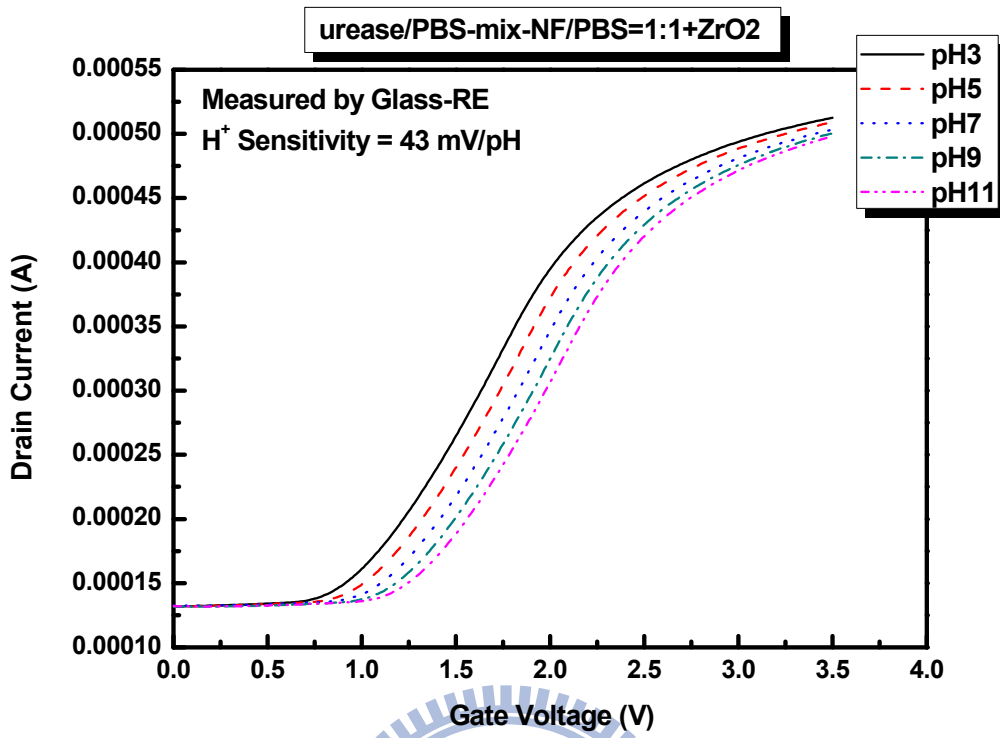


Fig. 4-2 The  $I_{DS}$ - $V_{GS}$  curves and sensitivity linearity of  $ZrO_2$ /urease-mix-NF urea-ENFET measure by glass reference electrode



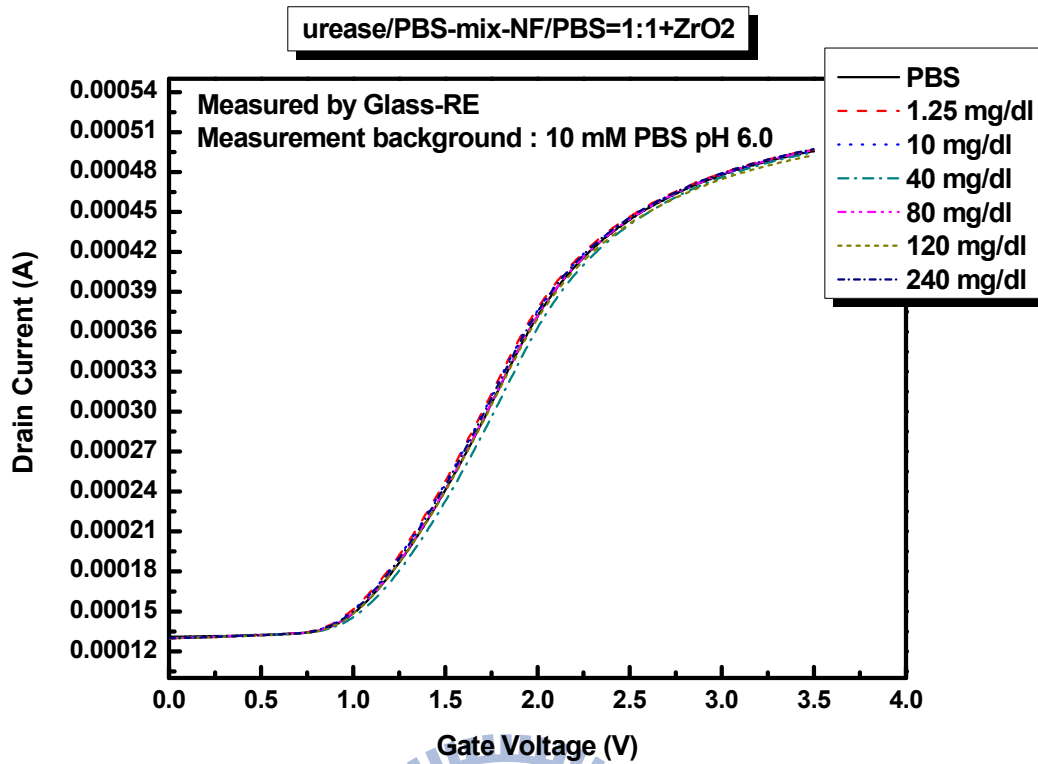


Fig. 4-3 The  $I_{DS}$ - $V_{GS}$  curves of  $ZrO_2$ /urease-mix-NF(1:1) urea-ENFET measure by glass reference electrode

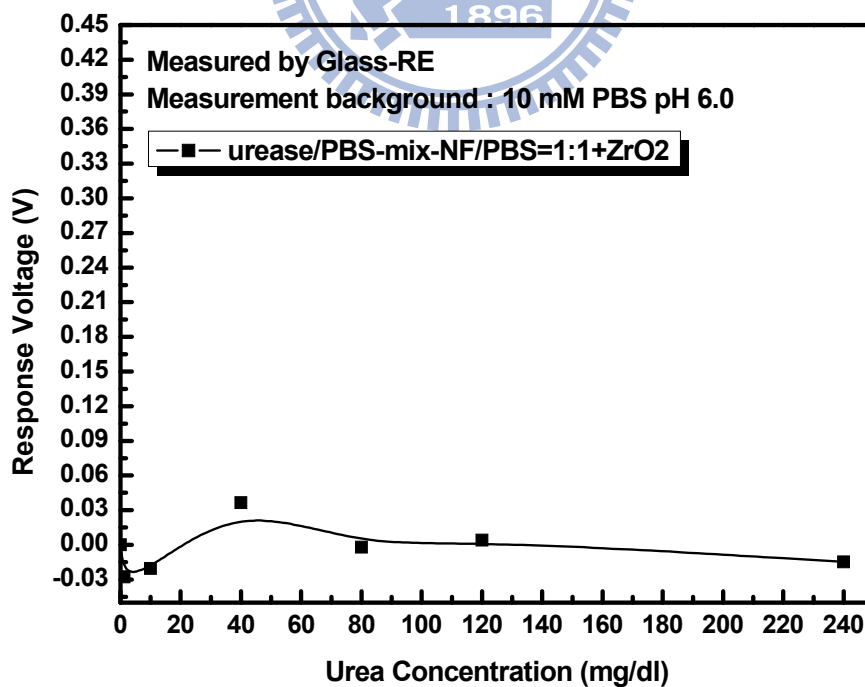


Fig. 4-4 Calibration curve of  $ZrO_2$ /urease-mix-NF(1:1) urea-ENFET measure by glass reference electrode

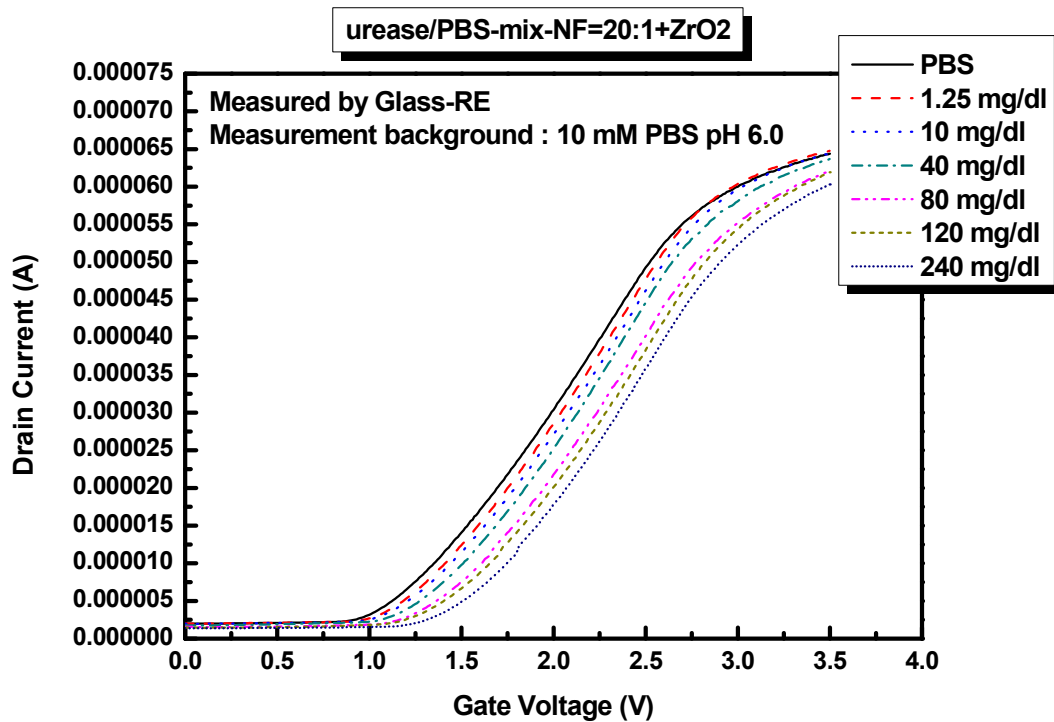


Fig. 4-5 The  $I_{DS}$ - $V_{GS}$  curves of  $ZrO_2$ /urease-mix-NF(20:1) urea-ENFET measure by glass reference electrode

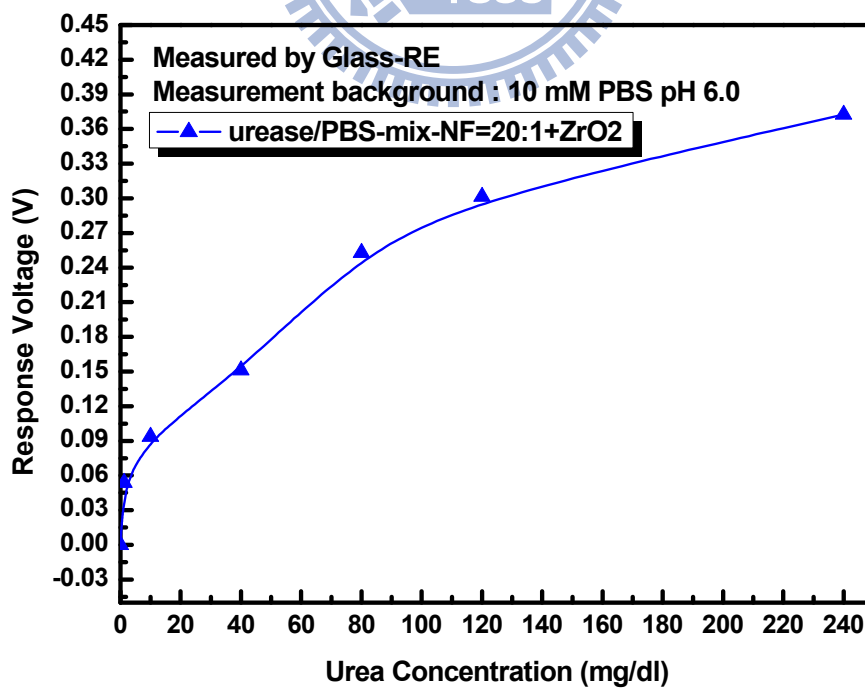


Fig. 4-6 Calibration curve of  $ZrO_2$ /urease-mix-NF(20:1) urea-ENFET measure by glass reference electrode

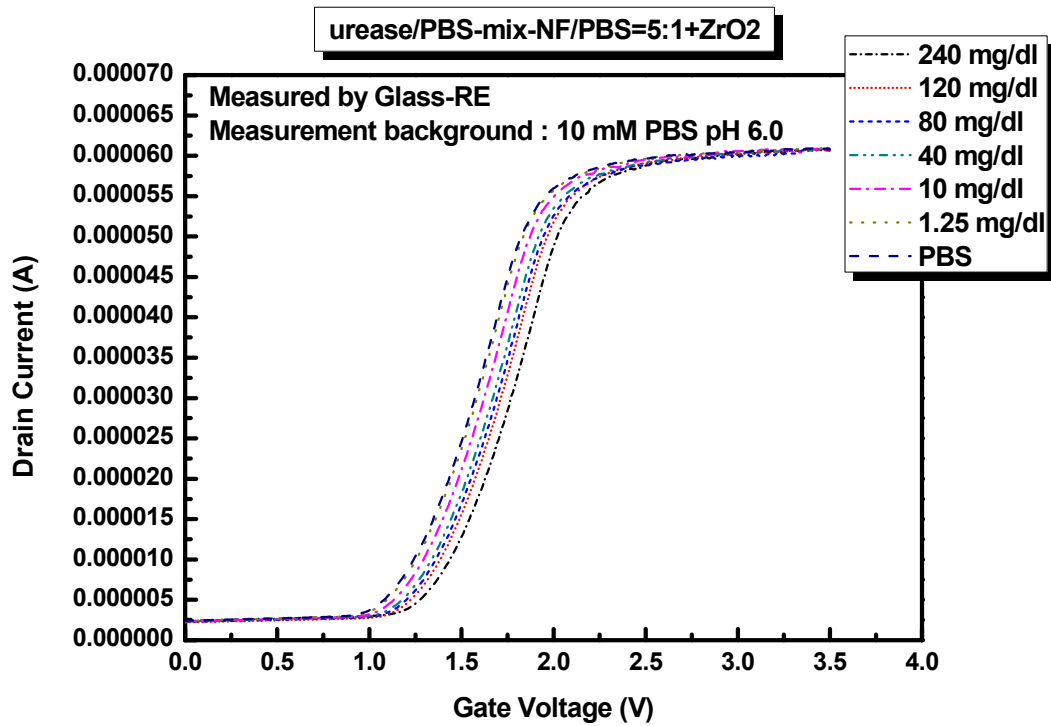


Fig. 4-7 The  $I_{DS}$ - $V_{GS}$  curves of  $ZrO_2$ /urease-mix-NF(5:1) urea-ENFET measure by glass reference electrode

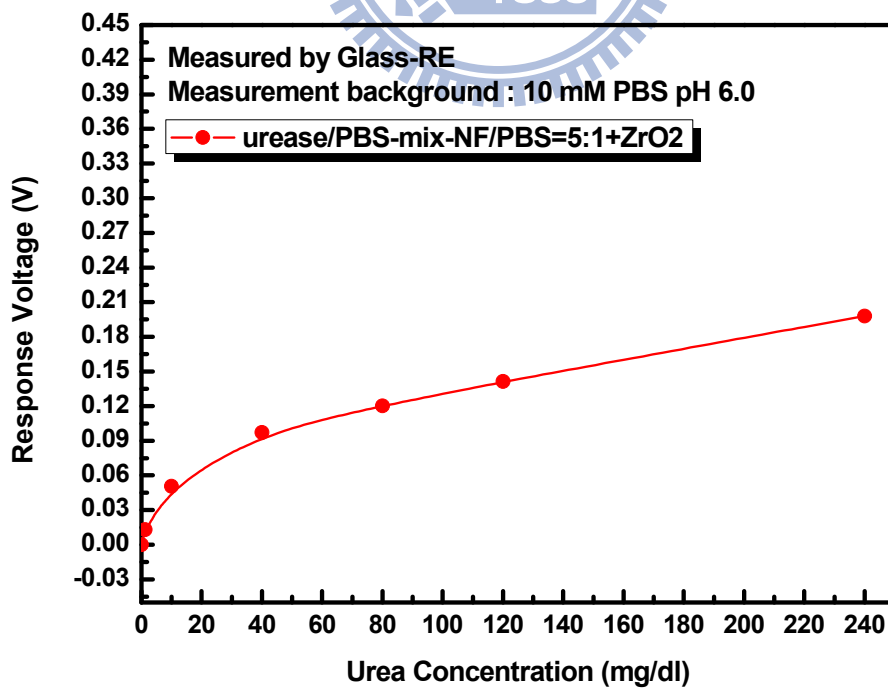


Fig. 4-8 Calibration curve of  $ZrO_2$ /urease-mix-NF(5:1) urea-ENFET measure by glass reference electrode

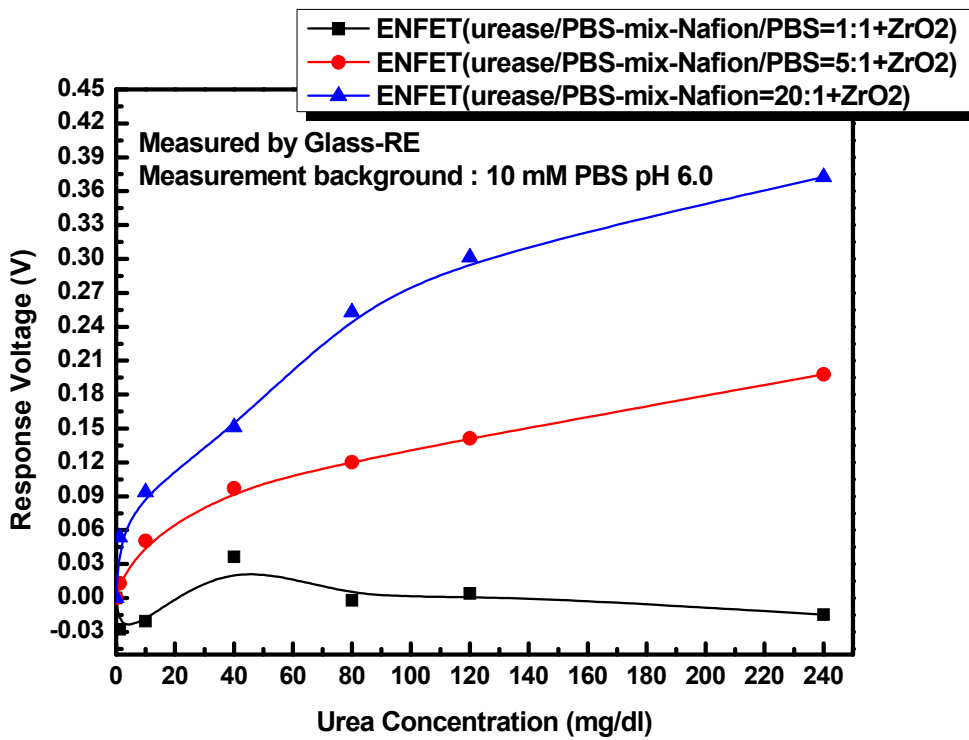


Fig. 4-9 Calibration curves of ZrO<sub>2</sub>/urease-mix-NF urea-ENFET measure by glass reference electrode

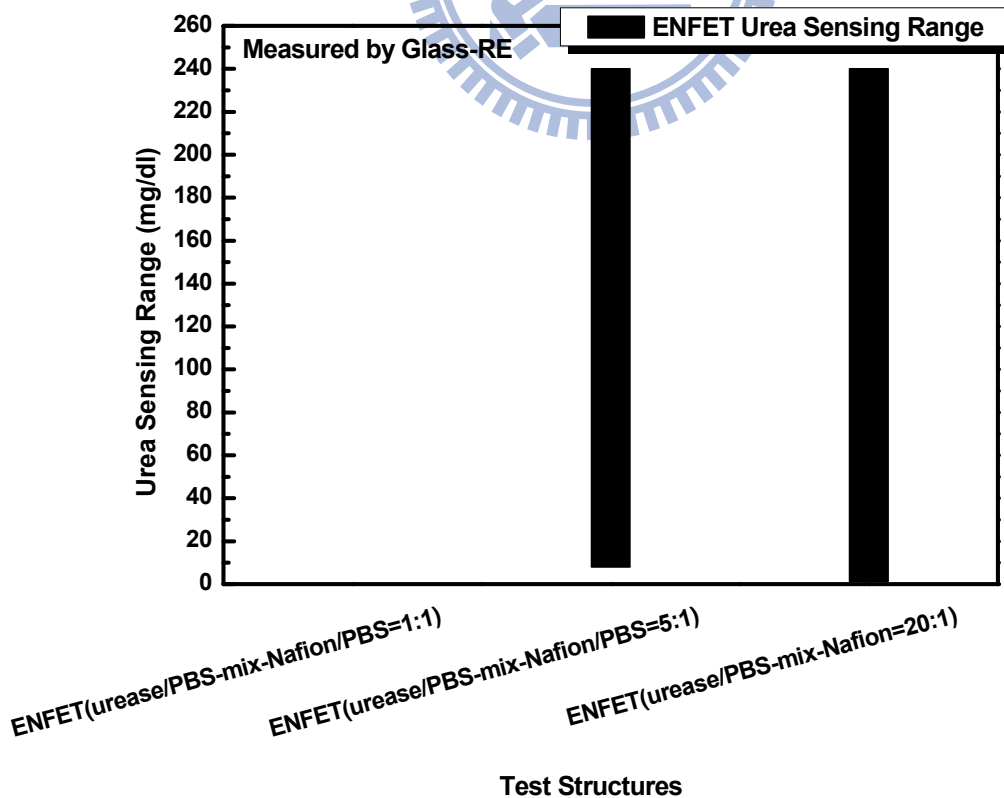


Fig. 4-10 Summary of urea sensing range for different test structures

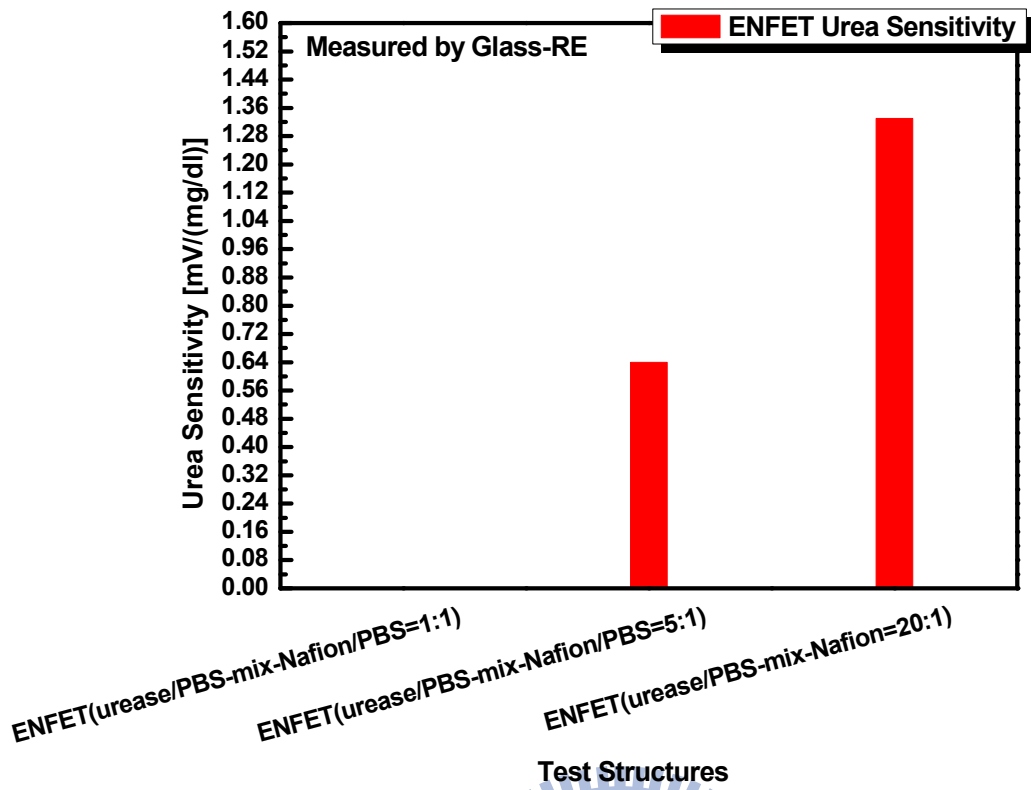


Fig. 4-11 Summary of urea sensitivity for different test structures

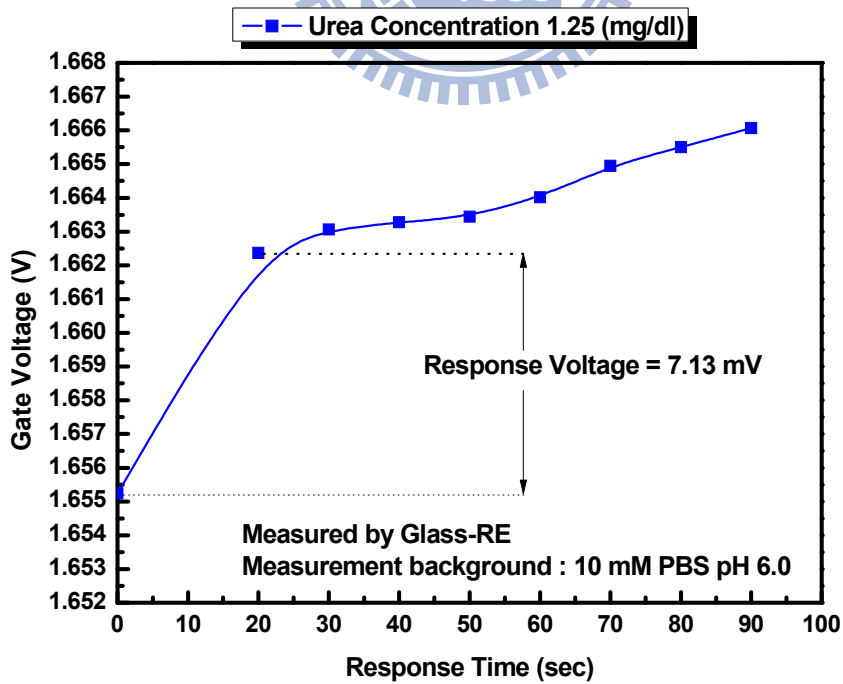


Fig. 4-12 Response signals of  $ZrO_2$ /urease-mix-NF(5:1) urea-ENFET with 1.25 mg/dl urea concentration

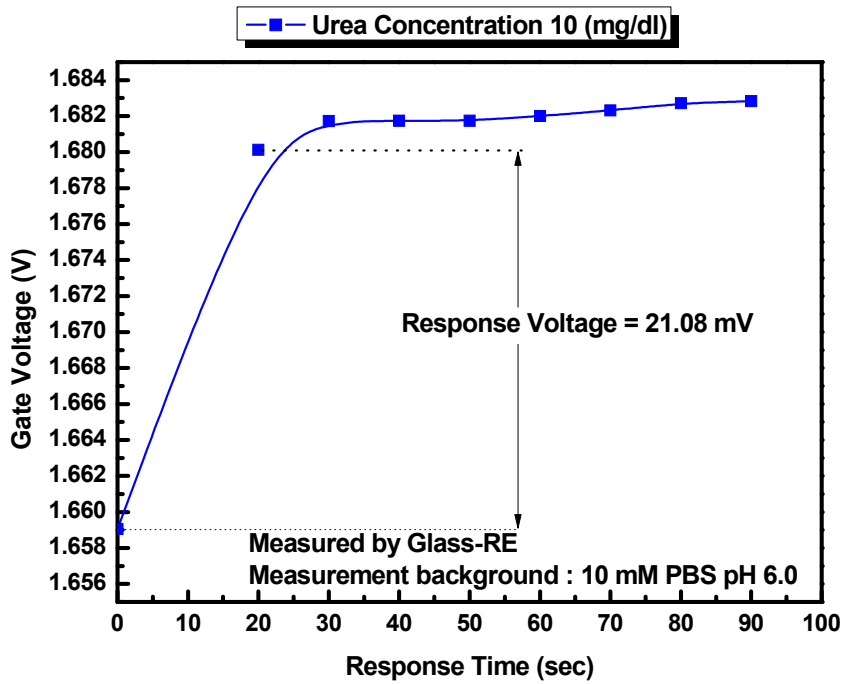


Fig. 4-13 Response signals of  $ZrO_2$ /urease-mix-NF(5:1) urea-ENFET with 10 mg/dl urea concentration

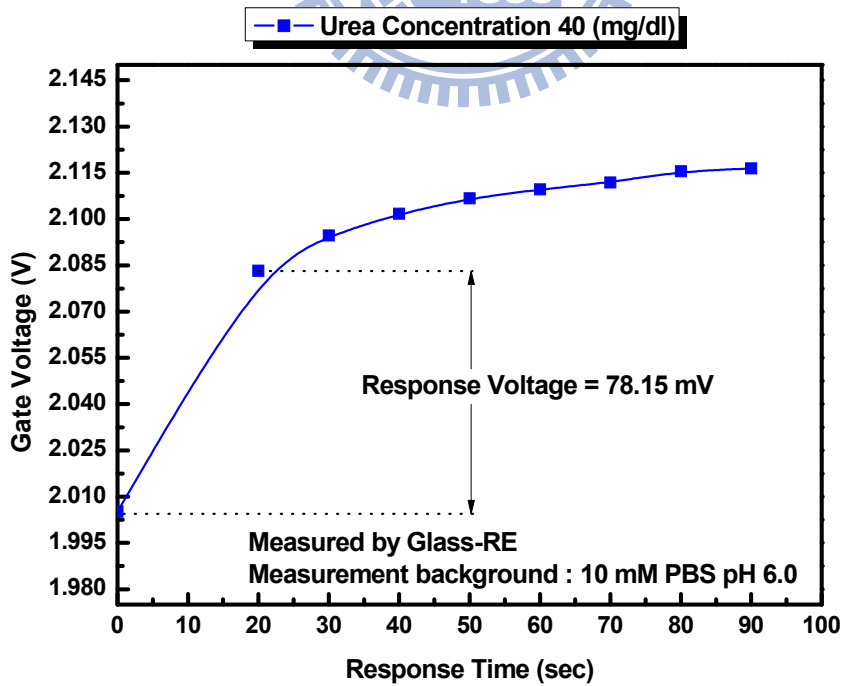


Fig. 4-14 Response signals of  $ZrO_2$ /urease-mix-NF(5:1) urea-ENFET with 40 mg/dl urea concentration

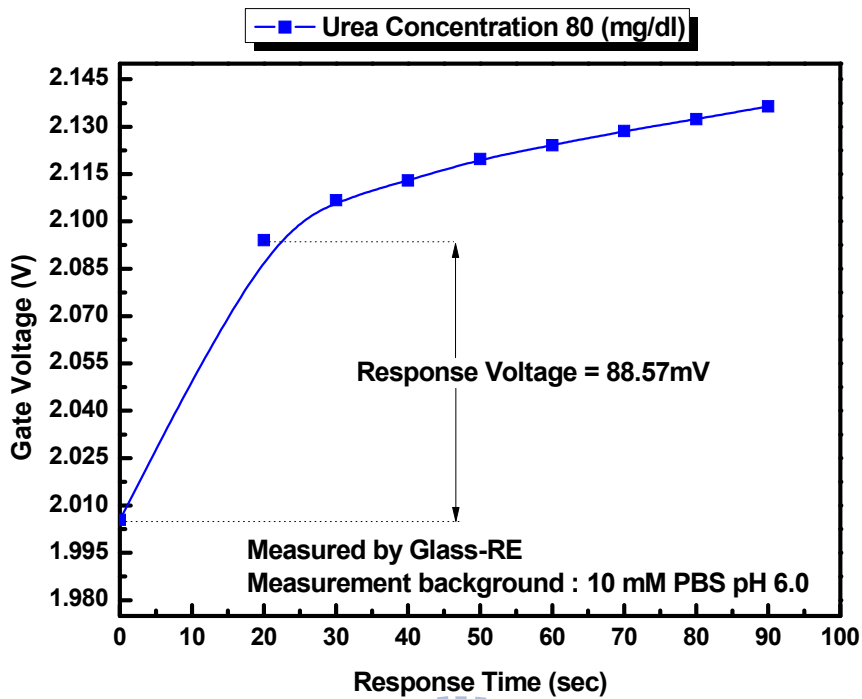


Fig. 4-15 Response signals of  $ZrO_2$ /urease-mix-NF(5:1) urea-ENFET with 80 mg/dl urea concentration

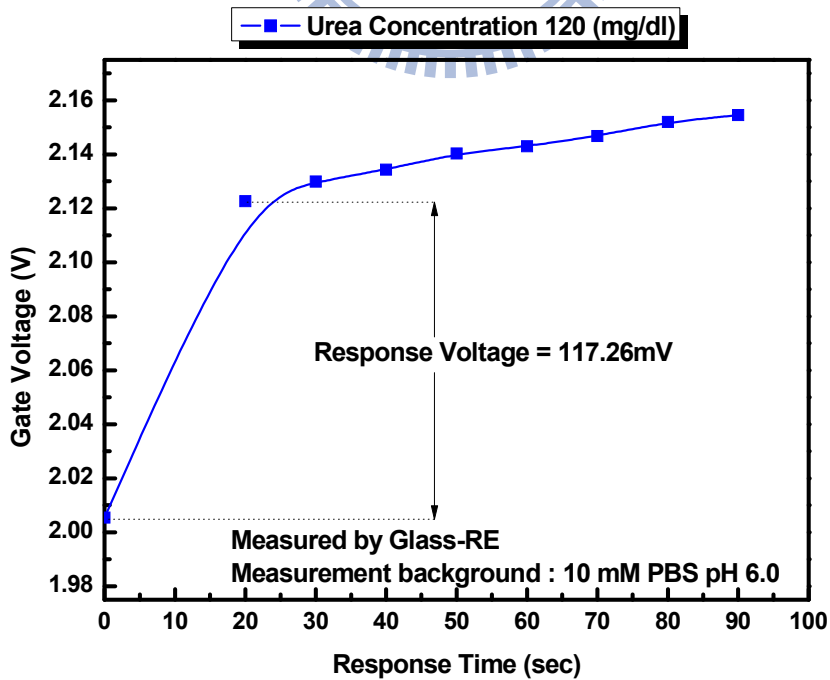


Fig. 4-16 Response signals of  $ZrO_2$ /urease-mix-NF(5:1) urea-ENFET with 120 mg/dl urea concentration

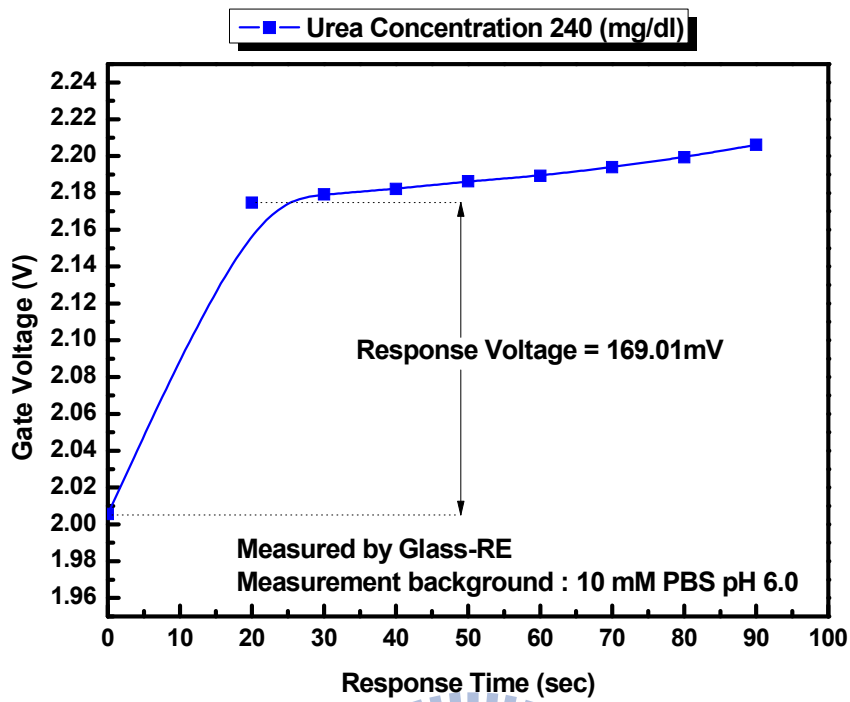


Fig. 4-17 Response signals of  $ZrO_2$ /urease-mix-NF(5:1) urea-ENFET with 240 mg/dl urea concentration

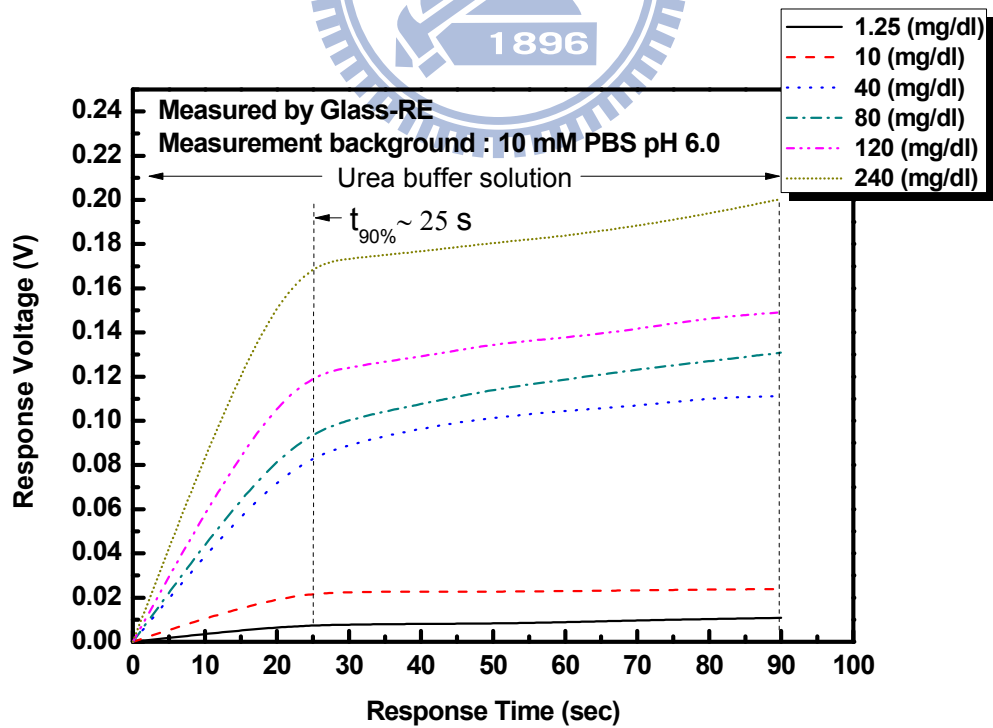


Fig. 4-18 Response signals of  $ZrO_2$ /urease-mix-NF(5:1) urea-ENFET with different urea concentrations



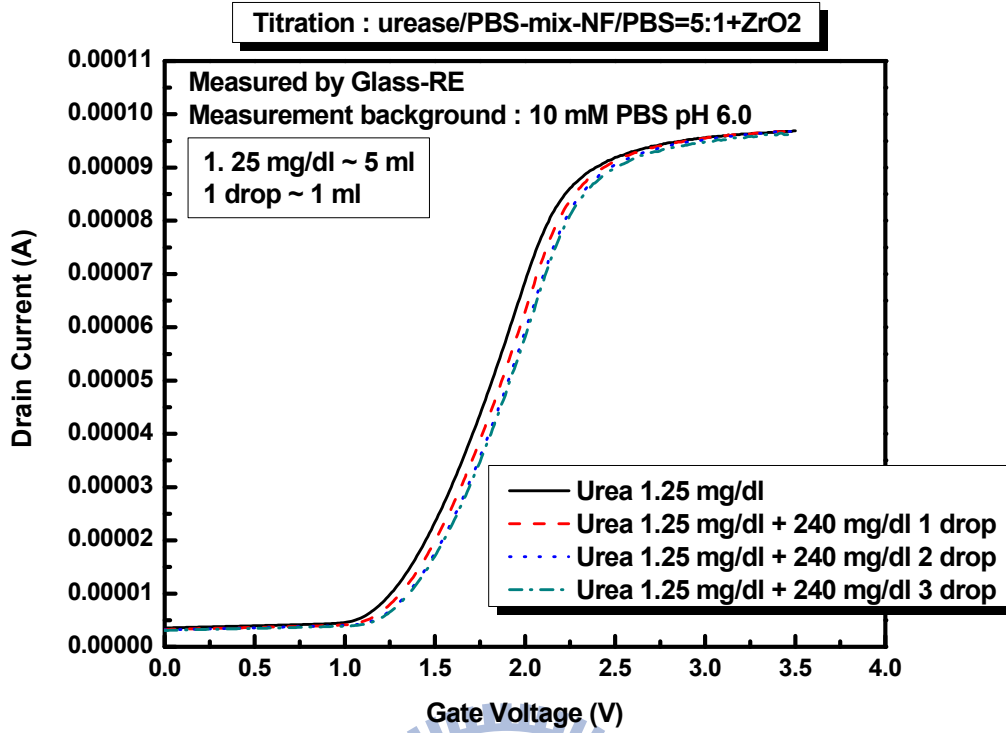


Fig. 4-19 The  $I_{DS}$ - $V_{GS}$  curves of  $ZrO_2$ /urease-mix-NF(5:1) urea-ENFET titration by high concentration urea

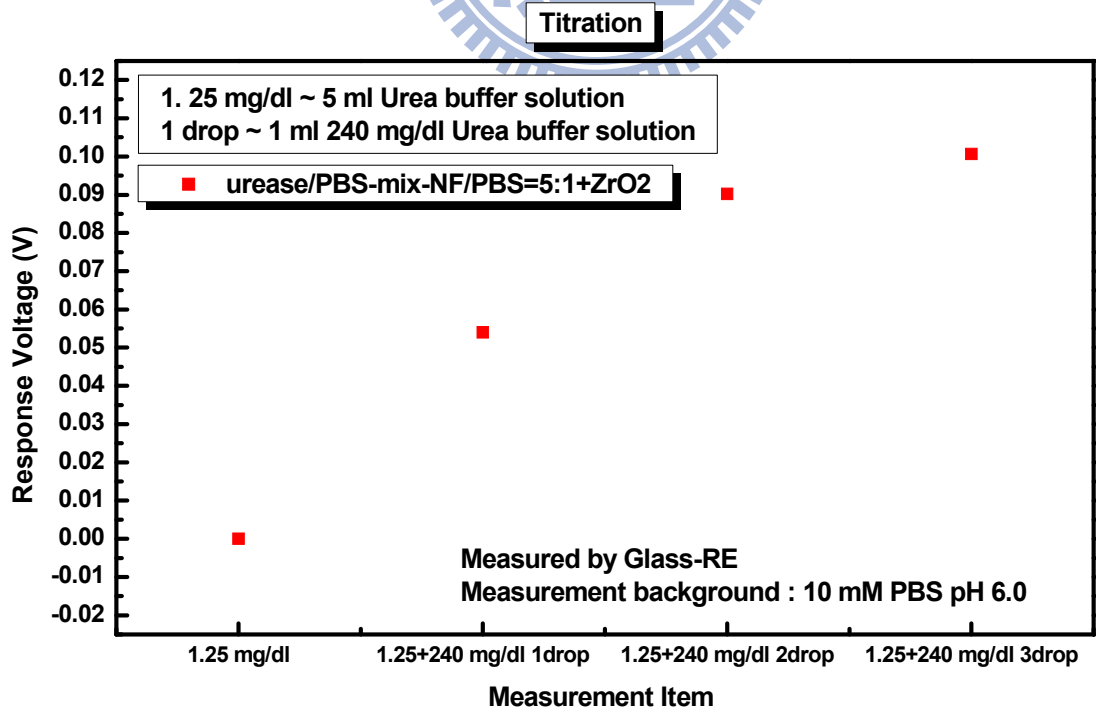


Fig. 4-20 Calibration signals of  $ZrO_2$ /urease-mix-NF(5:1) urea-ENFET titration by high concentration urea

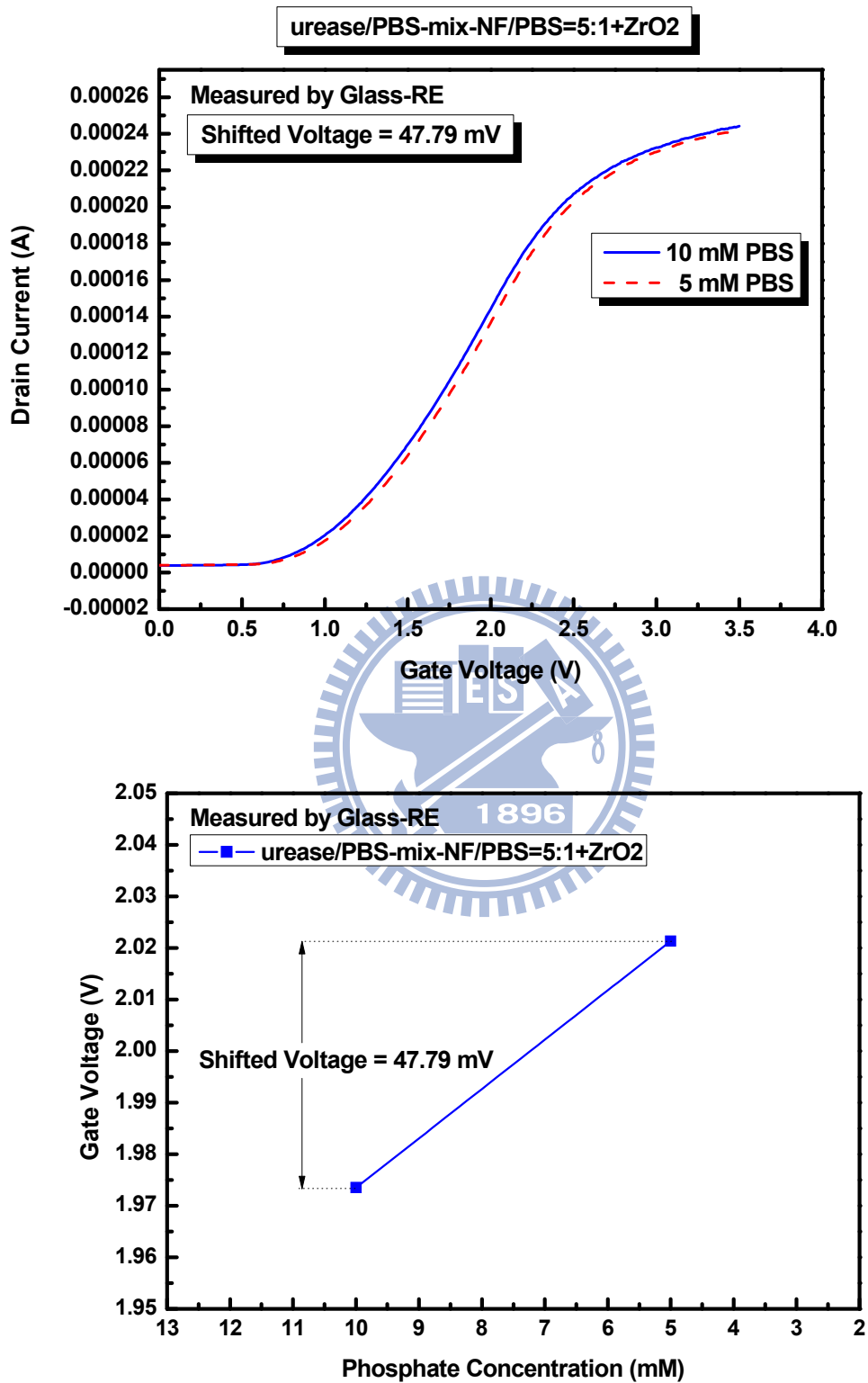


Fig. 4-21 The  $I_{DS}$ - $V_{GS}$  curves and calibration line of  $ZrO_2$ /urease-mix-NF(5:1) urea-ENFET with different phosphate buffer solutions

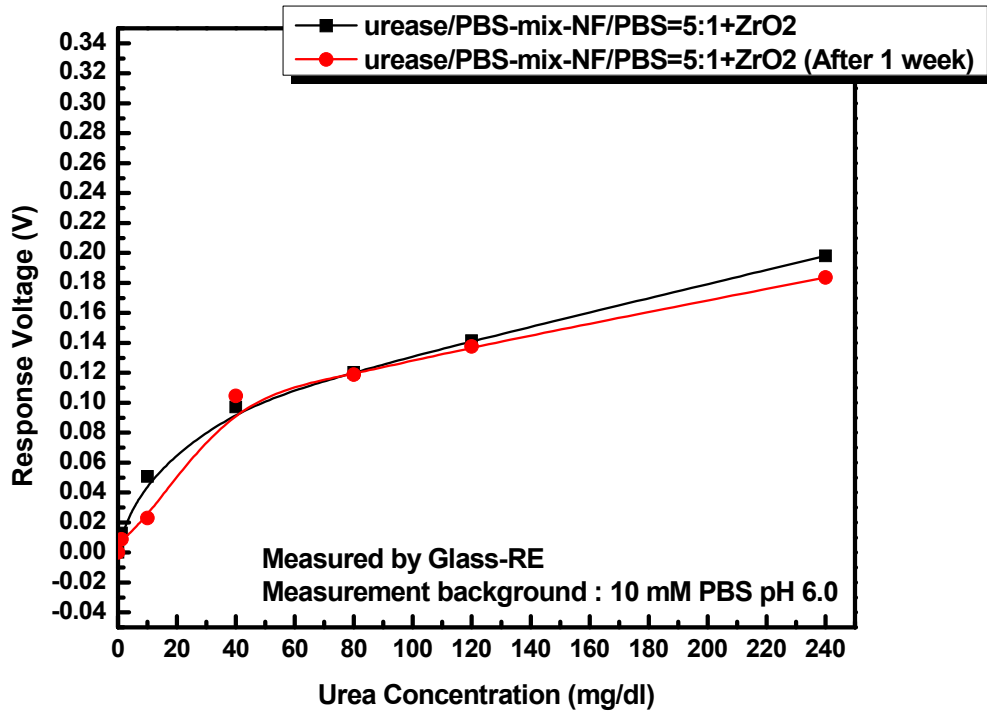


Fig. 4-22 Calibration curves of  $ZrO_2$ /urease-mix-NF(5:1) urea-ENFET in storage stability measurement

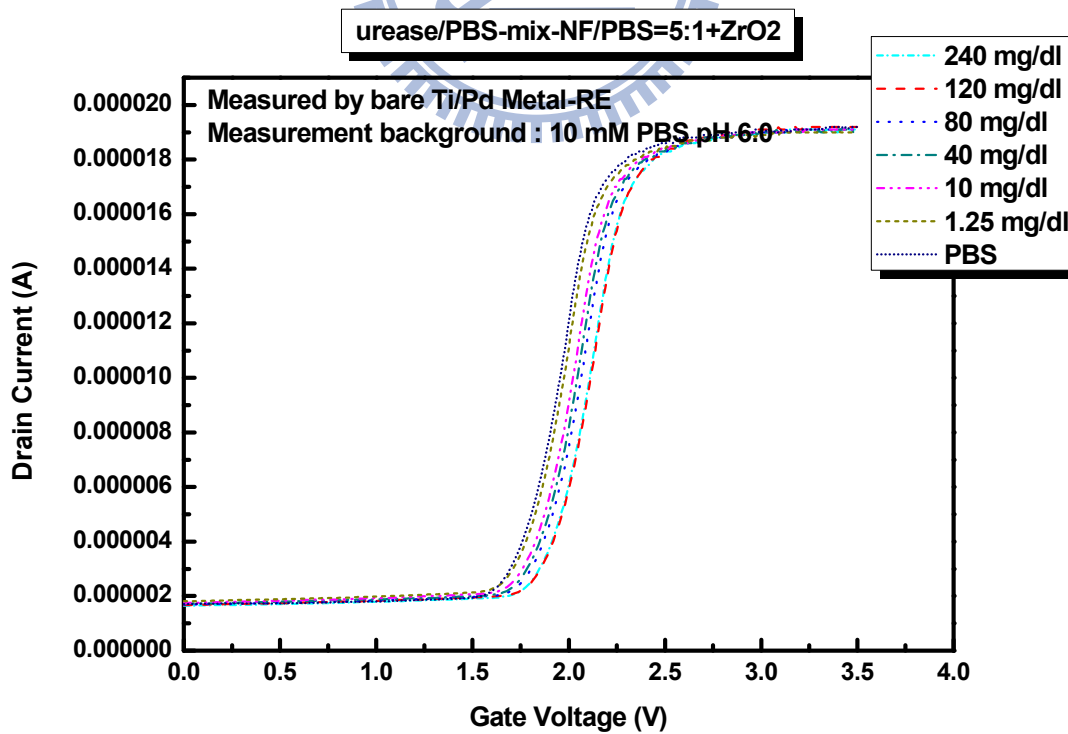


Fig. 4-23 The  $I_{DS}$ - $V_{GS}$  curves of  $ZrO_2$ /urease-mix-NF(5:1) urea-ENFET measure by bare Ti/Pd metal reference electrode

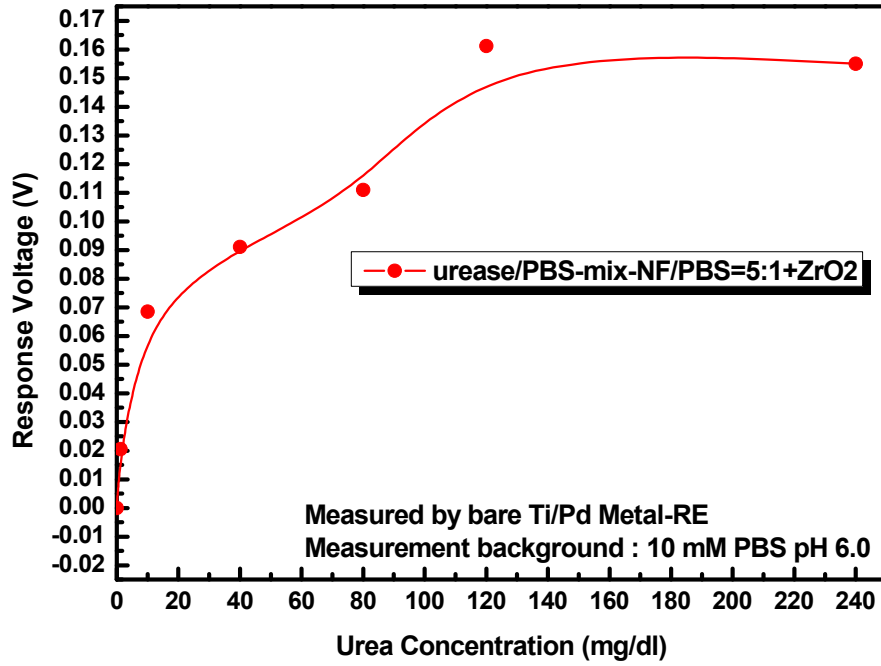


Fig. 4-24 Calibration curve of  $ZrO_2$ /urease-mix-NF(5:1) urea-ENFET measure by bare Ti/Pd metal reference electrode

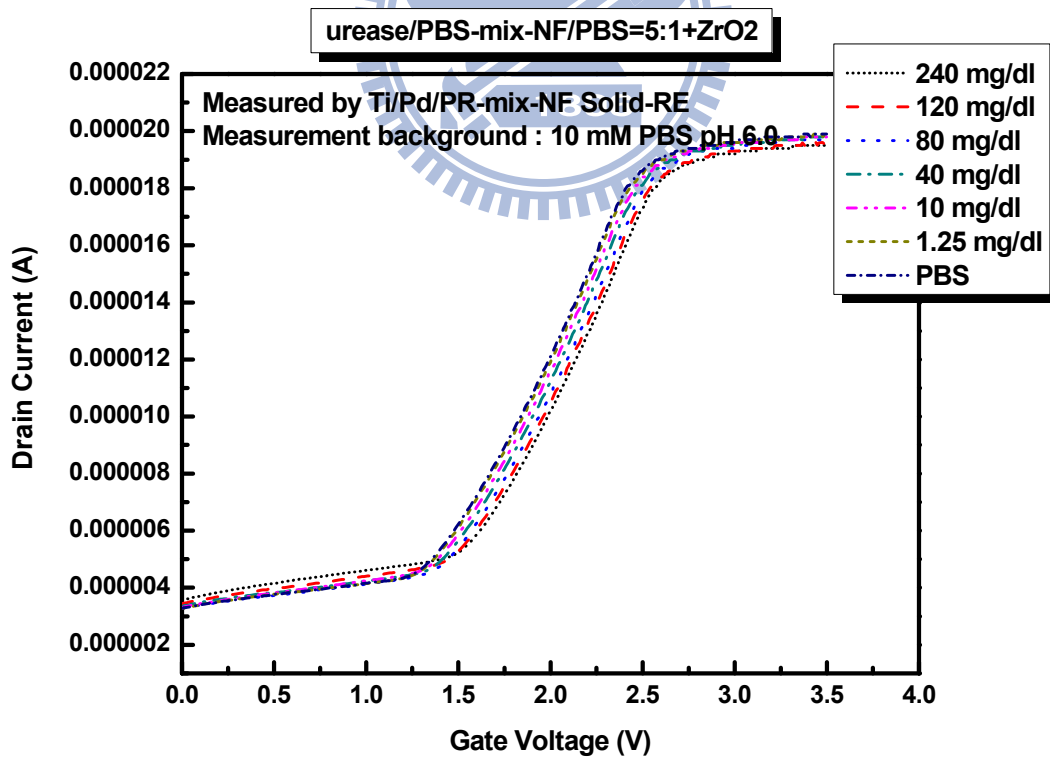


Fig. 4-25 The  $I_{DS}$ - $V_{GS}$  curves of  $ZrO_2$ /urease-mix-NF(5:1) urea-ENFET measure by Ti/Pd/PR-mix-NF solid-state reference electrode

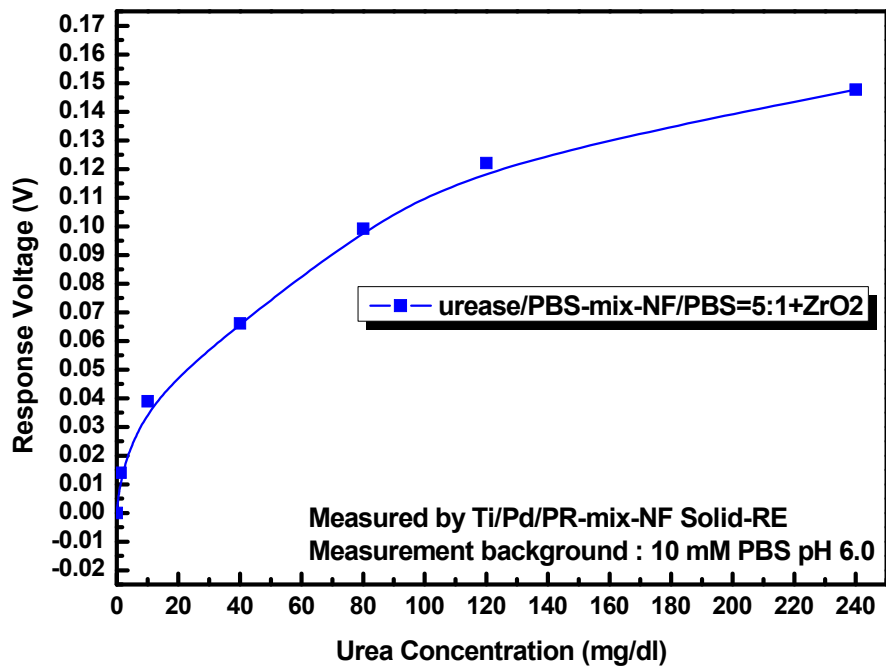


Fig. 4-26 Calibration curve of  $ZrO_2$ /urease-mix-NF(5:1) urea-ENFET measure by Ti/Pd/PR-mix-NF solid-state reference electrode

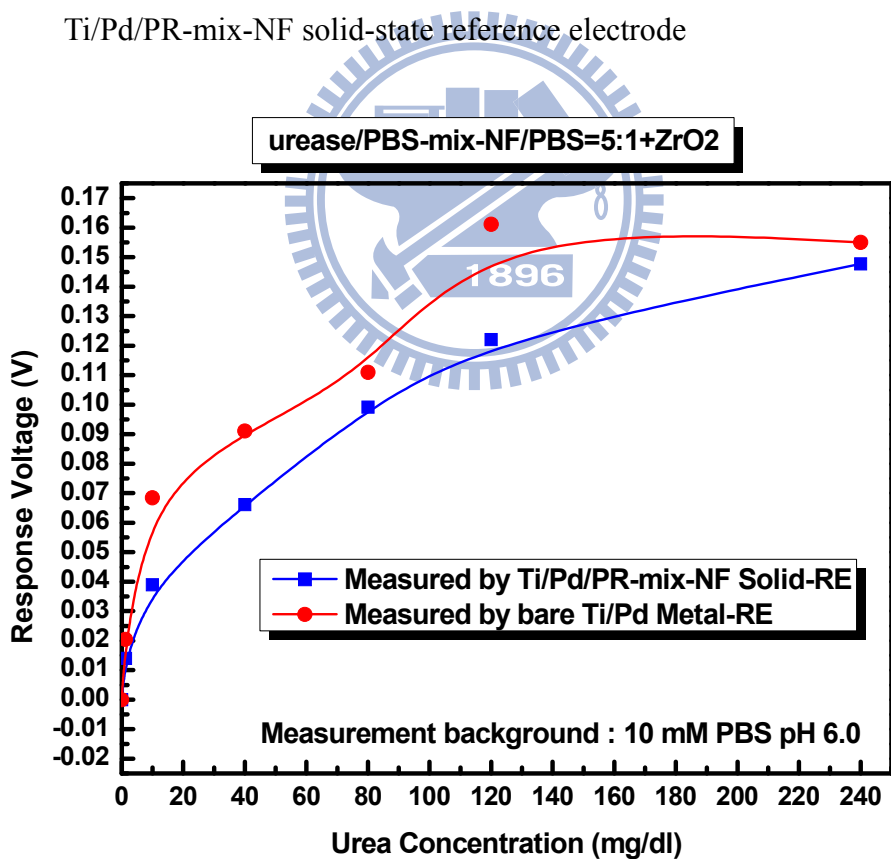


Fig. 4-27 Calibration curves of  $ZrO_2$ /urease-mix-NF(5:1) urea-ENFET measure by Ti/Pd/PR-mix-NF solid-state reference electrode and bare Ti/Pd metal reference electrode

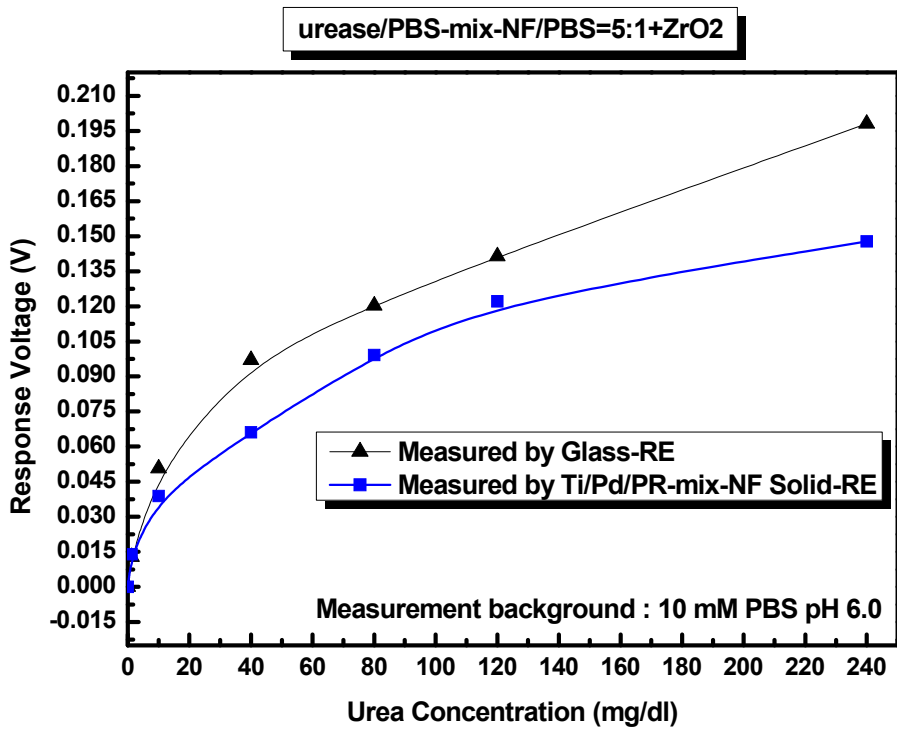


Fig. 4-28 Calibration curves of  $ZrO_2$ /urease-mix-NF(5:1) urea-ENFET measure by glass reference electrode and Ti/Pd/PR-mix-NF solid-state reference electrode

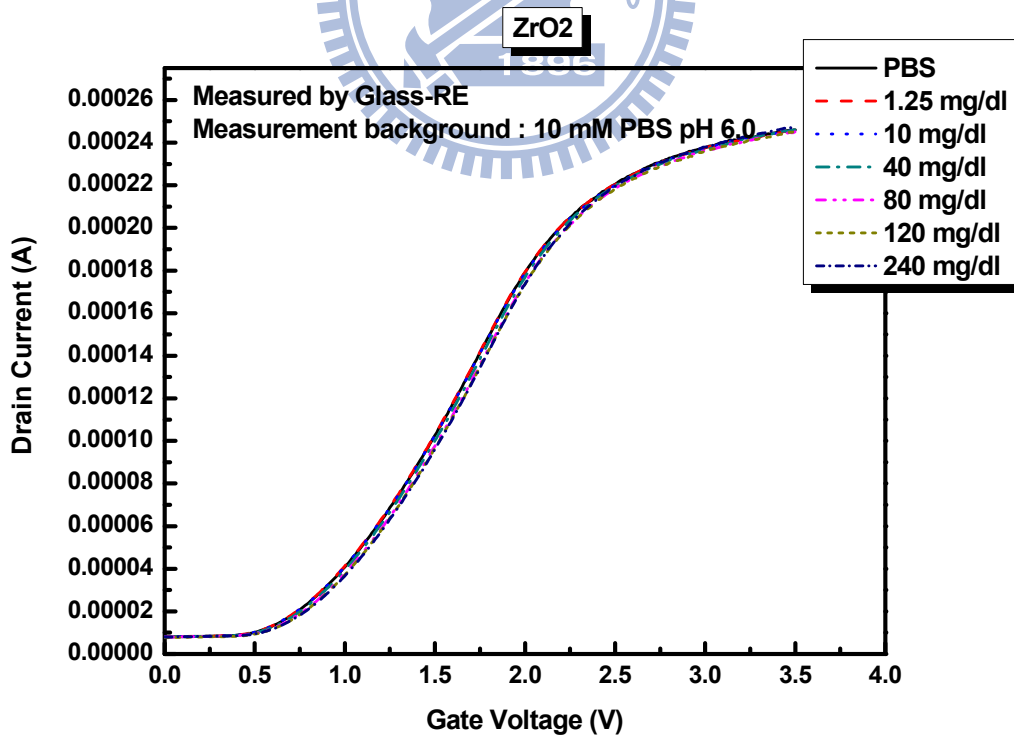


Fig. 4-29 The  $I_{DS}$ - $V_{GS}$  curves of  $ZrO_2$  ISFET measure by glass reference electrode

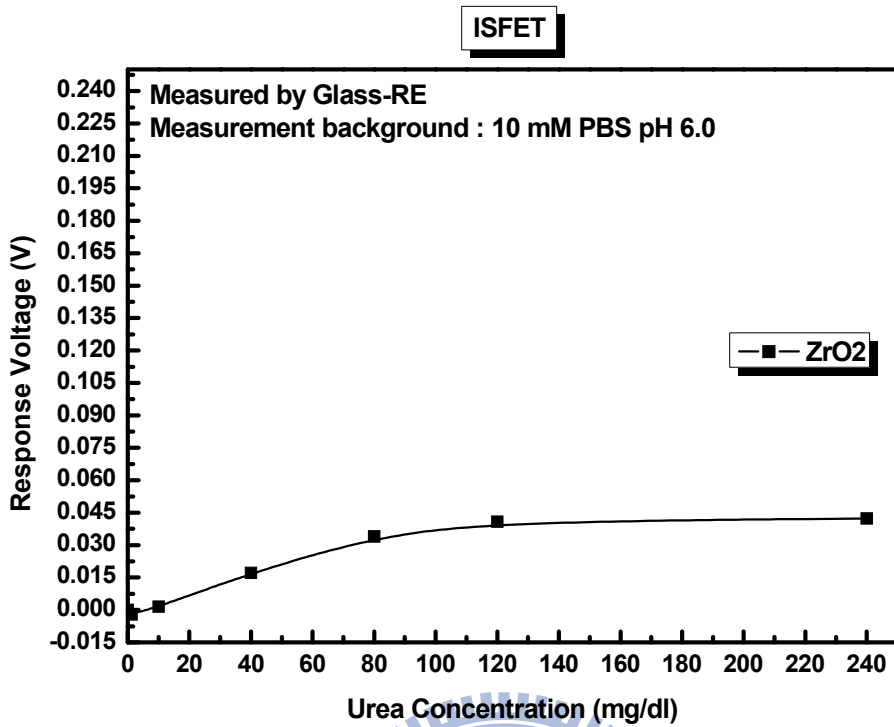


Fig. 4-30 Calibration curve of  $ZrO_2$  ISFET measure by glass reference electrode

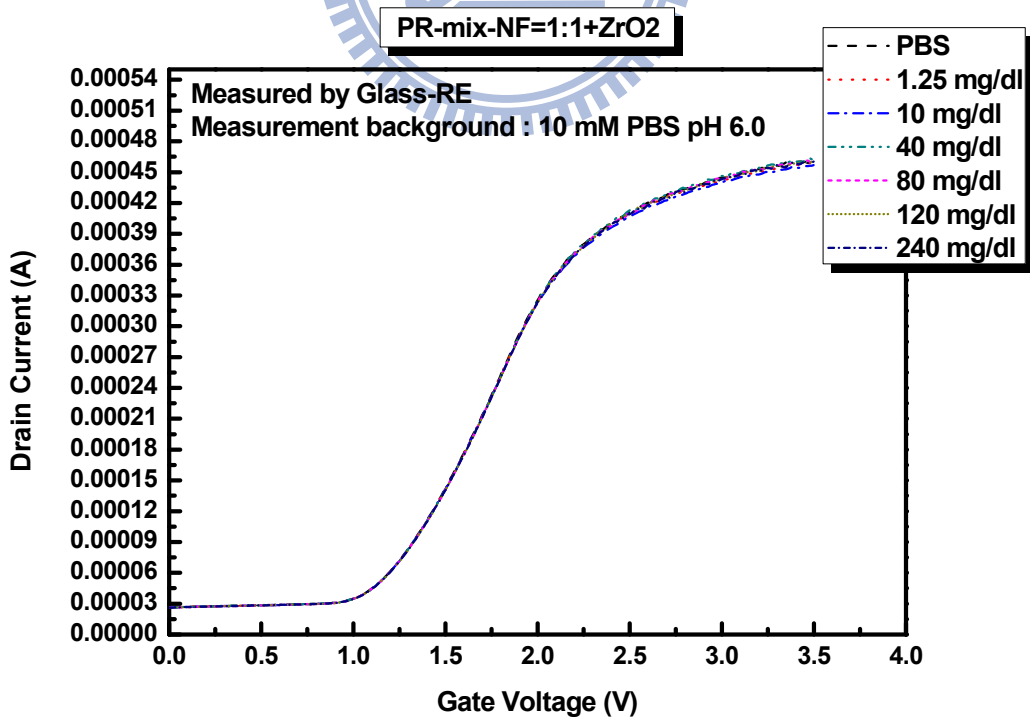


Fig. 4-31 The  $I_{DS}$ - $V_{GS}$  curves of  $ZrO_2/PR$ -mix-NF(1:1) REFET measure by glass reference electrode

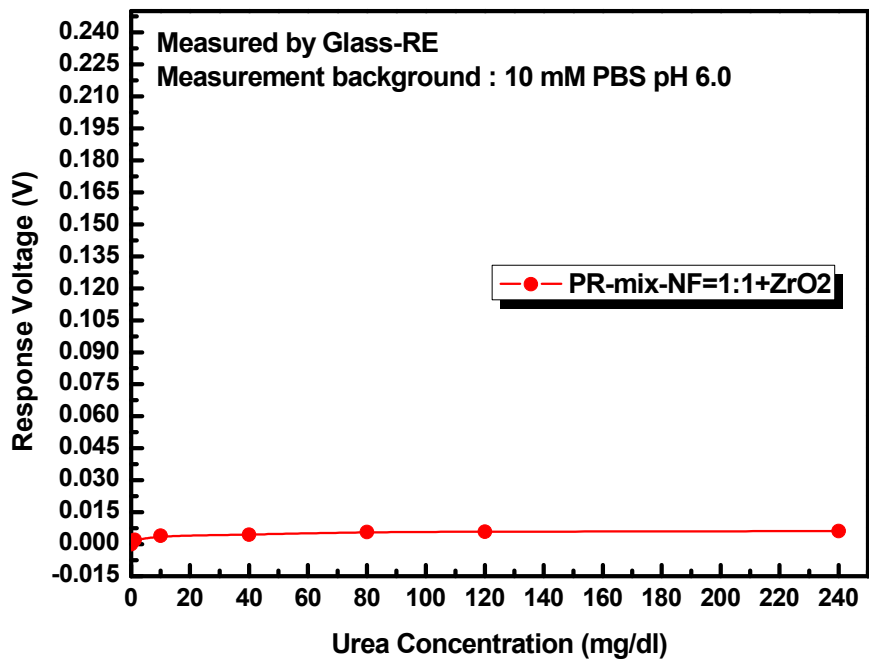


Fig. 4-32 Calibration curve of  $ZrO_2/PR\text{-mix-NF}(1:1)$  REFET measure by glass reference electrode

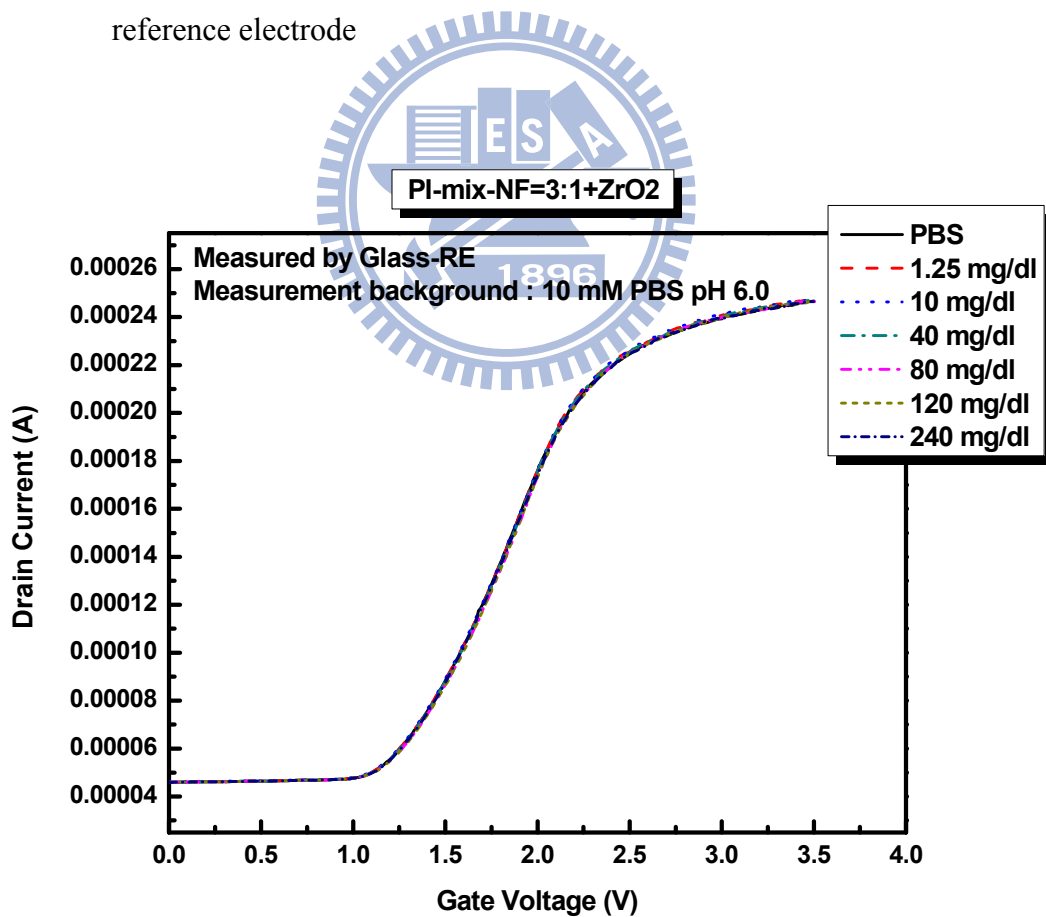


Fig. 4-33 The  $I_{DS}\text{-}V_{GS}$  curves of  $ZrO_2/PI\text{-mix-NF}(3:1)$  REFET measure by glass reference electrode



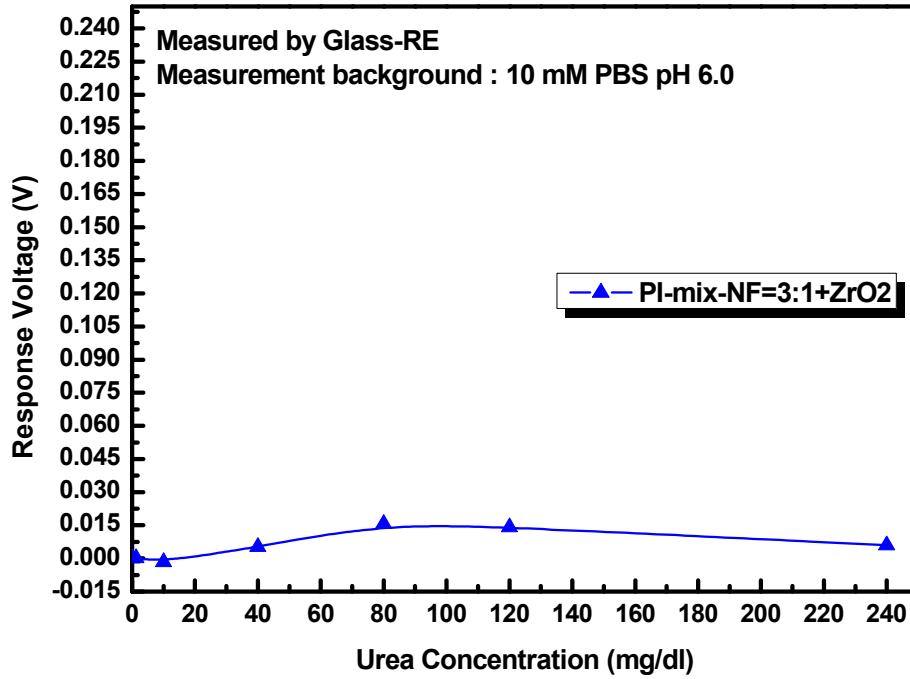


Fig. 4-34 Calibration curve of  $ZrO_2/PI\text{-mix-NF}(3:1)$  REFET measure by glass reference electrode

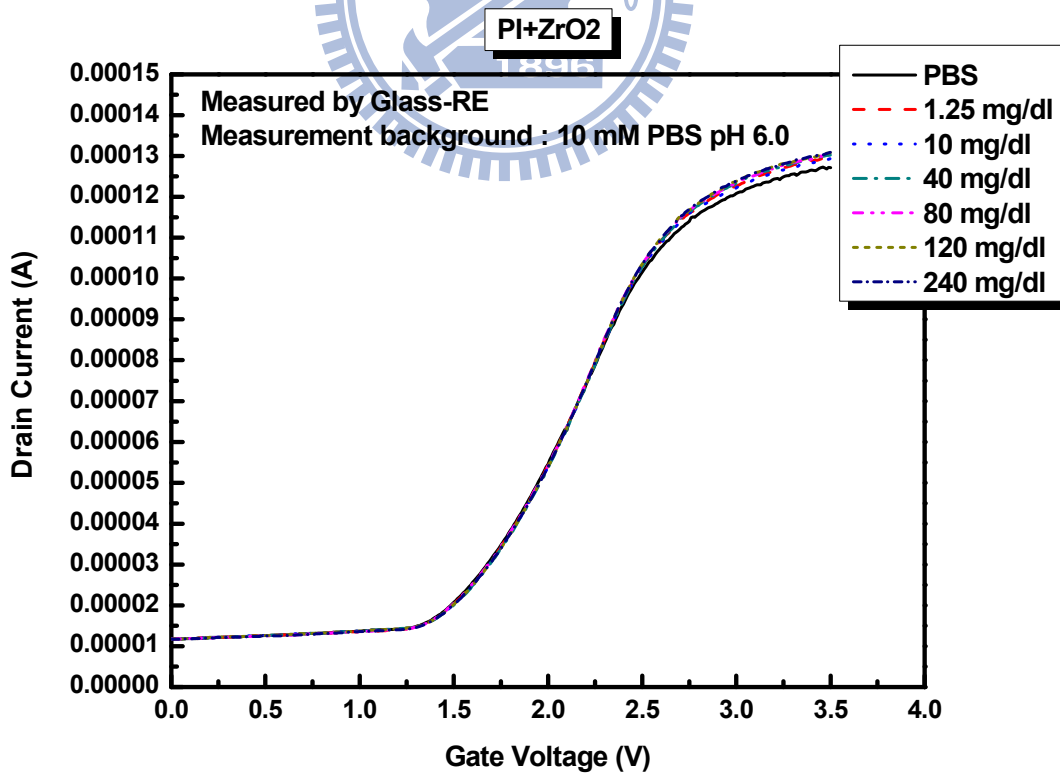


Fig. 4-35 The  $I_{DS}\text{-}V_{GS}$  curves of  $ZrO_2/PI$  REFET measure by glass reference electrode

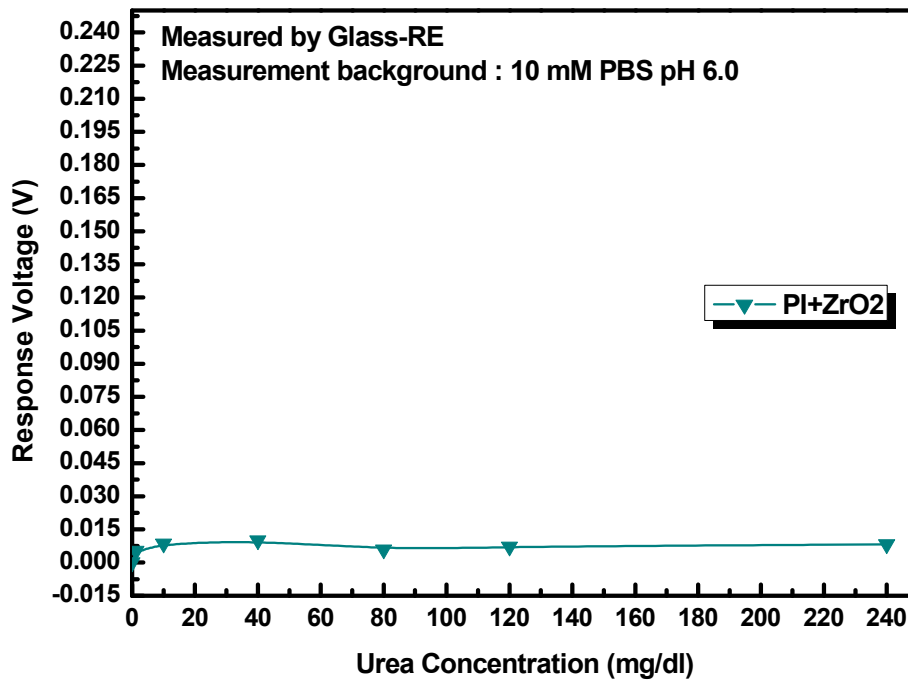


Fig. 4-36 Calibration curve of ZrO<sub>2</sub>/PI REFET measure by glass reference electrode

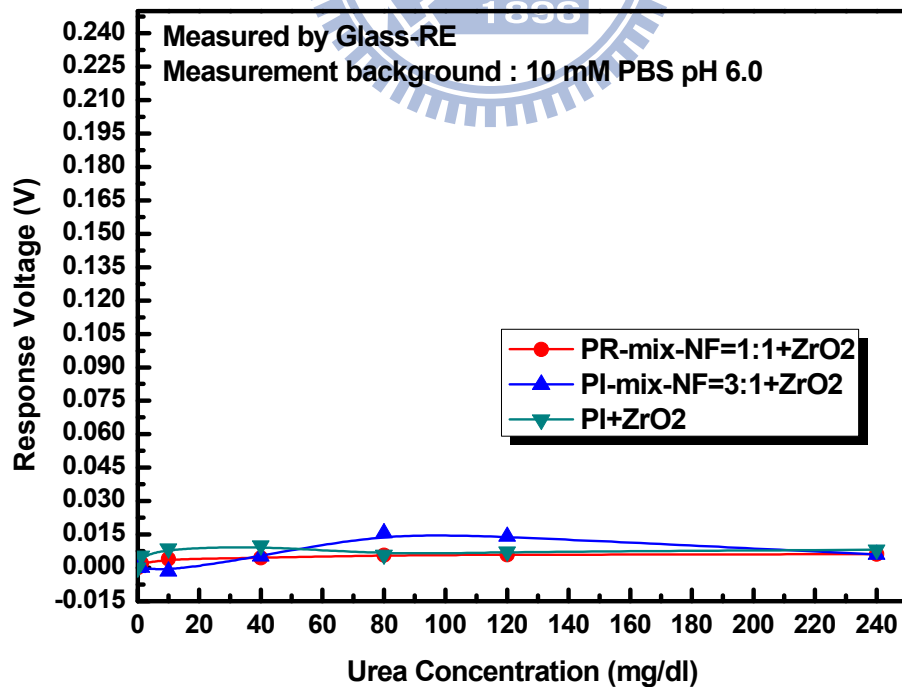


Fig. 4-37 Calibration curves of REFET with different structures measure by glass reference electrode

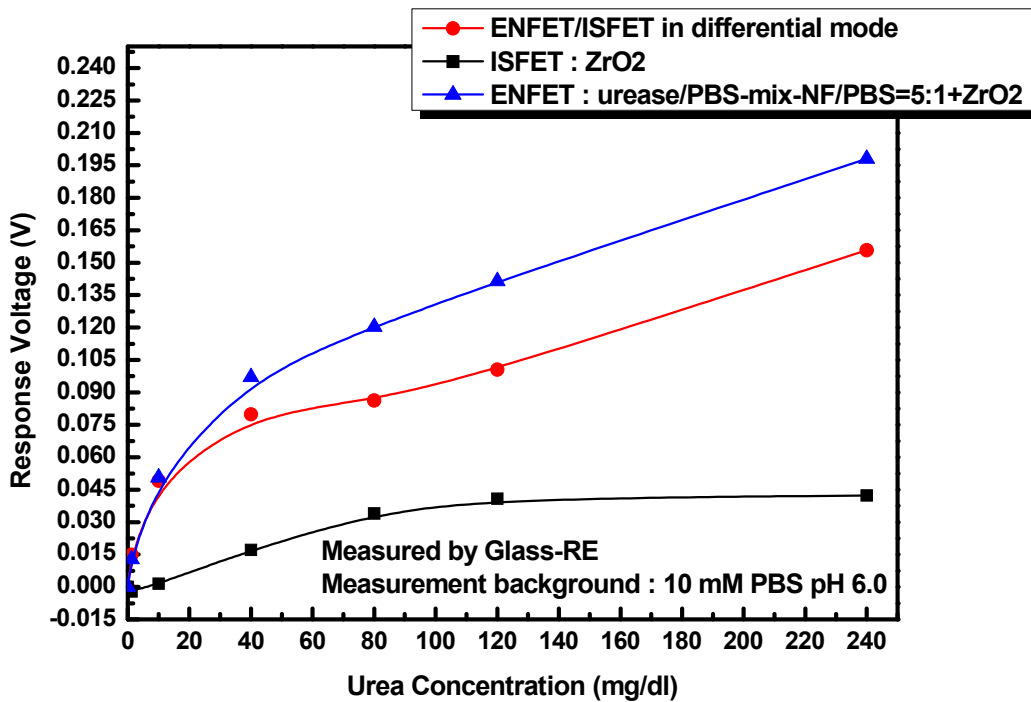


Fig. 4-38 Calibration curves of ENFET/ISFET( $ZrO_2$ ) in differential mode measure by glass reference electrode

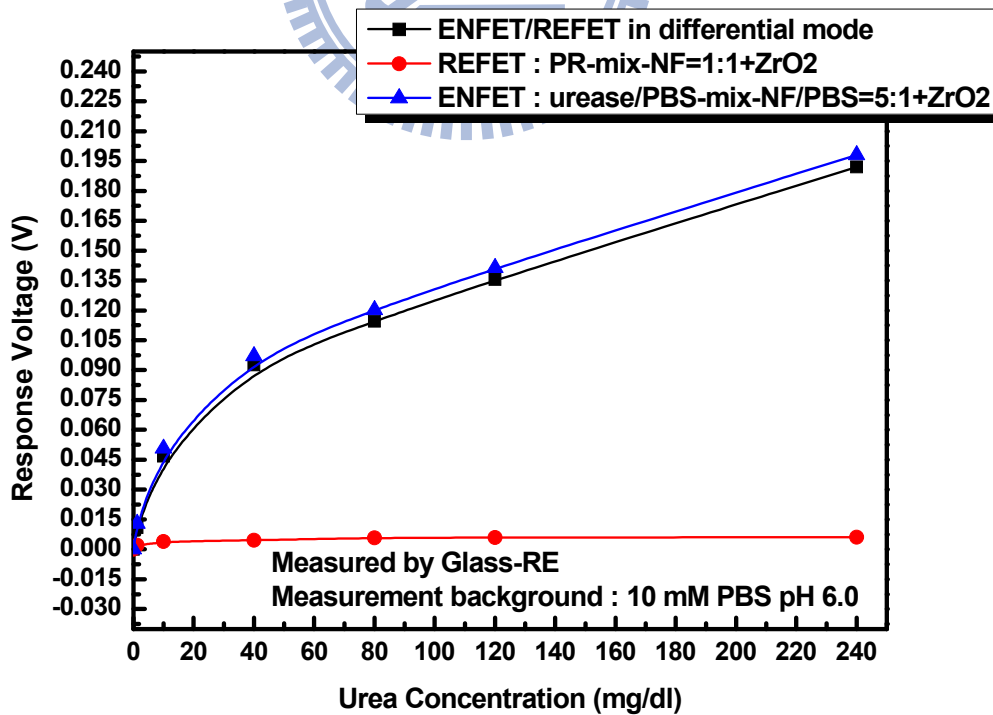


Fig. 4-39 Calibration curves of ENFET/REFET( $ZrO_2$ /PR-mix-NF) in differential mode measure by glass reference electrode

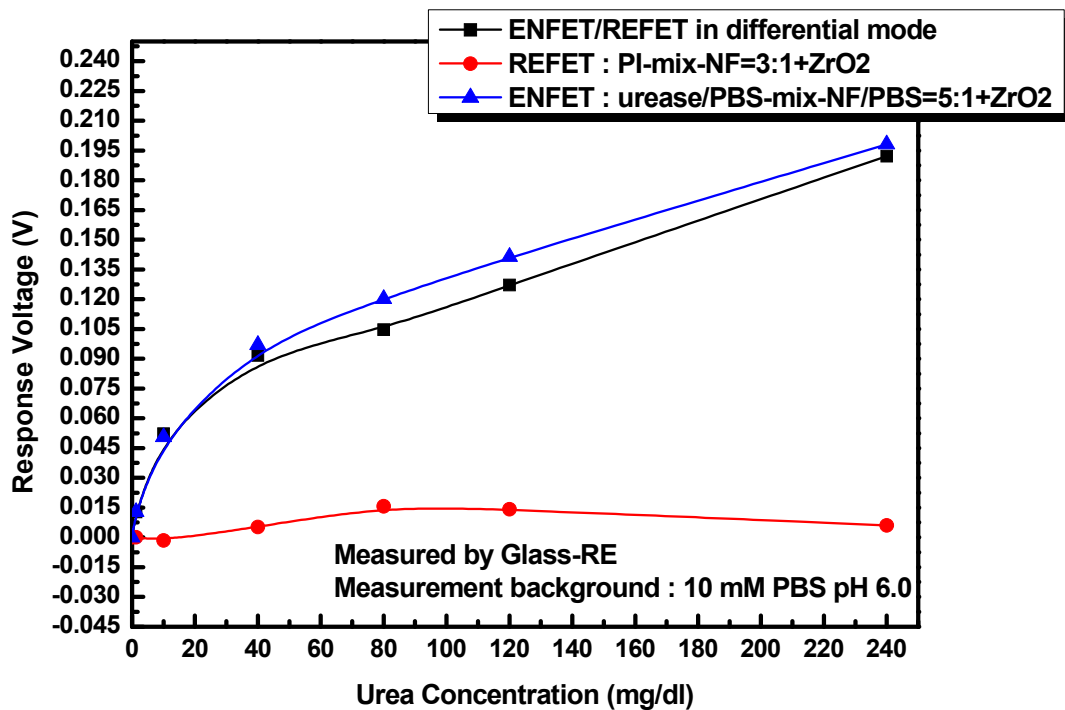


Fig. 4-40 Calibration curves of ENFET/REFET( $ZrO_2$ /PI-mix-NF) in differential mode measure by glass reference electrode

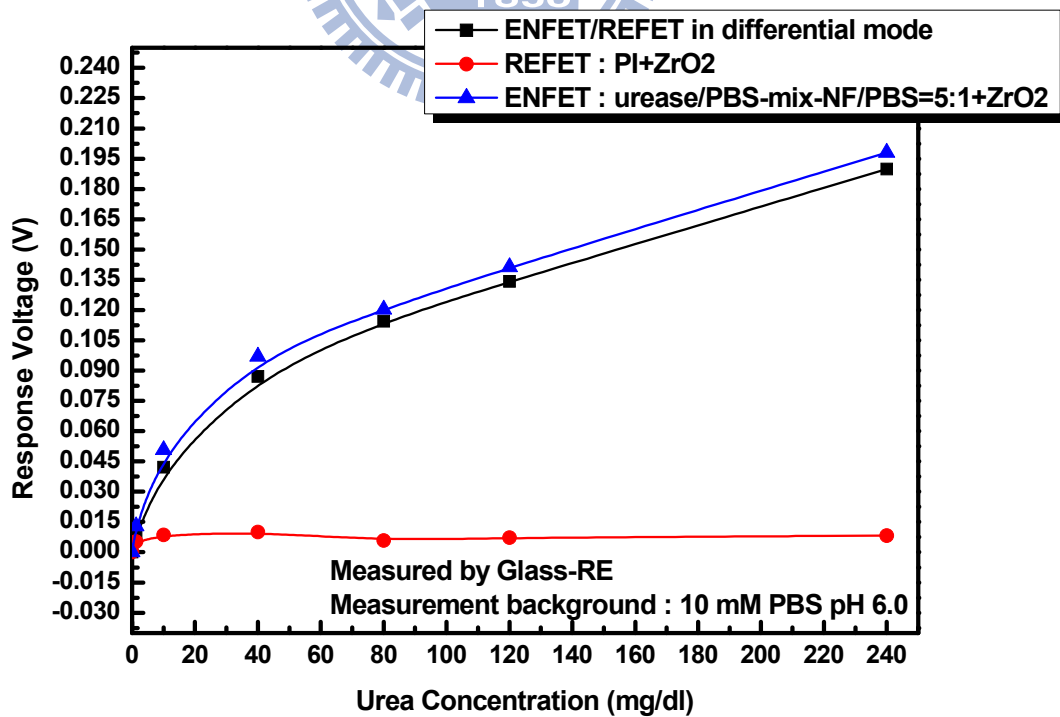


Fig. 4-41 Calibration curves of ENFET/REFET( $ZrO_2$ /PI) in differential mode measure by glass reference electrode

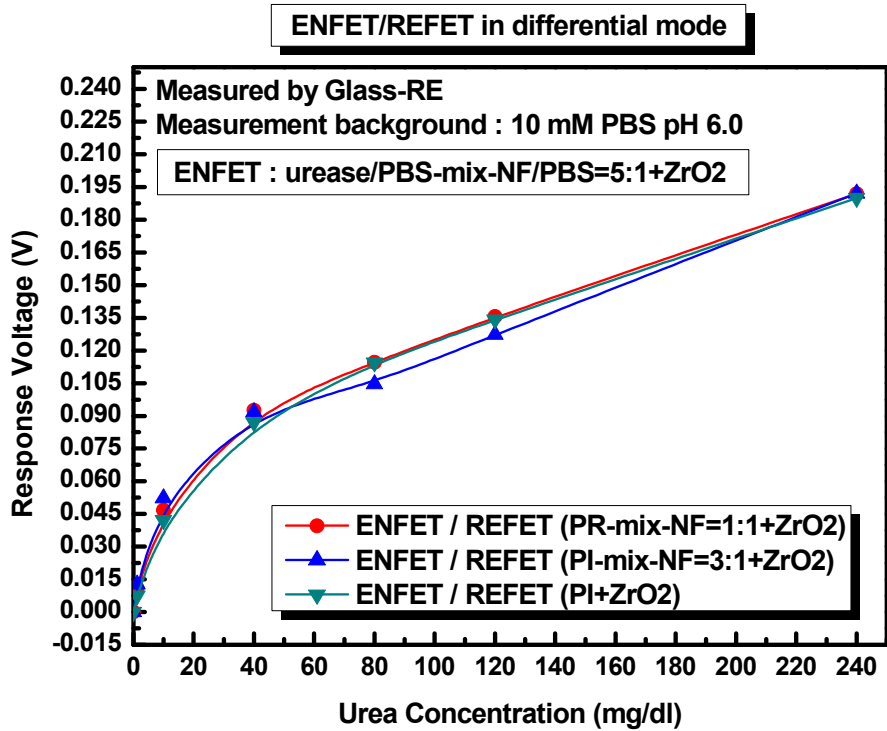


Fig. 4-42 Calibration curves of ENFET/REFET in differential mode measure by glass reference electrode

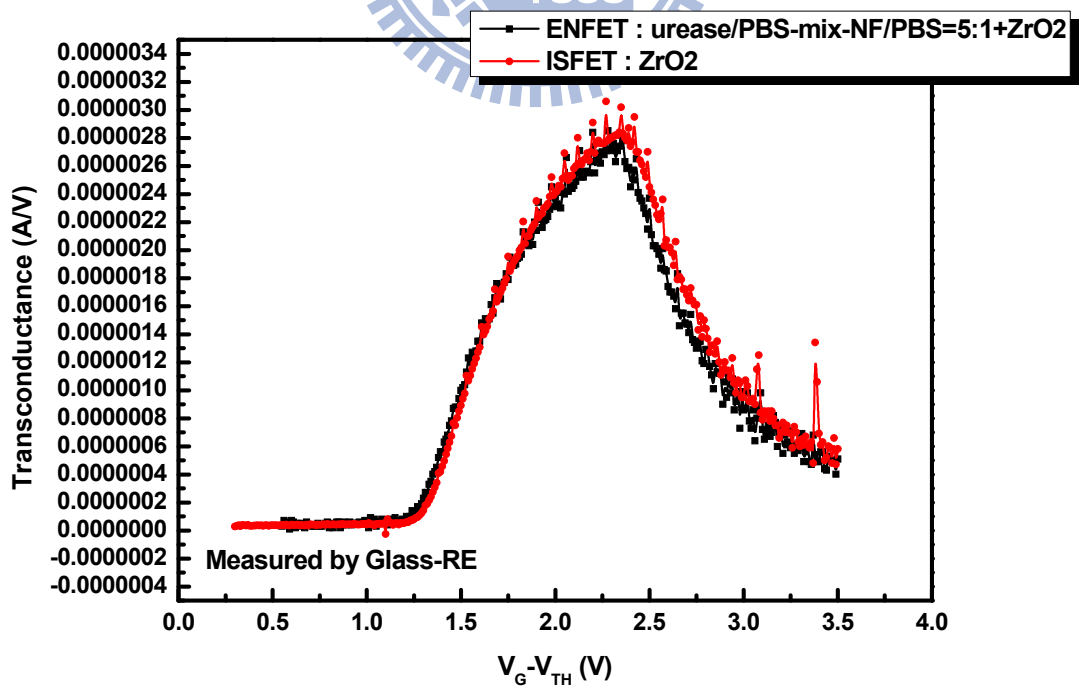


Fig. 4-43 Transconductance curves of ENFET/ISFET(ZrO<sub>2</sub>) in differential mode measure by glass reference electrode

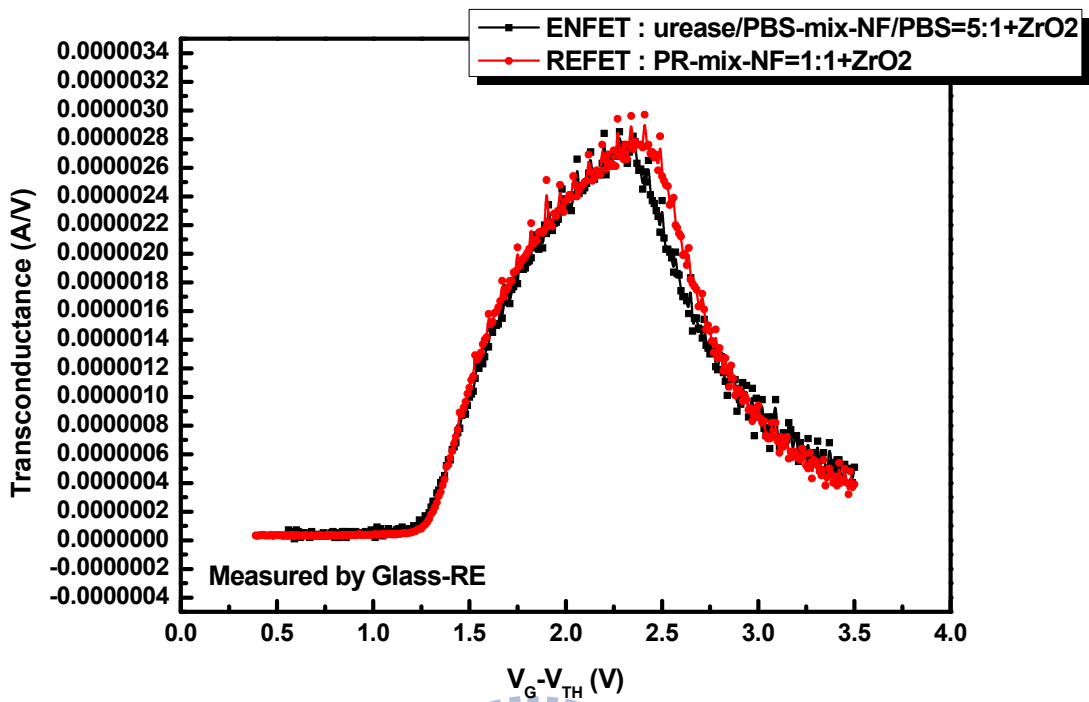


Fig. 4-44 Transconductance curves of ENFET/REFET(ZrO<sub>2</sub>/PR-mix-NF) in differential mode measure by glass reference electrode

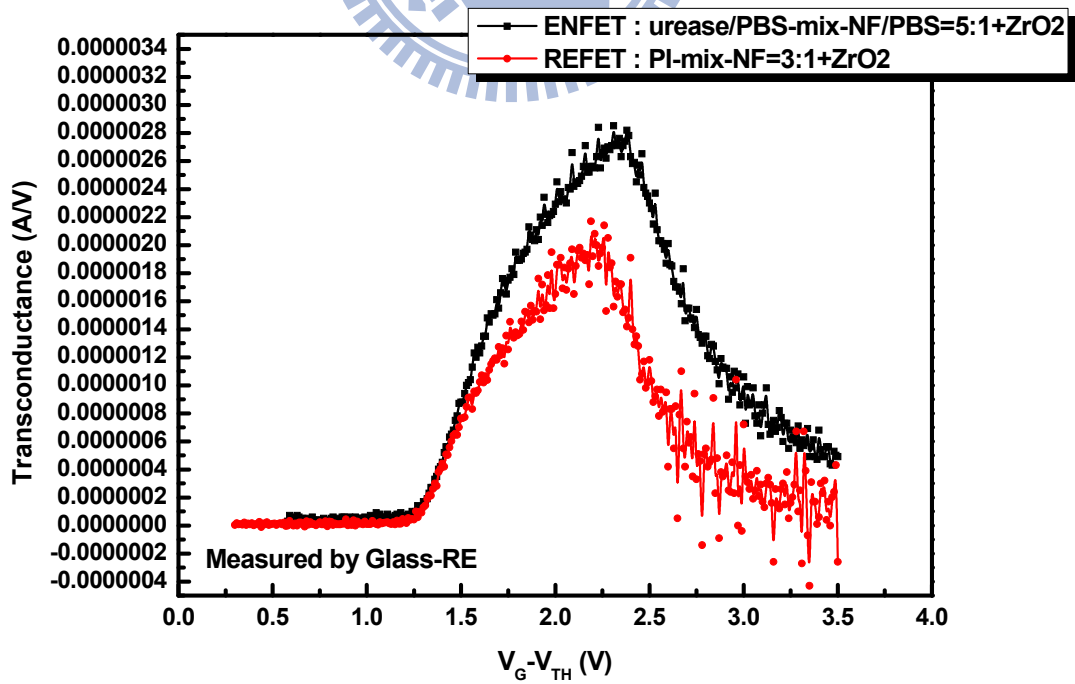


Fig. 4-45 Transconductance curves of ENFET/REFET(ZrO<sub>2</sub>/PI-mix-NF) in differential mode measure by glass reference electrode

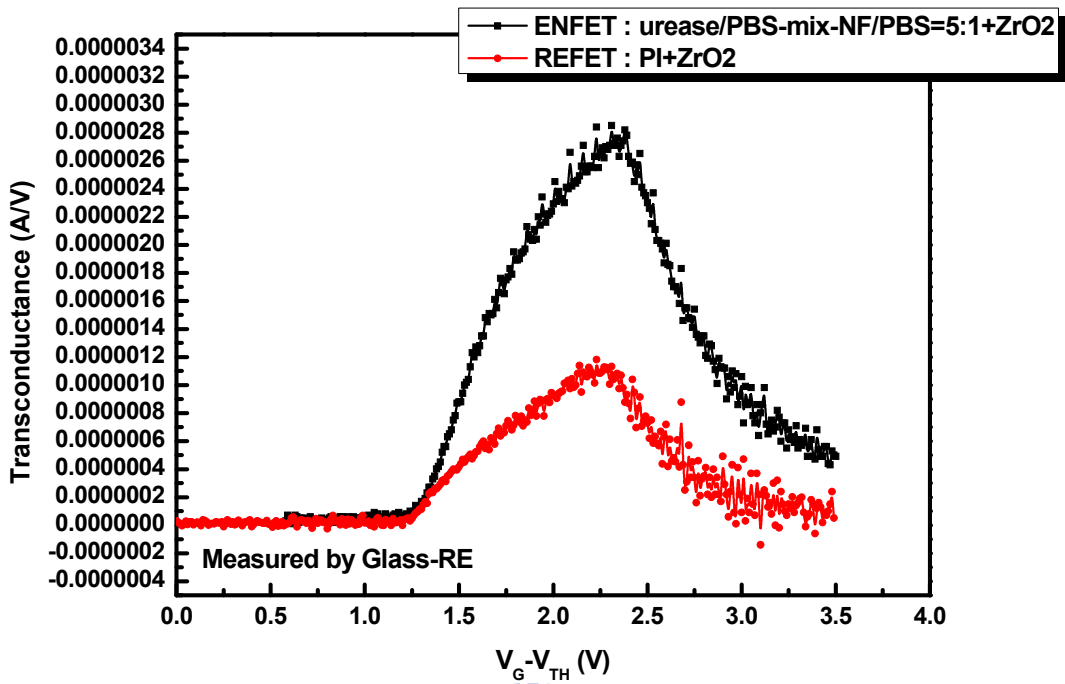


Fig. 4-46 Transconductance curves of ENFET/REFET( $ZrO_2/PI$ ) in differential mode measure by glass reference electrode

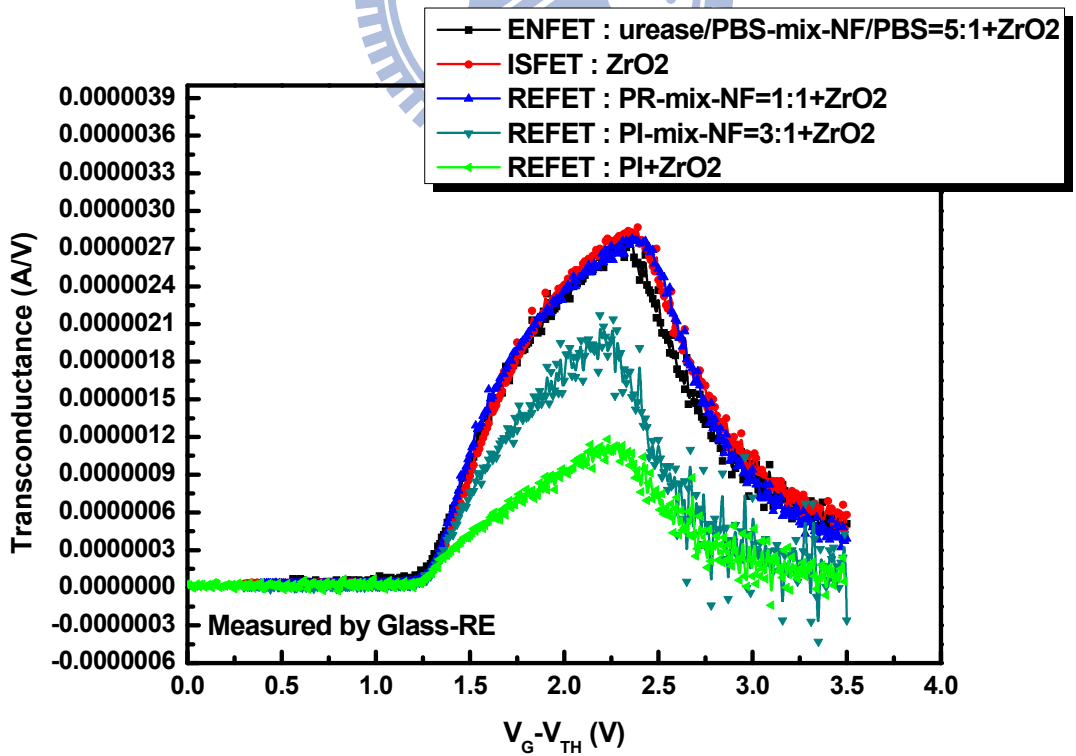


Fig. 4-47 Transconductance curves of ENFET/REFET(ISFET) in differential mode measure by glass reference electrode

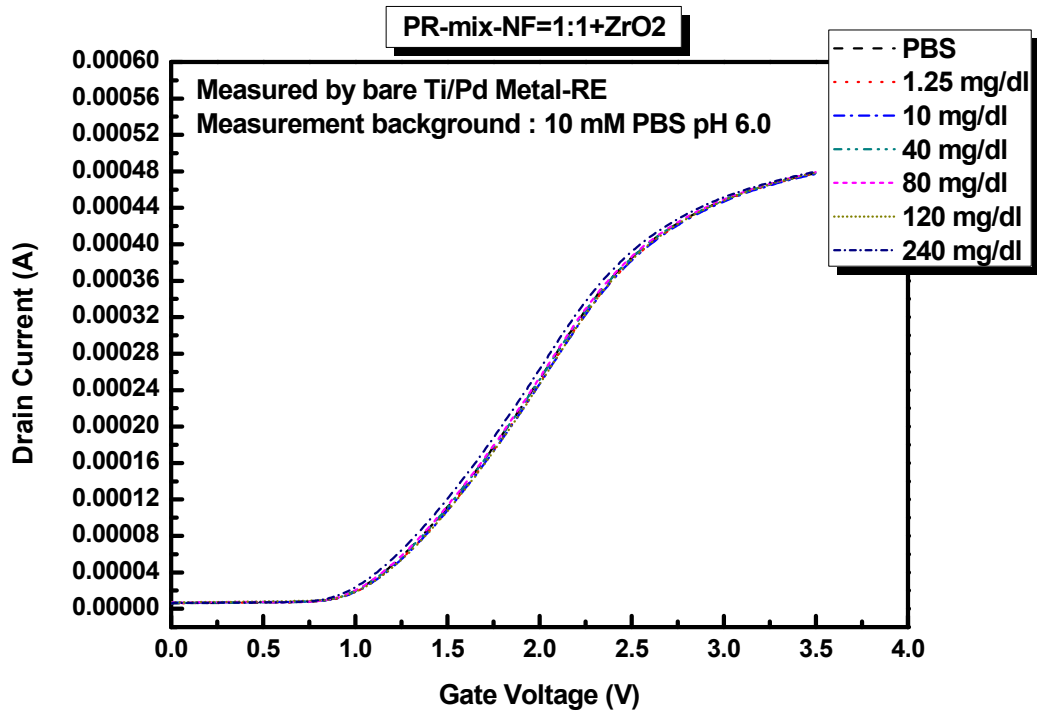


Fig. 4-48 The  $I_{DS}$ - $V_{GS}$  curves of  $ZrO_2/PR$ -mix-NF(1:1) REFET measure by bare Ti/Pd metal reference electrode

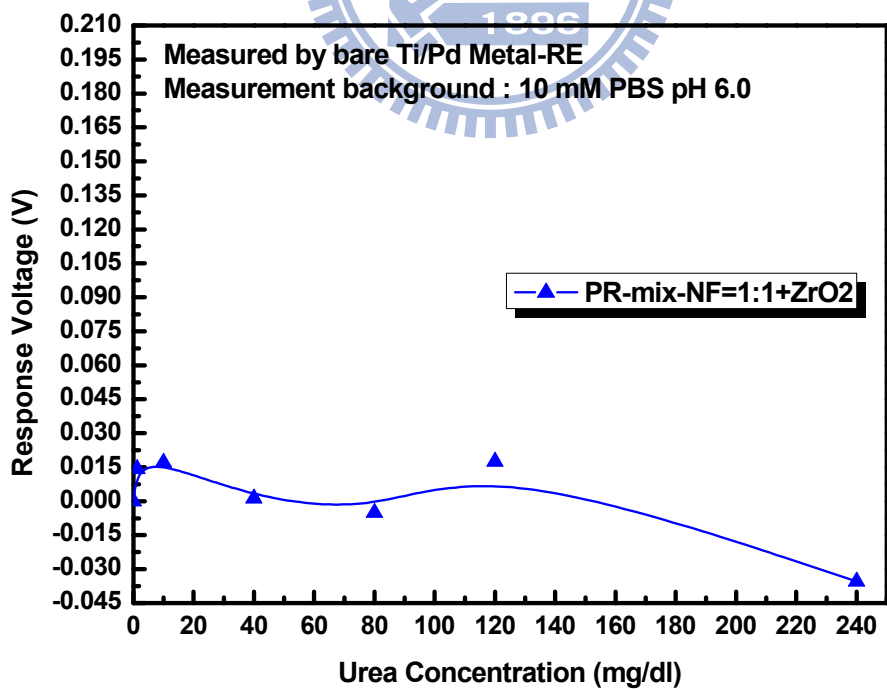


Fig. 4-49 Calibration curve of  $ZrO_2/PR$ -mix-NF(1:1) REFET measure by bare Ti/Pd metal reference electrode



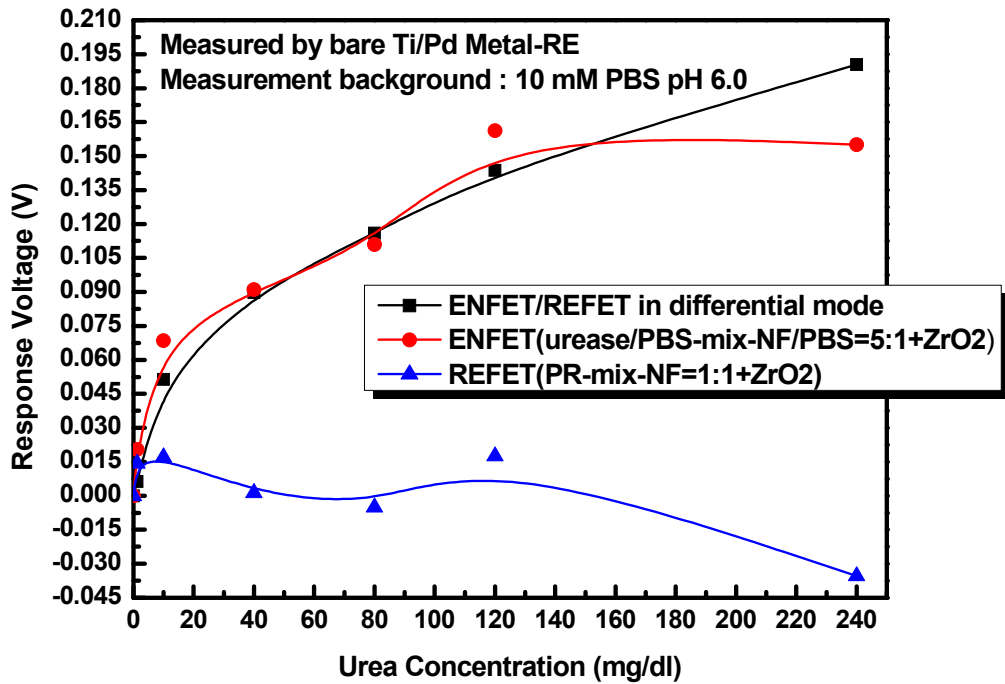


Fig. 4-50 Calibration curves of ENFET/REFET( $ZrO_2$ /PR-mix-NF) in differential mode measure by bare Ti/Pd metal reference electrode

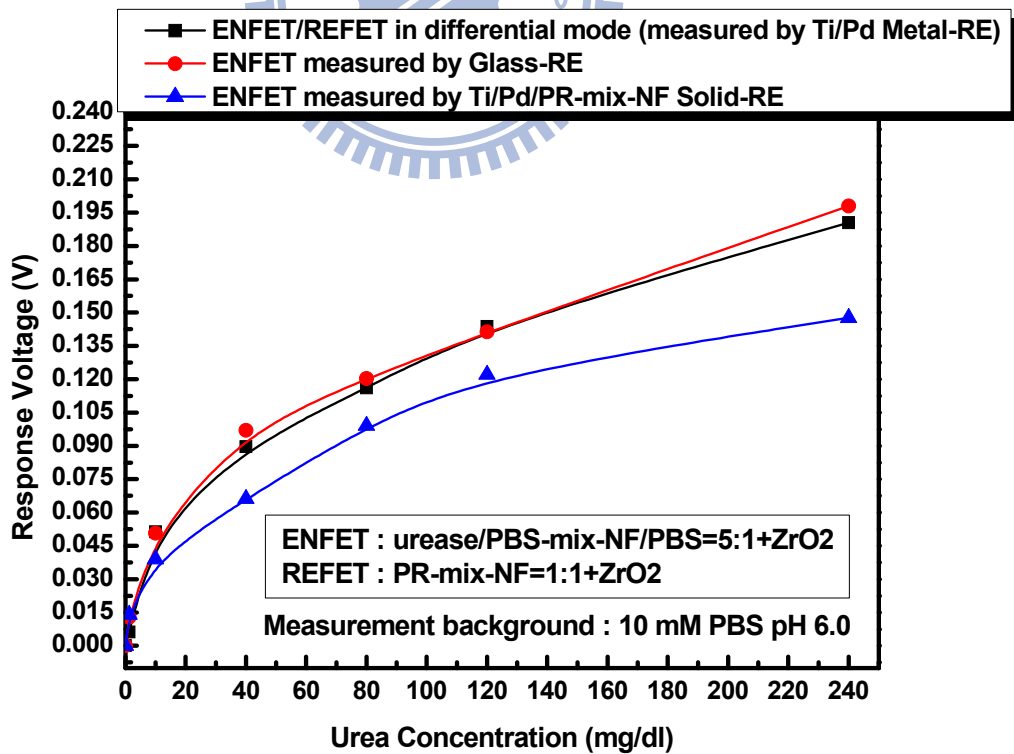


Fig. 4-51 Calibration curves of ENFET and ENFET/REFET differential pair measure by different reference electrodes

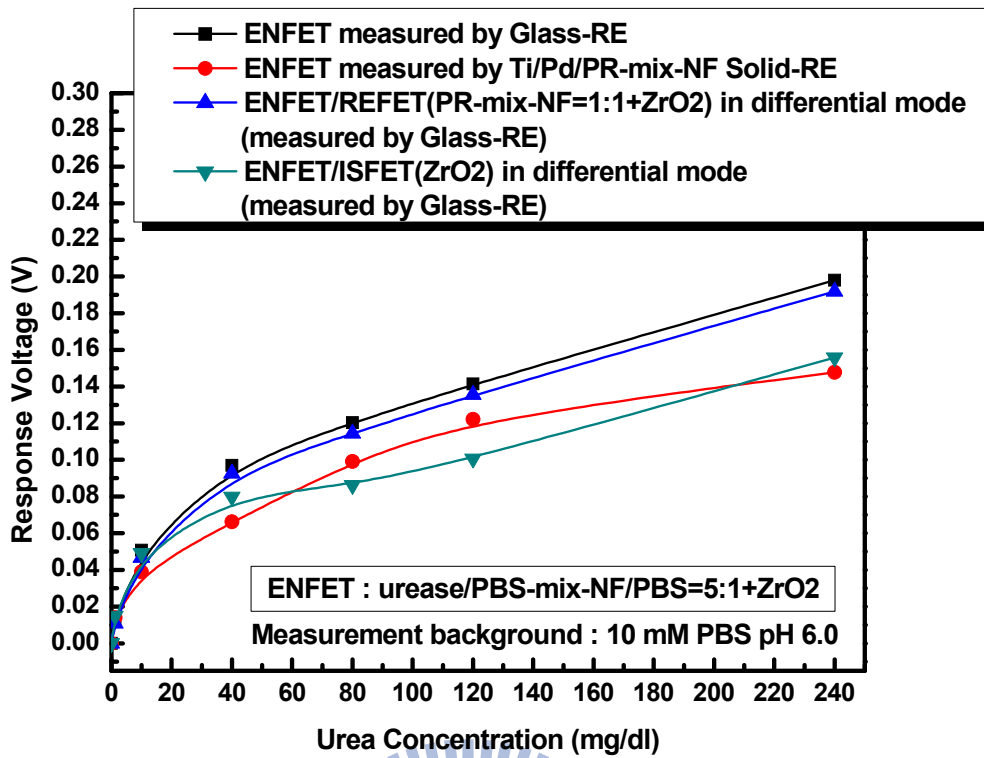


Fig. 4-52 Calibration curves of ENFET and ENFET/REFET(ISFET) differential pair measure by different reference electrodes

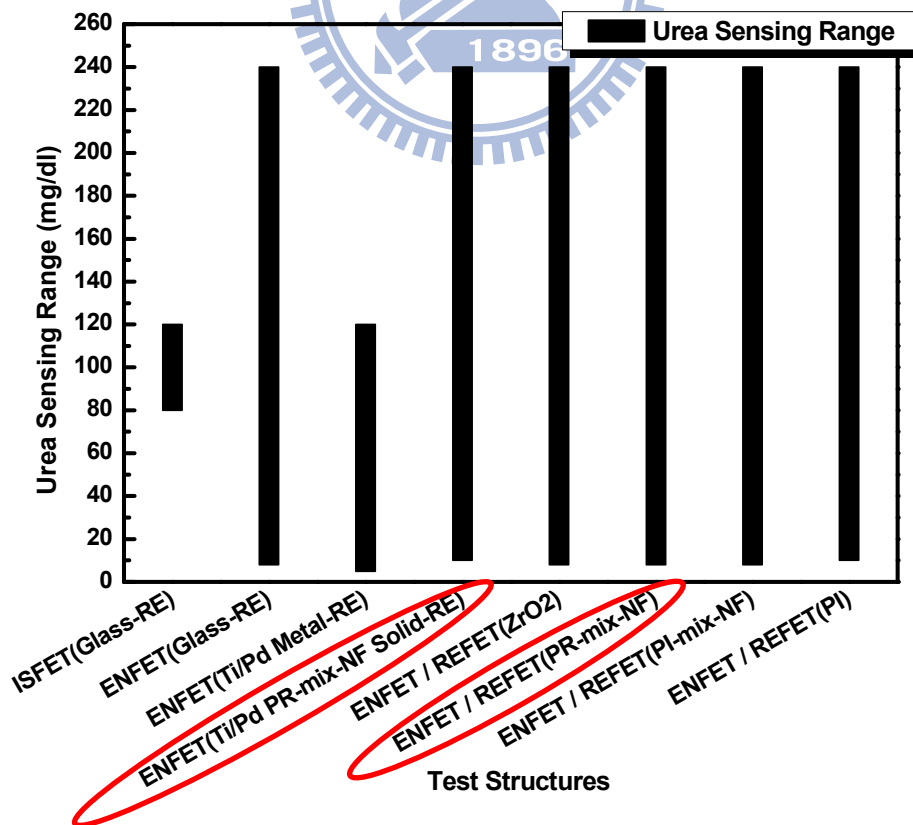


Fig. 4-53 Summary of urea sensing range for different test structures

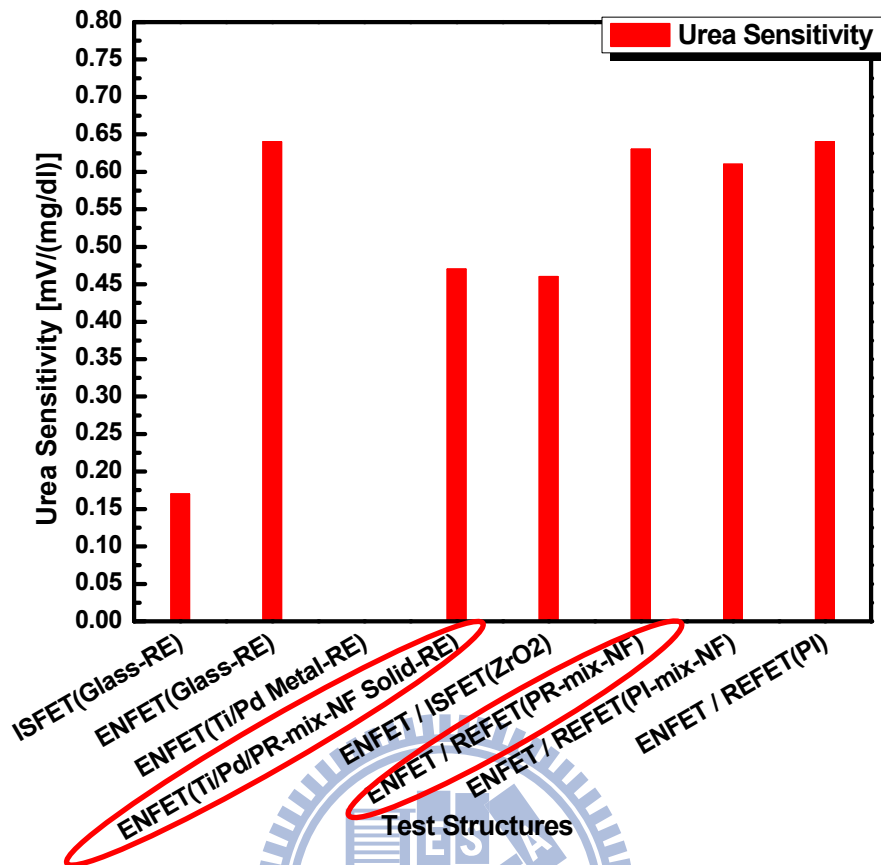


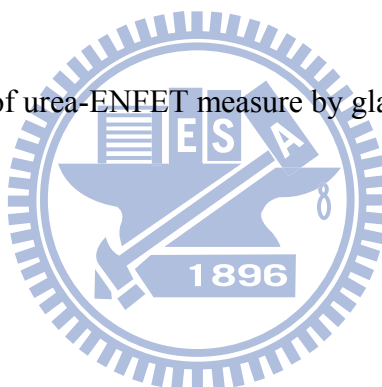
Fig. 4-54 Summary of urea sensitivity for different test structures

Measured By Glass-Reference Electrode			
	H <sup>+</sup> Sensitivity (mV/pH)	H <sup>+</sup> Linearity	pH Sensing Range
<b>ISFET</b> <b>ZrO<sub>2</sub></b>	55	0.9996	pH 1 ~ pH 13
<b>ENFET</b> <b>ZrO<sub>2</sub></b> <b>+</b> <b>Urease/PBS-mix-NF/PBS</b> <b>(1:1)</b>	43	0.9922	pH 3 ~ pH 11

Table 4-1 Summary of ZrO<sub>2</sub> ISFET and ZrO<sub>2</sub>/urease-mix-NF(1:1) ENFET measure by glass reference electrode

Operation Temperature : 25 °C / Measurement Environmental : 10 mM phosphate buffer solution, pH 6.0						
	Detection Limit (mg/dl)	Sensing Range (mg/dl)	Sensitivity [mV/(mg/dl)]	Lifetime	Response Time (sec)	Immobilization Method
Urease/PBS -mix- NF/PBS (1:1)	None	None	None	None	None	Entrapment (Nafion)
Urease/PBS -mix- NF/PBS (5:1)	8	8 ~ 240	0.64	> 7 days	25 ~ 60	Entrapment (Nafion)
Urease/PBS -mix- NF (20:1)	1.25	1.25 ~ 240	1.33	< 30 mins	None	Entrapment (Nafion)

Table 4-2 Summary of urea-ENFET measure by glass reference electrode

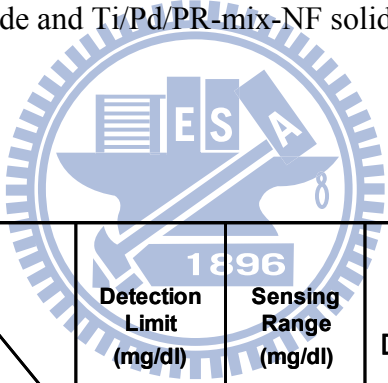


The ENFET biosensor were stored at 4 °C in darkness			
Urea Concentration (mg/dl)	Sensor Response (mV)	Sensor Response (mV) (After 1 week)	Storage Stability (% of sensor response)
1.25	12.9	8.8	68 %
10	50.7	23	45 %
40	97.1	104.6	92 %
80	120.3	118.7	99 %
120	141.4	137.6	97 %
240	198.1	183.6	93 %

Table 4-3 Storage stability of ZrO<sub>2</sub>/urease-mix-NF(5:1) ENFET measure by glass reference electrode

	Detection Limit (mg/dl)	Sensing Range (mg/dl)	Sensitivity [mV/(mg/dl)]
Bare Ti/Pd Metal-RE	5	5 ~ 120	None
Ti/Pd/PR-mix-NF Solid-RE	10	10 ~ 240	0.47

Table 4-4 Summary of ZrO<sub>2</sub>/urease-mix-NF(5:1) ENFET measure by bare Ti/Pd metal reference electrode and Ti/Pd/PR-mix-NF solid-state reference electrode



	Detection Limit (mg/dl)	Sensing Range (mg/dl)	Sensitivity [mV/(mg/dl)]
Glass-RE	8	8 ~ 240	0.64
Ti/Pd/PR-mix-NF Solid-RE	10	10 ~ 240	0.47

Table 4-5 Summary of ZrO<sub>2</sub>/urease-mix-NF(5:1) ENFET measure by glass reference electrode and Ti/Pd/PR-mix-NF solid-state reference electrode

<b>ENFET / ISFET in Differential Mode</b>			
	<b>Detection Limit (mg/dl)</b>	<b>Sensing Range (mg/dl)</b>	<b>Sensitivity [mV/(mg/dl)]</b>
<b>ENFET / ISFET (ZrO<sub>2</sub>) Glass-RE</b>	<b>8</b>	<b>8 ~ 240</b>	<b>0.46</b>

Table 4-6 Summary of ENFET/ISFET in differential mode measure by glass reference electrode

<b>ENFET / REFET in Differential Mode</b>			
	<b>Detection Limit (mg/dl)</b>	<b>Sensing Range (mg/dl)</b>	<b>Sensitivity [mV/(mg/dl)]</b>
<b>ENFET / REFET (ZrO<sub>2</sub>/PI) Glass-RE</b>	<b>10</b>	<b>10 ~ 240</b>	<b>0.64</b>
<b>ENFET / REFET (ZrO<sub>2</sub>/PI-mix-NF) (3:1) Glass-RE</b>	<b>8</b>	<b>8 ~ 240</b>	<b>0.61</b>
<b>ENFET / REFET (ZrO<sub>2</sub>/PR-mix-NF) (1:1) Glass-RE</b>	<b>8</b>	<b>8 ~ 240</b>	<b>0.63</b>

Table 4-7 Summary of ENFET/REFET in differential mode measure by glass reference electrode

<b>ENFET / REFET in Differential Mode</b>			
	<b>Detection Limit (mg/dl)</b>	<b>Sensing Range (mg/dl)</b>	<b>Sensitivity [mV/(mg/dl)]</b>
<b>ENFET / REFET (ZrO<sub>2</sub>/PR-mix-NF) Ti/Pd Quasi-RE</b>	<b>8</b>	<b>8 ~ 240</b>	<b>0.6</b>

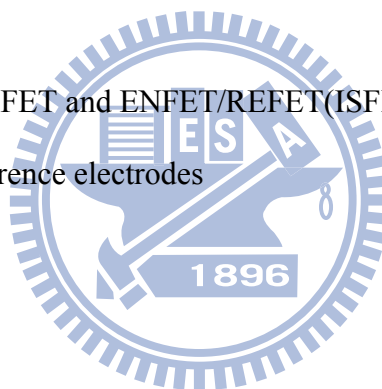
Table 4-8 Summary of ENFET/REFET in differential mode measure by Ti/Pd quasi-reference electrode

	<b>Detection Limit (mg/dl)</b>	<b>Sensing Range (mg/dl)</b>	<b>Sensitivity [mV/(mg/dl)]</b>
<b>Glass-RE</b>	<b>8</b>	<b>8 ~ 240</b>	<b>0.64</b>
<b>Ti/Pd/ PR-mix-NF Solid-RE</b>	<b>10</b>	<b>10 ~ 240</b>	<b>0.47</b>
<b>ENFET / REFET (ZrO<sub>2</sub>/PR-mix-NF) Differential Ti/Pd Quasi-RE</b>	<b>8</b>	<b>8 ~ 240</b>	<b>0.6</b>

Table 4-9 Summary of ENFET and ENFET/REFET differential pair measure by different reference electrodes

	Detection Limit (mg/dl)	Sensing Range (mg/dl)	Sensitivity [mV/(mg/dl)]
Glass-RE	8	8 ~ 240	0.64
Ti/Pd/ PR-mix-NF Solid-RE	10	10 ~ 240	0.47
ENFET / REFET (ZrO <sub>2</sub> /PR-mix-NF) Differential Glass-RE	8	8 ~ 240	0.63
ENFET / ISFET (ZrO <sub>2</sub> ) Differential Glass-RE	8	8 ~ 240	0.46

Table 4-10 Summary of ENFET and ENFET/REFET (ISFET) differential pair measure by different reference electrodes





## 簡 歷

姓 名：詹 昆 謀

性 別：男

出生日期：民國 73 年 03 月 05 日

籍 貫：高雄市

學 歷：國立台灣海洋大學電機工程學系

國立交通大學電子工程研究所

碩士論文：以 pH-ISFET 元件為基礎之尿素感測器之製造與研究

The fabrication and study for pH-ISFET based urea sensors

